BRIDGES BETWEEN QUANTUM AND CLASSICAL MECHANICS: DIRECTED POLYMERS, FLOCKING AND TRANSITIONLESS QUANTUM DRIVING

A Dissertation
Presented to
The Academic Faculty

By

Benjamin Loewe

In Partial Fulfillment
of the Requirements for the Degree
Doctor of Philosophy in the
School of Physics

Georgia Institute of Technology

May 2017

BRIDGES BETWEEN QUANTUM AND CLASSICAL MECHANICS: DIRECTED POLYMERS, FLOCKING AND TRANSITIONLESS QUANTUM DRIVING

Approved by:

Dr. Paul M. Goldbart, Advisor
School of Physics
Georgia Institute of Technology

Dr. Predrag Cvitanović
School of Physics
Georgia Institute of Technology

Dr. Michael Pustilnik
School of Physics
Georgia Institute of Technology

Dr. Elisabetta Matsumoto
School of Physics
Georgia Institute of Technology

Dr. Federico Bonetto
School of Mathematics
Georgia Institute of Technology

Date Approved: March 31, 2017

Qué es la vida? Un frenesí. Qué es la vida? Una ilusión, una sombra, una ficción, y el mayor bien es pequeño: que toda la vida es sueño, y los sueños, sueños son.
(What is this life? A frenzy, an illusion, a shadow, a delirium, a fiction. The greatest good's but little enough: for all life is but a dream, and dreams themselves are only dreams.)

Pedro Calderon de la Barca

To Danae.

ACKNOWLEDGEMENTS

First and foremost, I am deeply grateful to my parents for awakening in me a deep sense of curiosity and love for learning . Without your unconditional and constant support, I would not be here today. To my brothers and sister; thank you for all the laughs and music sessions. I am proud of being your brother, and I hope I was up to the task. Similarly, to my aunt Veronica I extend my deepest gratitude. With your emotional support and advice you have gone well beyond the call of duty.

To my dear friends Bo, DaLin, Alicia and Reinaldo, thank you very much for making us feel welcomed and loved in a foreign land. You are without a doubt a very important aspect of what made of Atlanta our beloved first home.

To Dr. Michael Loss and Dr. Ute Fischer, your generosity and goodwill exceed any expectation. During these years you have been more than friends and professors; you have been mentors, and because of this, I thank you.

A very special gratitude goes to Dr. Anton Souslov and Dr. Rafael Hipolito. Your coaching and advice have been important contributions to this work and to my career. Similarly, I would also like to thank Michael Dimitriyev for all the very interesting exchanges of ideas. To the three of you I can say that it has been a pleasure to collaborate with you.

A special thanks to Becas Chile, the School of Physics and the Goizueta foundation for their financial support.

To my advisor, Dr. Paul Goldbart, thank you for teaching me what makes a good scientist. Your love and passion for science has certainly permeated through the entire College

of Sciences and caused a strong impression on me. Thank you for taking the time to help me when I needed it.

Finally, to Danae, I am very grateful and honored to be able to call you my wife. Without you, this achievement would have been much more difficult. Thank you for so courageously embarking in this adventure with me. I cannot wait to share the next one. I love you very much, my dear Cubito.

TABLE OF CONTENTS

LIST OF FIGURES

LIST OF SYMBOLS

$\boldsymbol{q}$	Generalized coordinates
t	Time
S	Classical action
L	Classical Lagrangian (Ch. 1). Polymer's unstretched length (Ch. 2)
$\boldsymbol{p}$	Classical Momentum
H	Classical Hamiltonian
$\hat{H}$	Quantum Hamiltonian operator
$\{\ ,\ \}$	Poisson bracket
$[\ ,\ ]$	Commutator
$\{\ ,\ \}_M$	Moyal bracket
$\|A\rangle$	Quantum state
$\hat{x}$	Quantum position operator
$\hat{p}$	Quantum momentum operator
$\hbar$	Planck's reduced constant
δ_{ij}	Kronecker's delta
$\hat{U}$	Time evolution operator
∇	Del operator
$\hat{T}$	Time-ordering operator
$\langle\ \rangle$	Expectation value
K	Quantum propagator (Ch.s 1 and 2). Classical limit of the counterdiabatic term (Ch. 4)
$d[x]$	Functional measure

k_B	Boltzmann's constant
T	Temperature
β	Thermodynamic beta
A	Tension
Z	Partition function
X_i	Configuration of the polymers' positions at the lower (initial) end
X_f	Configuration of the polymers' positions at the upper (final) end
X_p	Intermediate configuration of the polymers' positions
Ψ_i	*A priori* initial probabiity distribution for the polymers' ends
Ψ_f	*A priori* final probabiity distribution for the polymers' ends
N	Number of polymers (Ch. 2). Number of self-propelled particles (Ch. 3)
M	An effective time-position-dependent mass (Ch. 2). The mass term in the N-th component theory
ω	Width of the one-dimensional box constraining the polymers
(x, y, z)	Cartesian coordinates
$\lvert\phi_{\text{gs}}\rangle$	Quantum groundstate
$E_{\text{g.s.}}$	Groundstate energy
F	Free energy of the polymer system
ϵ	Size of the time-steps in path-integrals and characteristic microscopic length of the polymer chain
r	Radial distance
θ	Polar angle or parameter used to parametrize the non-circular edge
R	The radius of a circle (or sphere) (Ch. 2). Range of the alignment interaction (Ch. 3). Generalized rotation operator (Ch. 4)
δ_n	Variation in θ for one time-step
s	Arclength parameter
$\hat{p}_\theta$	Momentum operator associated to θ in the quantum analogy

δ	Spread of the angular domain constraining the polymers
ρ	Distance traversed along the normal to the substrate (Ch. 1). The first angular Fourier mode of $P(\boldsymbol{r}, \theta)$ (Ch. 2)
$\boldsymbol{c}(\theta)$	Parametrization of the non-circular substrate
α	Dimensionless parameter that measures the non-circularity of the substrate (Ch. 2). Orientation of the alignment field (Ch. 3)
$\boldsymbol{n}(\theta)$	Normal vector to $\boldsymbol{c}(\theta)$
$\boldsymbol{t}(\theta)$	Tangent vector to $\boldsymbol{c}(\theta)$
$\hat{V}$	Perturbation potential in the polymer problem
δF_U	Universal correction to the Free Energy
$d(t)$	Center of the time-dependent box
$\ell(t)$	Width of the time-dependent box
Δs	Euclidean distance traversed by a polymer link
(θ, ϕ)	Angular spherical coordinates
$f(x, y)$	Function that gives the parametrization of the Monge patch
Ω	Auxiliary function
Λ	Auxiliary function
m	Mass (Ch. 1, 2 and 4). A measure of the orientational noise (Ch. 3)
$\boldsymbol{\sigma}$	Vector whose components are the Pauli matrices
σ_i	The i-th Pauli matrix
κ	A measure of the positional noise
$\hat{U}_\theta$	Rotation operator in the spinorial representation
$\boldsymbol{j}$	Vector formed with the second angular Fourier modes of $P(\boldsymbol{r}, \theta)$
$\boldsymbol{v}(\theta)$	Auxiliary vector that encodes the angular dependence of $P(\boldsymbol{r}, \theta)$
$\boldsymbol{r}$	Position variable in the Fokker-Planck equation
P	Probability density in $\boldsymbol{r}$ and θ associated to the system of self-propelled particles
χ	Imaginary part of the spinor's first component

$\boldsymbol{a}_\perp$	For any vector $\boldsymbol{a} = (a_x, a_y)$, $\boldsymbol{a}_\perp = (a_y, -a_x)$
$\boldsymbol{u}$	Drift vector
D	Diffusion Matrix
a	Auxiliar length-scale
$\boldsymbol{R}$	Position of a self-propelled particle in the Langevin equation (Ch. 3). Vector in parameter space (Ch. 4)
Σ	The matrix in the Langevin equation
$\boldsymbol{W}$	A Wiener process
$\boldsymbol{\xi}$	Positional Brownian noise
ξ_3	Orientational Brownian noise
α_ξ	Orientation of a positional Brownian kick
V_i	Alignment potential acting in the i-th particle
g	The strenght of the alignment interaction
$\boldsymbol{h}$	Alignment field
$\boldsymbol{j}_n$	The $(N+1)$-th Fourier mode of $P(\boldsymbol{r}, \theta)$
ρ_d	Density of self-propelled particles
λ	Measure of the strength of the correlation between positional and orientational noises (Ch. 3). The coupling of the term x^2 in the perturbed potential
ν_{eff}	Effective viscosity
$\boldsymbol{\Sigma}_N$	Velocity/spin operator for the N-component theory
$\boldsymbol{\Sigma}'_N$	Corrected velocity/spin operator for the N-component theory
$\boldsymbol{C}_N$	Correction matrices
$\boldsymbol{\Sigma}_N$	Spin vector for the N-component theory
M	The mass term in the N-th component theory
τ	Time-scale for the Hamiltonian's variation in time, and the coupling of the x^4 term in the perturbed potential
γ_n	Berry's phase

$\boldsymbol{A}_n$	Gauge potential associated to γ_n
$\boldsymbol{B}$	A time dependent magnetic field
$\hat{K}$	Counterdiabatic term
$\hat{\Gamma}$	A transitionless Hamiltonian
$\hat{\boldsymbol{S}}$	A three-dimensional spin operator
$\tilde{H}$	The image of $\hat{H}$ under to transformation to the co-moving frame
V	Classical or quantum potential associated to K and $\hat{K}$, respectively
O_W	The Weyl symbol of an operator $\hat{O}$
(x, p)	Phase space coordinates (x: position, p: momentum)
K_{nW}^m	K_W expanded up to orders m in perturbation theory and n in the semi-classical approximation
PDE	Partial differential equation
TQD	Transitionless quantum driving

SUMMARY

Often considered separated worlds, classical and quantum mechanics share numerous connections with one another. Indeed, as classical mechanics corresponds to a limiting case of quantum mechanics, certain concepts and elements of physical intuition developed in one theory can be and have been used to tackle issues in the other. Nevertheless, these connections do not only cover conceptual issues but also numerous techniques. Indeed, the inherently probabilistic nature of quantum mechanics and its close resemblance to Markovian stochastic processes opens the door to the application of a broad range of powerful methods, initially developed for quantum mechanics, in classical equilibrium and non-equilibrium statistical mechanics. In this thesis we develop progress in three subjects by taking advantage of either a conceptual or a methodological connection between quantum and classical mechanics.

First, we develop the well-known mapping between systems of strongly repelling, two-dimensional directed lines and systems of one-dimensional fermions in order to extend the directed polymer problem to richer geometries. By expressing path integrals in generalized curvilinear coordinates, we successfully generalize the model to settings such as polymers anchored to curved edges, polymers constrained to uneven walls, and polymers constrained to curved surfaces. In each case, we identify the Hamiltonian of an analogous quantum system, which, because of the new geometry of each setting, develops features such as a time- and position-dependent mass and an external electromagnetic vector potential. Along the way, we perform an in-depth analysis of the approximations made and establish regimes of their validity. Finally, in order to obtain analytical results, we employ an extension of the time-dependent perturbation theory scheme of quantum mechanics to imaginary time. Complementing this with the assumption of ground-state dominance, we obtain compact expressions for universal shifts in the free energies of the various systems that allows for

isolation of the effects of the distinct geometrical properties of each system.

The second piece of work presented into this thesis relates to the non-equilibrium setting of active particles. Strongly interacting, self-propelled particles can form a spontaneously flowing, polar (i.e. motionally aligned), active fluid. The study of the connection between the microscopic dynamics of a single, self-propelled particle and the macroscopic dynamics of a liquid comprising such particles can yield insights into experimentally realizable active flows, but this connection is well understood in only a few select cases. Here, we introduce a model of self-propelled particles that is based on an analogy with the motion of an electron subject to strong spin-orbit coupling. We find that, within our model, self-propelled particles experience an analog of the Heisenberg uncertainly principle that instead relates positional and rotational noise. An extension to many-component (and hence more classical) spinors, under which this uncertainty relation vanishes, contributes to the justification of this interpretation. Furthermore, by coarse-graining the microscopic model, we find expressions for the coefficients of the hydrodynamic Toner-Tu equations, established some time ago to describe an active liquid composed of active spins. The connection between self-propelled particles and quantum spins may possibly provide a route for realizing exotic phases of matter using active liquids, via inspiration hailing from systems composed of strongly correlated electrons.

The third and final piece of work to be presented on this thesis consists of a semiclassical approach to Transitionless Quantum Driving (TQD). TQD is a method, developed by means of a reverse engineering strategy, under which non-adiabatic transitions in time-dependent quantum systems are, in M. V. Berry's words, "stifled" through the introduction of a specific auxiliary Hamiltonian. This Hamiltonian comes, however, expressed as a formal sum of outer products of the original instantaneous eigenstates and their time-derivatives. Generically, how to actually create such an operator in the laboratory is thus

rarely evident. The operator may even be non-local. By following a semi-classical approach, we obtain a recipe that yields the auxiliary Hamiltonian explicitly, in terms of the fundamental operators of the system (e.g., position and momentum). By using this formalism, we are able to ascertain criteria for the locality of the auxiliary Hamiltonian, and also to determine its exact form in certain special cases. Lastly, the explicit connection between the auxiliary Hamiltonian and the observables of the system allows for a perturbation scheme in cases in which an exact solution is not easily achievable. This scheme shows that, even in situations in which an exact local auxiliary term cannot be achieved, under special circumstances it is possible to achieve an operator that is local and still approximately stifles non-adiabatic transitions.

CHAPTER 1
INTRODUCTION

The theories of classical and quantum mechanics are amongst the greatest achievements in human history. The former one is the crowning jewel of the great founders of science in the seventeenth century; the latter one is result of the audacious work of physicists in the early twentieth century. Although they are usually considered separate theories, applicable in different energy, time and length scales, it is more precise to say that quantum mechanics is the more fundamental theory, and thus classical mechanics is nothing but a limit of this theory. To understand this bridge between the two requires the reformulation of the classical theory as was achieved during the eighteenth and nineteenth centuries.

Even though the classical theory is a limit, and thus it should not be able to grant any knowledge about quantum mechanics, the algebraic structure between the two seems to be preserved. Therefore, classical mechanics can often be used to gain insight about what a quantum problem may entail. This is formally structured in terms of semi-classical approximations; classical results with quantum corrections whose size is determined by powers of $\hbar$, Planck's fundamental constant, which sets the scales of quantum phenomena. This, the first kind of bridge that we can formulate between the two theories, can in a certain sense be considered a true blessing. Indeed, consider the Rutherford experiment that unraveled the structure of the atom and revealed the existence of the atomic nucleus, a length-scale in which quantum mechanics reigns at full force. In this experiment, Rutherford compared an experimental scattering cross-section with the theoretical *classical* scattering cross-section of the Coulomb potential. The fact that in the first Born approximation the quantum and classical results coincide – and it is not obvious that this should happen – allowed Rutherford to successfully interpret his experiment. Without this, the discovery of the structure of

matter and quantum laws may have taken far much longer.

The idea behind this first bridge, to gain insights from classical mechanics has been also used in other contexts such as the WKB formula. Since the world in which we live is the natural setting for classical mechanics, we are more used to this theory that the quantum one, and therefore its insights can be easier to obtain.

However, this is not the only bridge that we can construct. Although it can appear strange, it is also possible to reach for concepts from *quantum* mechanics and use them to solve *classical* problems. The connection between the two in this case is achieved through the use of the powerful mathematical tools developed to study quantum mechanics. For example, the similarity between the quantum-mechanical composition formula for the transition amplitude $\langle x_f, t_f | x_i, t_i \rangle$, i.e.,

$$\langle x_f, t_f | x_i, t_i \rangle = \int dx \langle x_f, t_f | x, t \rangle \langle x, t | x_i, t_i \rangle \tag{1.1}$$

with the Chapman-Kolmogorov equation for the transition probability between states x_i and x_f, $P(x_f|x_i)$ in a Markovian chain:

$$P(x_f|x_i) = \int dx \, P(x_f|x) \, P(x|x_i), \tag{1.2}$$

allows for the harnessing of quantum-mechanical techniques in stochastic and statistical-mechanic problems. This is, e.g., the basic principle that allows the use of path integrals in both formalisms.

The use of the structure and tools of quantum mechanics to solve classical statistical problems has also been used in other situations. For example, second quantization of quantum mechanics can be used to deal with classical statistical problems in which the number

of particles is not conserved [1, 2]. Similarly, an operator language can be used to deal with Asymmetric Diffusion [3], and finally the Pauli exclusion principle can be used to deal with problems that exhibit strong repulsion [4].

In this thesis we cover three problems in which establishing bridges between quantum and classical mechanics helps to find solutions:

- We use a quantum analogy to compute the equilibrium thermal properties of strongly repulsive directed polymer systems in non-trivial geometries [5].
- We find a bridge between the Schrödinger equation with a spin-orbit coupling term and the statistical study of flocking in active media [6].
- And we use a semi-classical approach to find explicit solutions to a commutator equation in order to find a Hamiltonian that could drive a system without inducing quantum transitions [7].

The thesis is structured as follows: We dedicate the rest of this chapter to a quick review of both classical and quantum mechanics, putting special emphasis in the tools that we shall need. In chapter 2 we explore the problem of directed polymers in complicated geometries. We first introduce the directed polymer problem and the mapping to quantum mechanics envisioned by de Gennes [4] to then show how to extend the method to more general coordinates and geometries. In chapter 3 we study the relationship between the Schrödinger equation with a spin orbit coupling term and a stochastic system of self-propelled particles. Through the use of a Fokker-Planck equation we incorporate interactions so that we may explore the flocking transition and the hydrodynamic behavior. Finally, in chapter 4 we study the problem of transitionless quantum driving using a semi-classical approach. We first introduce the concept of adiabatic evolution and Berry's reverse engineering method [8] to accelerate this evolution. We then find a commutator equation which, by using a semi-classical expansion, can be used to obtain explicit expressions and undertake perturbation theory.

1.1 Classical mechanics in a nutshell

The laws of classical mechanics, as introduced by Newton in the *Philosophiae Naturalis Principia Mathematica*, state that:

- In an inertial reference frame, a body either remains at rest or travels at constant velocity, unless subject to a force.
- In an inertial frame the trajectory of a body, described by $\boldsymbol{r}(t)$, satisfies

$$m\frac{d^2}{dt^2}\boldsymbol{r}(t) = \boldsymbol{F}, \tag{1.3}$$

  in where m denotes the mass of the object and $\boldsymbol{F}$ is the sum of all external forces.
- If a body exerts a force on another, the latter exerts on the former a force equal in magnitude but with opposite direction.

If the external forces are conservative then they can be expressed as the negative of the gradient of a potential function $V(\boldsymbol{r})$. In this case the second law becomes

$$m\frac{d^2}{dt^2}\boldsymbol{r}(t) = -\nabla V(\boldsymbol{r}). \tag{1.4}$$

Given initial conditions $\boldsymbol{r}(0) = \boldsymbol{r}_0$ and $\dot{\boldsymbol{r}}(0) = \boldsymbol{v}_0$, where the dots denote time derivatives, Eq. (1.4) then (in principle) provides the trajectories of the object for all future times, and thus classical mechanics is completely deterministic.

An alternative formulation of classical mechanics, which facilitates the use of generalized coordinates, is based on Hamilton's principle of stationary action. This principle exhibits classical mechanics as a variational problem. It states that the trajectory of a system described by the generalized coordinates $\boldsymbol{q} = (q_1, q_2, \ldots, q_N)$ between two specific states $\boldsymbol{q}(t_1)$ and $\boldsymbol{q}(t_2)$ at times t_1 and t_2 is a stationary point of a functional, $S[\boldsymbol{q}(\cdot), \boldsymbol{q}(t_1), \boldsymbol{q}(t_2)]$,

called the action. In other words, the dynamical evolution of the system can be determined by the equation

$$\frac{\delta S[\boldsymbol{q}(\cdot), \boldsymbol{q}(t_1), \boldsymbol{q}(t_2)]}{\delta \boldsymbol{q}(t)} = 0, \tag{1.5}$$

in where $\delta/\delta\boldsymbol{q}$ denotes a functional derivative. Usually, this functional can be written in terms of a function of the coordinates and their time derivatives, $L(\boldsymbol{q}, \dot{\boldsymbol{q}})$, called the Lagrangian, such that

$$S[\boldsymbol{q}(\cdot), \boldsymbol{q}(t_1), \boldsymbol{q}(t_2)] = \int_{t_1}^{t_2} dt L(\boldsymbol{q}, \dot{\boldsymbol{q}}, t). \tag{1.6}$$

The equations of motion are then the Euler-Lagrange equations:

$$\frac{d}{dt}\left(\frac{\partial L(\boldsymbol{q}, \dot{\boldsymbol{q}}, t)}{\partial \dot{\boldsymbol{q}}}\right) - \frac{\partial L(\boldsymbol{q}, \dot{\boldsymbol{q}}, t)}{\partial \boldsymbol{q}} = 0. \tag{1.7}$$

One needs then to identify the appropriate form of the Lagrangian. This can be readily achieved for a point-particle system described in Cartesian coordinates. To start with, notice that if the particles are free of external forces then the Lagrangian cannot depend on the position of the particles, because space is homogeneous. In a similar way, since space is also isotropic, the Lagrangian cannot depend on the directions of the velocities. As a consequence, the Lagrangian can only depend on the modulus of the velocities. By comparing with Eq. (1.4), we see that a good fit is given by

$$L(\boldsymbol{r}, \dot{\boldsymbol{r}}, t) = \frac{1}{2} m |\dot{\boldsymbol{r}}(t)|^2 \equiv T(\dot{\boldsymbol{r}}), \tag{1.8}$$

in which we identify $T(\dot{\boldsymbol{r}})$ as the kinetic energy of the system. Finally, if we include external conservative forces, and thus, potentials, Eq. (1.7) must still yield Eq. (1.4). This comparison finally leads to

$$L(\boldsymbol{r}, \dot{\boldsymbol{r}}, t) = T(\dot{\boldsymbol{r}}) - V(\boldsymbol{r}). \tag{1.9}$$

When using generalized coordinates, this result generalizes to

$$L(\boldsymbol{q}, \dot{\boldsymbol{q}}, t) = T(\boldsymbol{q}, \dot{\boldsymbol{q}}, t) - V(\boldsymbol{q}, t). \tag{1.10}$$

classical mechanics, formulated in this way, is known as the Lagrangian formalism. It is of great help to identify symmetries of the system since, by Eq. (1.7), a transformation that leaves the Lagrangian invariant will yield the same equations of motion. The symmetries will lead then to conserved quantities [9]. One conserved quantity that is easy to recognize arises in the case in which the Lagrangian does not depend on some particular coordinate, say $\boldsymbol{q}_i$. Then, via Eq. (1.7), one obtains the conserved quantity:

$$p_i \equiv \frac{\partial L(\boldsymbol{q}, \dot{\boldsymbol{q}}, t)}{\partial \dot{q}_i} = \text{const.} \tag{1.11}$$

We call the quantity p_i the momentum conjugated to q_i. Equation (1.11) suggests that in some cases, $\boldsymbol{p}$ could give a simpler description of the system than $\dot{\boldsymbol{q}}$. The set of variables $\boldsymbol{q}$ and $\boldsymbol{p}$, are called canonical variables, and their use leads to Hamiltonian dynamics.

The formal change of variables is achieved via the Legendre transformation:

$$H(\boldsymbol{q}, \boldsymbol{p}, t) = \sum_i \dot{q}_i \, p_i - L(\boldsymbol{q}, \boldsymbol{p}, t), \tag{1.12}$$

in where H is a function of $\boldsymbol{q}$ and $\boldsymbol{p}$ called the Hamiltonian. For simple particle systems described in Cartesian coordinates $\boldsymbol{r}$, Eq. (1.12) gives

$$H(\boldsymbol{r}, \boldsymbol{p}) = \frac{\boldsymbol{p}^2}{2m} + V(\boldsymbol{r}) = T + V, \tag{1.13}$$

and thus we can physically interpret the Hamiltonian as the total energy of the system.

This interpretation however does not hold for general systems. A comparison of the total differentials of L and H, together with Eq. (1.7), leads us to the equations of motion for $\boldsymbol{p}$ and $\boldsymbol{q}$, known as Hamilton's equations:

$$\dot{\boldsymbol{p}} = -\frac{\partial H}{\partial \boldsymbol{q}}, \quad \dot{\boldsymbol{q}} = \frac{\partial H}{\partial \boldsymbol{p}}, \quad \frac{\partial H}{\partial t} = \frac{\partial L}{\partial t}. \tag{1.14}$$

In particular, this last equation implies that if the system is explicitly time-independent then the Hamiltonian is a conserved quantity. For the simple systems described above, this just states the conservation of energy.

Equations (1.14) can then be used to determine the evolution of any function that depends on both $\boldsymbol{q}$ and $\boldsymbol{p}$. Indeed, notice that if f is a sufficiently smooth but otherwise general function, then

$$\frac{d}{dt} f(\boldsymbol{q}, \boldsymbol{p}, t) = \dot{\boldsymbol{q}} \cdot \frac{\partial f}{\partial \boldsymbol{q}} + \dot{\boldsymbol{p}} \cdot \frac{\partial f}{\partial \boldsymbol{p}} + \frac{\partial f}{\partial t}. \tag{1.15}$$

Thus, by using Hamilton's equations (1.14) to replace $\dot{\boldsymbol{q}}$ and $\dot{\boldsymbol{p}}$ we obtain

$$\frac{d}{dt} f(\boldsymbol{q}, \boldsymbol{p}, t) = \frac{\partial f}{\partial \boldsymbol{q}} \cdot \frac{\partial H}{\partial \boldsymbol{p}} - \frac{\partial f}{\partial \boldsymbol{p}} \cdot \frac{\partial H}{\partial \boldsymbol{q}} + \frac{\partial f}{\partial \boldsymbol{t}}. \tag{1.16}$$

By defining the Poisson bracket

$$\{A, B\} \equiv \sum_i \frac{\partial A}{\partial q_i} \cdot \frac{\partial B}{\partial p_i} - \frac{\partial A}{\partial p_i} \cdot \frac{\partial B}{\partial q_i}, \tag{1.17}$$

Eq. (4.54) can then be rewritten as

$$\frac{d}{dt} f(\boldsymbol{q}, \boldsymbol{p}, t) = \{f, H\} + \frac{\partial f}{\partial \boldsymbol{t}}. \tag{1.18}$$

The Poisson bracket plays then an important role in Hamiltonian dynamics, as it drives the time evolution of the system. In particular, by noticing that

$$\{q_i, p_j\} = \delta_{ij} \tag{1.19}$$

and using (1.18) we recover Hamilton's equation (1.14). Finally, the Poisson bracket determines the *algebra* behind the group structure of Hamilton's equations. A transformation of coordinates $\boldsymbol{q} \to \boldsymbol{Q}$, $\boldsymbol{p} \to \boldsymbol{P}$, $H \to K$, preserves the structure of Eqs. (1.14), i.e.

$$\dot{\boldsymbol{P}} = -\frac{\partial K}{\partial \boldsymbol{Q}}, \quad \dot{\boldsymbol{Q}} = \frac{\partial K}{\partial \boldsymbol{P}}, \tag{1.20}$$

if and only if the Poisson bracket is preserved, i.e.,

$$\{q_i, p_j\} = \{Q_i, P_j\} = \delta_{ij}, \quad \{q_i, q_j\} = \{p_i, p_j\} = \{Q_i, Q_j\} = \{P_i, P_j\} = 0. \tag{1.21}$$

Since transformations of this kind send canonical systems into canonical systems, they are called Canonical Transformations, and they are deeply related to symmetries and conserved quantities. Indeed, let us study canonical transformations that depend on a continuous parameter λ, i.e.,

$$\boldsymbol{Q} = \boldsymbol{Q}_\lambda(\boldsymbol{q}, \boldsymbol{p}, \lambda), \quad \boldsymbol{P}_\lambda = \boldsymbol{P}(\boldsymbol{q}, \boldsymbol{p}, \lambda), \tag{1.22}$$

such that $Q(\boldsymbol{q}, \boldsymbol{p}, 0) = \boldsymbol{q}$, $P(\boldsymbol{q}, \boldsymbol{p}, 0) = \boldsymbol{p}$. Then, for a time-independent canonical transformation and an infinitesimal λ it is possible to show that there is a function of the canonical variables $G(\boldsymbol{q}, \boldsymbol{p})$ such that [10]

$$\begin{aligned} \delta\boldsymbol{q} &= \boldsymbol{Q}(\lambda) - \boldsymbol{q} = \lambda \frac{\partial G}{\partial \boldsymbol{p}}, \\ \delta\boldsymbol{p} &= \boldsymbol{P}(\lambda) - \boldsymbol{p} = -\lambda \frac{\partial G}{\partial \boldsymbol{q}}. \end{aligned} \tag{1.23}$$

Taking the reverse route, one can also show that infinitesimal transformations defined

through Eqs. (1.23) lead to canonical transformations for any function $G(\boldsymbol{q}, \boldsymbol{p})$ [10].

In other words, for all one-parameter families of canonical transformations there is a function G and for all functions G there is a one-parameter family of canonical transformations. Given this correspondence, G is frequently called the generator of the transformation.

As an example, take the one-dimensional translation $p \to p$ and $q \to q + \lambda$. Then, $G(q, p) = p$. Thus, the canonical momentum is the generator of translations.

Given that every function of $\boldsymbol{q}$ and $\boldsymbol{p}$ generates a canonical transformation, we can ask: What is the canonical transformation associated to $H(\boldsymbol{q}, \boldsymbol{p})$? By replacing in Eqs. (1.23) and letting $\lambda = t$, we find that these equations take the form of Hamilton's equations (1.14), and thus H drives $\boldsymbol{p}(t)$ to $\boldsymbol{p}(t + dt)$ and $\boldsymbol{q}(t)$ to $\boldsymbol{q}(t + dt)$. In other words, the Hamiltonian is quite literally the generator of time evolution.

1.2 Quantum mechanics in a nutshell

In this section we briefly review the main aspects of quantum mechanics. For our derivations we follow closely Ref. [11].

Striking experimental observations at the beginning of the twentieth century – such as the radiation spectrum of a black body and ultraviolet catastrophe, the photoelectric effect and the impossibility of understanding the stability of the atom – led physicists to understand that the principles that ruled classical mechanics did not apply at microscopic length-scales. The apparent corpuscular behavior of light, appearing in packets or quanta of discretized energy named photons, cannot be explained by classical electrodynamics, in which light its a wave. An analogous contradiction appeared with the theoretical prediction by De Broglie which stated the exact opposite situation for matter, i.e., that massive, classically point-like objects can behave as a wave.

After several attempts to explain phenomena such as these – quantization of energy and wave-like behavior– success was finally achieved in 1925 almost simultaneously by Schrödinger and Heisenberg. While the former established the theory in terms of wavefunctions and partial differential equations and the latter in terms of matrices, both approaches were shortly thereafter proven to be equivalent.

The success of these methods in obtaining the spectrum of the hydrogen atom, solving along the way the issue of its stability, contrasted with the adjacent predictions about the nature of the microscopic world. The most striking one is the loss of determinism. The theory is at its heart probabilistic. After Born's interpretation of the wavefunction as a probability amplitude for finding a particle in a given neighborhood, the concept of a trajectory no longer has a place in quantum mechanics. Not only can we not be certain about the position of a particle but also, as encapsulated in Heisenberg's uncertainty principle, an attempt to increase the precision of this measurement would yield a complementary loss of information about the particle's velocity. There is in general no way to know, *a priori*, the result of a measurement, and measurements themselves generally influence the state of the object being measured.

Accepting this findings, the theory can be expressed then in terms of states, represented by vectors in a Hilbert space. Each classical observable has its quantum counterpart in the form of an operator, and these operators have states with associated definite, and possibly quantized, values. Mathematically, to a classical observable A there is an associated hermitian linear operator $\hat{A}$ with a complete set of eigenvectors $|A\rangle$ that satisfy

$$\hat{A}|A\rangle = A|A\rangle. \tag{1.24}$$

The state of the system, also represented by a vector in Hilbert space $|\Psi\rangle$, is then described

by a linear superposition of the eigenstates of $\hat{A}$:

$$|\Psi\rangle = \sum_n c_n |A_n\rangle, \tag{1.25}$$

and the coefficients c_n of this linear combination are the probability amplitudes of finding the system in a definite state $|A_n\rangle$. In other words, the probability that a measurement of A will yield the result A_n is given by $|c_n|^2$. Given this interpretation, we should then have

$$\sum_n |c_n|^2 = 1 \tag{1.26}$$

Denoting the inner product between states as $\langle \Psi_1 | \Psi_2 \rangle$, and using the fact that eigenstates of hermitian operators form an orthonormal basis, we have then that the norm of the state must be given by

$$\langle \Psi | \Psi \rangle = 1. \tag{1.27}$$

Moreover, notice that in order to extract the probability amplitude associated with $|A_n\rangle$ we can simply take the inner product of the associated eigenvector $|A_n\rangle$ with $|\Psi\rangle$; thus

$$\langle A_n | \Psi \rangle = c_n. \tag{1.28}$$

Combining all these results, we then see that

$$\langle \Psi | \hat{A} | \Psi \rangle = \sum_n |c_n|^2 A_n = \langle A \rangle \,, \tag{1.29}$$

i.e., the expectation value of an operator $\hat{A}$ is given by $\langle \Psi | \hat{A} | \Psi \rangle$.

Finally, notice that since the eigenvectors of $\hat{A}$ form a complete basis of our Hilbert space, we must have that:

$$\sum_n |A_n\rangle\langle A_n| = \hat{I}, \tag{1.30}$$

in where $\hat{I}$ denotes the identity operator in the Hilbert space.

Until now we have discussed general operators. A particular operator that we should pay attention to is then the position operator $\hat{\boldsymbol{x}}$. Let us denote its eigenvectors as $|\boldsymbol{x}\rangle$, which satisfy

$$\hat{\boldsymbol{x}}|\boldsymbol{x}\rangle = \boldsymbol{x}|\boldsymbol{x}\rangle. \tag{1.31}$$

Since, as far as we know, space is a continuum, this operator must have a continuous set of eigenvalues, and thus a special normalization is needed:

$$\langle \boldsymbol{x}'|\boldsymbol{x}\rangle = \delta(\boldsymbol{x} - \boldsymbol{x}'), \tag{1.32}$$

in where $\delta(\boldsymbol{x})$ is the (three-dimensional) Dirac delta function. However, these states continue on to be complete, and thus we must have

$$\int d\boldsymbol{x}|\boldsymbol{x}\rangle\langle\boldsymbol{x}| = \hat{I}. \tag{1.33}$$

Then, given equation (1.28) we must have that

$$\langle \boldsymbol{x}|\Psi\rangle = \Psi(\boldsymbol{x}), \tag{1.34}$$

i.e., $\Psi(\boldsymbol{x})$ is the probability amplitude for finding a particle near position $\boldsymbol{r}$, viz., the wavefunction.

What about the momentum operator? As we learned from classical mechanics, the momentum operator is the generator of translations, and thus, one should get insight about

it by exploring the infinitesimal translation from $|\boldsymbol{x}\rangle$ to $|\boldsymbol{x} + d\boldsymbol{x}\rangle$. Call the operator that connects these two states $\hat{J}(d\boldsymbol{x})$. After a translation, a state continues to describe a valid physical system and, as such, its norm should not change. This constrains $\hat{J}(d\boldsymbol{x})$ to satisfy $\hat{J}^{\dagger}(d\boldsymbol{x})\,\hat{J}(d\boldsymbol{x}) = \hat{I}$. On the other hand, a translation by $(d\boldsymbol{x})$ followed by a translation by $-(d\boldsymbol{x})$ should leave the system invariant. Thus, we conclude that: $\hat{J}(-d\boldsymbol{x}) = \hat{J}^{\dagger}(d\boldsymbol{x})$, which also leads to the conclusion that: $\hat{J}(d\boldsymbol{x})\hat{J}^{\dagger}(d\boldsymbol{x}) = \hat{I}$. Therefore, $\hat{J}(d\boldsymbol{x})$ must be unitary.

Other constraints that $\hat{J}(d\boldsymbol{x})$ must satisfy are that the composition of two translations is also a translation, i.e.,

$$\hat{J}(d\boldsymbol{x}_1)\hat{J}(d\boldsymbol{x}_2) = \hat{J}(d\boldsymbol{x}_1 + d\boldsymbol{x}_1), \tag{1.35}$$

and that a translation by zero should yield the identity operator, i.e.,

$$\hat{J}(0) = \hat{I}. \tag{1.36}$$

A quick computation would conclude that by writing

$$\hat{J}(d\boldsymbol{x}) = \hat{I} - d\boldsymbol{x} \cdot \frac{\hat{\boldsymbol{p}}}{\hbar} \tag{1.37}$$

with $\boldsymbol{p}$ a hermitian operator and $\hbar$ being Planck's (reduced) constant, we satisfy all of the previous requirements up to linear order in $d\boldsymbol{x}$. As the operator $\hat{\boldsymbol{p}}$ generates the translation, we identify it with the momentum operator. Furthermore, notice that

$$(\hat{\boldsymbol{x}}\hat{J}(d\boldsymbol{x}) - \hat{J}(d\boldsymbol{x})\hat{\boldsymbol{x}})|\boldsymbol{x}\rangle \approx d\boldsymbol{x}|\boldsymbol{x}\rangle. \tag{1.38}$$

As this is true for any state $|\boldsymbol{x}\rangle$, we conclude that

$$\left[\hat{\boldsymbol{x}}, \hat{J}(d\boldsymbol{x})\right] = d\boldsymbol{x}\hat{I}. \tag{1.39}$$

In terms of $\hat{\boldsymbol{p}}$, this translates to

$$[\hat{x}_i, \hat{p}_j] = i\hbar\delta_{i\,j}\hat{I}, \tag{1.40}$$

in where [,] denotes the commutator, i.e., $[\hat{A}, \hat{B}] = \hat{A}\hat{B} - \hat{B}\hat{A}$. Equation (1.40) seems then to be the quantum counterpart to the classical equation Eq. (1.19). Thus, there seems to be a relationship between the commutator and the Poisson bracket. We shall discuss this further below.

An important consequence of Eq. (1.40) is that since $\hat{\boldsymbol{x}}$ and $\hat{\boldsymbol{p}}$ do not commute they do not share a common basis of eigenstates. In other words, they are not compatible operators and cannot be measured simultaneously. Mathematically, this leads to the result that

$$\Delta x \Delta p \geq \frac{\hbar}{2}, \tag{1.41}$$

in where Δx and Δp are the standard deviations of x and p, respectively.

Finally, one can establish that

$$\langle \boldsymbol{x'}|\hat{\boldsymbol{p}}|\boldsymbol{x}\rangle = -i\nabla\delta(\boldsymbol{x'} - \boldsymbol{x}), \tag{1.42}$$

and that if $|\boldsymbol{p}\rangle$ denotes an eigenstate of $\hat{\boldsymbol{p}}$ then

$$\langle \boldsymbol{x}|\boldsymbol{p}\rangle = \frac{1}{(2\pi\hbar)^{3/2}} e^{i\frac{\boldsymbol{p}\cdot\boldsymbol{x}}{\hbar}}. \tag{1.43}$$

This completes our review of the momentum operator. However, as we saw in the classical case, there is another important generator: the Hamiltonian, which drives time

evolution. Following the same line of thought we used with the momentum operator, let us define a time evolution operator $\hat{U}(t, t_0)$, which satisfies

$$|\Psi(t)\rangle = \hat{U}(t, t_0)|\Psi(t_0)\rangle, \tag{1.44}$$

i.e., it transforms our state at time t_0 in to its form at a later time, t. By demanding that this operators keeps the norm of states constant, and that it satisfies the composition property

$$\hat{U}(t, t_1)\hat{U}(t_1, t_0) = \hat{U}(t, t_0), \tag{1.45}$$

we conclude that it must also be a unitary operator. By analogy to the momentum operator then, one can prove that for an infinitesimal timestep we have

$$\hat{U}(t + dt, t) = \hat{I} - \frac{i}{\hbar}\hat{H}, \tag{1.46}$$

where $\hat{H}$ is the operator counterpart of the classical Hamiltonian. (This satisfies all the constraints up to order dt^2.) Notice then that

$$\hat{U}(t + dt, t_0) = \hat{U}(t + dt, t)\,\hat{U}(t, t_0). \tag{1.47}$$

By expanding up to first order, this leads to:

$$\hat{U}(t + dt, t_0) - \hat{U}(t, t_0) = -\frac{i}{\hbar}\hat{H}\hat{U}(t, t_0)dt. \tag{1.48}$$

This can be recast as

$$\frac{d}{dt}\hat{U}(t, t_0) = -\frac{i}{\hbar}\hat{H}\hat{U}(t, t_0). \tag{1.49}$$

This is the Schrödinger equation for the time evolution operator. Furthermore, by considering the state$|\Psi(t_0)\rangle$ we finally arrive at

$$i\hbar\frac{d}{dt}|\Psi(t)\rangle = \hat{H}|\Psi(t)\rangle, \tag{1.50}$$

which is the Schrödinger equation for the state $|\Psi(t)\rangle$. Then we have that if the classical Hamiltonian is given by

$$H = \frac{\boldsymbol{p}^2}{2m} + V(\boldsymbol{x}), \tag{1.51}$$

then, in configuration space, Eq. (1.50) acquires its usual form, i.e.,

$$i\hbar\frac{\partial}{\partial t}\Psi(\boldsymbol{x}) = \left(-\frac{\hbar^2}{2m}\nabla^2 + V(\boldsymbol{x})\right)\Psi(\boldsymbol{x}). \tag{1.52}$$

We finish this quick recap of quantum mechanics by finding formal solutions to Eq. (1.49). There are three possible cases. (i) If the operator $\hat{H}$ is time independent then it is evident that

$$\hat{U}(t,t_0) = e^{-\frac{i}{\hbar}(t-t_0)\hat{H}}. \tag{1.53}$$

(ii) If the Hamiltonian depends on time but it commutes with itself at all pairs of times, i.e., $[\hat{H}(t_1), \hat{H}(t_2)] = 0$, then the solution of Eq. (1.49) is also relatively simple:

$$\hat{U}(t,t_0) = e^{-\frac{i}{\hbar}\int_{t_0}^{t} dt'\hat{H}(t')}. \tag{1.54}$$

(iii) Finally, if $\hat{H} = \hat{H}(t)$ but $[\hat{H}(t_1), \hat{H}(t_2)] \neq 0$ then the solution to Eq. (1.49) is formally given by

$$\hat{U}(t,t_0) = \hat{T}\left(e^{-\frac{i}{\hbar}\int_{t_0}^{t} dt'\hat{H}(t')}\right), \tag{1.55}$$

where $\hat{T}$ is the time-ordering operator. This solution is only a formal expression. In order to use it, one needs to expand the exponential in series and, using the time-ordering operator,

compute each term.

1.3 Connection between quantum and classical mechanics: The classical limit

There are several ways to examine the connection between classical and quantum mechanics. As the latter is the more fundamental theory, we expect to have a limit in which classical mechanics becomes a good approximation. As we shall see, this limit is achieved by letting $\hbar$ become vanishingly small. In this way, $\hbar$ stands as the universal constant that identifies the scale at which quantum phenomena become relevant.

1.3.1 Heisenberg's equations, the commutator and the Moyal bracket

One of the clearest way to make the quantum-classical connection is via the Heisenberg Equations of Motion. These are achieved by changing the picture of time evolution. Instead of setting the observables as stationary operators and letting the wavefunction carry the time evolution (i.e., the Schrödinger picture), we can instead let the wavefunction be time independent and have the operators evolve. This is achieved through the unitary transformation:

$$\hat{U}(t) = e^{-\frac{i\hat{H}t}{\hbar}}. \tag{1.56}$$

Indeed, we know that for any state $|\Psi(t)\rangle$ we have

$$|\Psi(t)\rangle = \hat{U}(t)|\Psi(0)\rangle. \tag{1.57}$$

This allows us to look at the computation of the expectation value of an observable $\hat{A}$ in two different ways:

$$\langle \hat{A} \rangle = \langle \Psi(t) | \hat{A} | \Psi(t) \rangle = \langle \Psi(0) | \hat{U}^{\dagger}(t)\, \hat{A}\, \hat{U}(t) | \Psi(0) \rangle = \langle \Psi(0) | \hat{A}(t) | \Psi(0) \rangle, \tag{1.58}$$

where we have defined the Heisenberg time-dependent operator via

$$\hat{A}(t) \equiv \hat{U}^{\dagger}(t)\, \hat{A}\, \hat{U}(t). \tag{1.59}$$

By explicitly derivating Eq. (1.59) with respect to time, we determine that the dynamical equation for $\hat{A}$ is

$$\frac{d\hat{A}}{dt} = \frac{i}{\hbar}[A, \hat{H}] + \frac{\partial \hat{A}}{\partial t}. \tag{1.60}$$

The formal similarity between Eq. (1.60) and its classical counterpart, Eq. (1.18), suggests that the classical limit is achieved by exchanging the commutator operator for the Poisson bracket, i.e.,

$$[\ \ ,\ \ ] \rightarrow i\hbar\{\ \ ,\ \ \}. \tag{1.61}$$

Is the commutator the quantum version of the Poisson bracket? Equations (1.60) and the observation that through (1.61) one can compute many commutators led Dirac to conjecture that this is indeed the case [12]. However, as was observed by Groenewold in Ref. [13], a general, systematic and consistent correspondence between the commutator and the Poisson bracket can not exist. Indeed, the Poisson bracket is not enough. As Moyal showed in Ref. [14], a proper formulation of quantum mechanics in phase space and Weyl quantization requires instead the use of the more elaborate prescription:

$$[\hat{A}(q,p),\hat{B}(q,p)] \to i\hbar\{A(q,p),B(q,p)\}_M \equiv A(q,p)2i\sin\left(\frac{\hbar}{2}(\overleftarrow{\partial_q}\vec{\partial_p}-\overleftarrow{\partial_p}\vec{\partial_q}\right)B(q,p). \tag{1.62}$$

In this notation the derivative $\vec{\partial}$ acts only on the function to the right while $\overleftarrow{\partial}$ acts only on functions to the left.

Equation (1.62) defines the Moyal bracket (also known as Sine bracket) and it should be understood as a series in derivatives. Notice that as $\hbar \to 0$ it becomes the Poisson bracket, thus making the match with classical mechanics. Notice also that this expression opens up the door for semi-classical expansions, i.e. it results in a series in $\hbar$, which can be understood as a classical result plus quantum corrections. Since, in order to secure a full quantum result, one needs the entire series and thus an unlimited number of derivatives, this exhibits the non-local character of quantum mechanics. Speaking in classical terms, when going from one position to another in a certain amount of time, the particle traverses all of space. Although this idea is not evident from Eq. (1.62), it is at the heart of the path-integral formalism of quantum mechanics, which we briefly introduce next.

1.3.2 Path-integral formalism

In this section we briefly review the path-integral formalism. For simplicity, we discuss the one-dimensional case. The extension to higher dimensions is not difficult to achieve. For all derivations, we follow Ref. [15].

As described in the previous sections, the dynamical evolution in quantum mechanics is encoded in the time-evolution operator $\hat{U}(t,t_0)$. The matrix elements of this operator in configuration space, i.e.,

$$K(x', t; x, t_0) \equiv \langle x'|\hat{U}(t, t_0)|x\rangle, \tag{1.63}$$

also called the kernel or propagator, encodes then the same information. Indeed, notice that by inserting an identity operator Eq. (1.57) is equivalent to

$$\Psi(x', t) = \int dx\, K(x', t; x, t_0)\Psi(x, t_0). \tag{1.64}$$

Therefore, computing K is formally equivalent to solving the quantum dynamics problem. The path-integral formalism achieves this computation by taking advantage of the composition property (1.45) and dividing the total evolution time $t - t_0$ in N infinitesimal timesteps, i.e.,

$$\langle x'|\hat{U}(t, t_0)|x\rangle = \langle x'| \left[\prod_{k=0}^{N-1} \hat{U}(t_{k+1}, t_k)\right] |x\rangle, \tag{1.65}$$

in where $t_N = t$, and $t_{k+1} - t_k = \epsilon$, with ϵ being infinitesimal. For the resulting short-time evolution, the form of $\hat{U}$ is straightforward to obtain. Indeed, via Eq. (1.49) we see that

$$\hat{U}(t_{k+1}, t_k) = -\frac{i}{\hbar}\epsilon\hat{H}(t_k) \approx e^{-\frac{i}{\hbar}\epsilon\hat{H}(t_k)}, \tag{1.66}$$

up to first order in ϵ. Then, by inserting $N - 1$ resolutions of the identity in Eq. (1.65), we see that

$$\langle x'|\hat{U}(t, t_0)|x\rangle = \int \left(\prod_{i=1}^{N-1} dx_i\right) \left[\prod_{k=0}^{N-1} \langle x_{k+1}|e^{\frac{-i}{\hbar}\epsilon\hat{H}(t_k)}|x_k\rangle\right]. \tag{1.67}$$

From now on, we consider a Hamiltonian of the form

$$\hat{H} = \frac{\hat{p}^2}{2m} + V(\hat{x}). \tag{1.68}$$

in were both the mass and the potential could, in principle, be time dependent. Then, by

means of the Baker-Campbell-Hausdorff formula [15],

$$e^{\epsilon(\hat{A}+\hat{B})} = e^{\epsilon\hat{A}}e^{\epsilon\hat{B}}e^{\epsilon^2\hat{C}}, \tag{1.69}$$

with

$$\hat{C} = \frac{1}{2}[\hat{A},\hat{B}] - \frac{\epsilon}{6}\Big([\hat{A},[\hat{A},\hat{B}]] - 2[[\hat{A},\hat{B}],\hat{B}]\Big) + O(\epsilon^2), \tag{1.70}$$

we have that, up to order ϵ,

$$\langle x_{k+1}|e^{\frac{-i}{\hbar}\epsilon\hat{H}(t_k)}|x_k\rangle \approx \langle x_{k+1}|e^{\frac{-i\epsilon}{\hbar}\frac{\hat{p}^2}{2m}}e^{\frac{-i\epsilon}{\hbar}V(x)}|x_k\rangle. \tag{1.71}$$

Then, by inserting a complete set of momentum eigenstates and observing that $V(\hat{x})$ depends only on position we can rewrite

$$\langle x_{k+1}|e^{\frac{-i}{\hbar}\epsilon\hat{H}(t_k)}|x_k\rangle \approx \int \frac{dp}{2\pi\hbar}\langle x_{k+1}|e^{\frac{-i\epsilon}{\hbar}\frac{\hat{p}^2}{2m}}|p\rangle\langle p|x_k\rangle e^{\frac{-i\epsilon}{\hbar}V(x_k)}, \tag{1.72}$$

or:

$$\langle x_{k+1}|e^{\frac{-i}{\hbar}\epsilon\hat{H}(t_k)}|x_k\rangle \approx \int \frac{dp}{2\pi\hbar}e^{\frac{-i\epsilon}{\hbar}\frac{p^2}{2m}+i\frac{(x_{k+1}-x_k)p}{\hbar}}e^{\frac{-i\epsilon}{\hbar}V(x_k)}. \tag{1.73}$$

Finally, by performing the Fresnel integral in momentum (i.e., the imaginary version of the Gaussian integral), we obtain

$$\langle x_{k+1}|e^{\frac{-i}{\hbar}\epsilon\hat{H}(t_k)}|x_k\rangle \approx \sqrt{\frac{m}{2\pi\hbar i}}e^{\frac{i\epsilon}{\hbar}\left[\frac{m}{2}\left(\frac{x_{k+1}-x_k}{\epsilon}\right)^2 - V(x_k)\right]}. \tag{1.74}$$

Inserting this into our original expression for the propagator, Eq. (1.67), we obtain

$$\langle x'|\hat{U}(t,t_0)|x\rangle \approx \sqrt{\frac{m}{2\pi i\hbar\epsilon}}\int d^N[x]e^{\frac{i\epsilon}{\hbar}\sum_{k=0}^{N-1}\left[\left(\frac{m}{2}\frac{x_{k+1}-x_k}{\epsilon}\right)^2 - V(x_k)\right]}, \tag{1.75}$$

in which we have used the definition

$$d^N[x] = \prod_{i=1}^{N-1} \sqrt{\frac{m}{2\pi i\hbar\epsilon}}\, dx_i\,. \tag{1.76}$$

Finally, we take the continuum limit by letting $\epsilon \to 0$ and $N \to \infty$ such that $N\epsilon = t - t_0$. In this limit

$$\sum_{k=0}^{N-1} \left[\left(\frac{x_{k+1} - x_k}{\epsilon} \right)^2 - V(x_k) \right] \to \int_{t_0}^{t} dt' \left(\frac{1}{2} m\dot{x}^2 - V(x) \right). \tag{1.77}$$

We then recognize the integrand as the classical Lagrangian, Eq. (1.9). Thus, we identify the integral as the classical action, Eq. (1.6). By defining the functional measure, $d[x]$ as the limit of $d^N[x]$ as $N \to \infty$ we can then finally write

$$K(x_f, t_f; x_i, t_i) = \int_{x(t_i)=x_i}^{x(t_f)=x_f} d[x] e^{\frac{i}{\hbar}\int_{t_0}^{t} dt' \left(\frac{1}{2}m\dot{x}^2 - V(x)\right)} = \int_{x(t_i)=x_i}^{x(t_f)=x_f} d[x] e^{\frac{i}{\hbar}S[x_f,t_f,x_i,t_i]}. \tag{1.78}$$

The interpretation of this equation yields the same non-locality that we observed from the Moyal bracket. This integral is a functional integral, and the variable of integration is the trajectory of the particle. Therefore, this integral sums over all possible paths joining x_f and x_i in a time $t_f - t_i$ and the contribution from each path to the propagator is weighted in by the factor $e^{\frac{i}{\hbar}S}$. In other words, the evolution of the particle is a superposition of all possible trajectories, not only the classical one. Because of this, even if a potential is localized far away from a particle, when the particle propagates there will be paths that enter the support of the potential, hence affecting propagation. Notice again that the strength of this effect depends again on the size of $\hbar$. As $\hbar \to 0$ the weight factor $e^{\frac{i}{\hbar}S}$ oscillates very quickly as S increases. As a consequence, contributions from different paths cancel each other. The exception is the classical path, as it is a stationary point of the action. In this regard, $\hbar$ acts like temperature in statistical mechanics; indeed, because of the Boltzmann weight $\exp(-E/k_BT)$, when the temperature goes to zero the only configurations

that contribute are those with the minimal energy. Increasing the temperature allows additional configurations to become more accessible to the system. We shall see in chapter two how explicit this analogy can be.

We end this chapter by mentioning that path-integrals are one of the main tools shared between quantum mechanics and classical statistical mechanics. In its field version, it can be used to either model the most fundamental particles and interactions known today [16, 17], i.e., the Standard Model, to also explore the universal properties of phase transitions [18]. Their application is not only limited to the realm of physics, but they also are a strong element in the tool kit of researchers studying stochastic processes [19, 2] and, by extension, stock markets [15, 20]. As such, path-integrals can be seen as one of the hallmarks of bridges between fields that we explore, with a reduced scope, in this thesis. It is no surprise, then, that our first bridge between quantum and classical problems will employ them at full force.

CHAPTER 2
DIRECTED POLYMERS

Since its introduction by Wiener [21] in 1921, and further employment in physics by Dirac [22] in 1933 and Feynman [23] in 1948, path integral methods have proven to be extremely powerful tools to the development of not only quantum mechanics and quantum field theory but also in the modeling of many other physical phenomena, specially in statistical mechanics. One setting in which the use of path-integrals appears natural is the statistical modeling of polymers and systems of polymers.

As polymers are long flexible molecules composed of many repeating units, time-sliced path-integrals are well suited to described the contribution from each individual link in the chain. From free chain models to more realistic models with angular rigidity and self-avoidance, these problems can be stated in terms of paths integrals in the continuum limit, yielding in this way results such as end-to-end distributions and the thermodynamics of the molecule. For more details in these topics, see Ref. [15].

In this chapter, we focus in the study of the equilibrium statistical mechanics of the conformations of systems of many, directed, strongly repelling polymers. By the term directed polymers we understand polymers that have been put under tension along a preferred direction, making them acquire a stretched-string like shape. As a result of this tension, the energy cost associated to each possible configuration of the polymer is proportional to its total length and, therefore, shorter configurations are energetically preferred.

The study of such a system has two main difficulties, the first being that in order to compute the partition function of the system one needs to sum over all possible shapes of

the polymer. This difficulty is solved by using path-integrals. The second issue is the strong repulsion between the polymers, which makes the use of perturbative techniques inappropriate, and thus, leaves us in the need of a smart trick.

This trick came through the hand of de Gennes [4], who realized that, under certain approximations to be specified out later, the equilibrium statistical mechanics of a two-dimensional system of strongly repelling polymers could be mapped to the quantum dynamics, in imaginary time, of a system of free fermionic particles moving in one dimension. In this setting, the role of repulsion is taken over by the Pauli Exclusion Principle, thus reducing the problem to the solution of the Schrödinger equation for non-interacting particles in imaginary time. This idea was later extended in order to answer more elaborate questions such as the influence of topological obstacles [24], general polymer interactions [25], three-dimensional systems [26] and polymers on a lattice with bending rigidity [27].

All of these extensions considered flat systems directed over one preferred Cartesian direction. Even though this is a good approximation in many settings, the question of how different geometries could affect the problem has not been yet addressed. For example, we know that one natural physical realization of these systems happens at the cellular level, where the pericellular coat of certain cellular membranes acts as the polymer fluid. In this system, polymers are not anchored to a flat surface bur rather to a curved one. How does this special configuration affect the previous results? Among the same lines, one could also ask: What happens in systems in which the polymers are put under tension over a curved surface? How does the extrinsic and intrinsic curvature of such surface affects the statistical mechanics of the system? In a more general sense, how far can we push this analogy between polymers and quantum mechanics? These are the kind of questions that we address in this work [5] .

This chapter is structured as follows: In the next section we provide a detailed de-

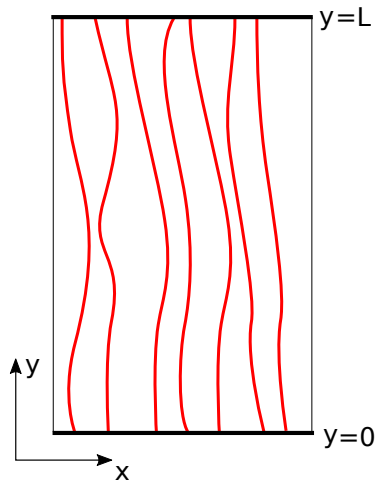

Figure 2.1: Depiction of a two-dimensional directed polymer system: Many polymers put under tension between two parallel lines and allowed to thermally fluctuate in the plane. The strong repulsion between polymers forbids crossing configurations

scription of the problems of interest and our proposed extensions. Afterward, we provide a review of the main ideas and techniques behind the quantum analogy devised by de Gennes [4] and employed by Rocklin et al [24]. We then analyze in detail the approximations and conditions assumed by the quantum analogy. In the final three sections, we present our results of polymers in non-trivial geometries: first polymers anchored to curved edges, then geometric effects due to finite polymer chains and finally, polymers stretched over curved surfaces.

2.1 Generalized systems of directed polymers

As mentioned previously, we focus in systems composed of a large number of spatially confined directed polymers, whose typical configuration is depicted in Figure 2.1.

First, consider polymers such as the ones sketched in Figure 2.1, that is to say, two-dimensional polymers with unstretched length L, confined to a sub-region of width w of the plane, and directed along the Cartesian y axis by a tension A. Furthermore, we consider systems in thermal equilibrium with a heat bath of temperature T. The kinetic energy of the

polymers, quadratic in the instantaneous velocities of each link, contributes a trivial factor to the partition function, and we shall therefore restrict our attention to the, non trivial, configurational partition function.

Now, call $\{X_i\}$ and $\{X_f\}$ the positions of the polymers at the ends of the system. We call the lower end initial and the upper end final. Then, given that all polymers are under the same tension A, the energy of a particular configuration of the system described by polymers shapes $\{x_i(y)\}_{i=1}^{N}$ is given by

$$U\left[\{x_n(\cdot)\}_{n=1}^{N}\right] = \sum_{i=1}^{N} A \int_0^L dy \sqrt{1+\left(\frac{dx_n}{dy}\right)^2}, \tag{2.1}$$

and therefore the configuration has a Boltzmann weight proportional to

$$\exp\left(-\beta U\left[\{x_n(\cdot)\}_{n=1}^{N}\right]\right), \tag{2.2}$$

where, as usual, $\beta \equiv 1/k_B T$. As we see, the Boltzmann weight of each configuration is a functional of the paths that each polymer describes. Therefore, to compute the partition function of the system, Z, which sums these Boltzmann weights over all possible configurations, we must use functional integration (i.e., path-integrals); thus we have

$$Z\left[X_i, X_f\right] \propto \int \prod_{n=1}^{N} [dx_n] \exp\left(-\beta U\left[\{x_n(\cdot)\}_{n=1}^{N}\right]\right). \tag{2.3}$$

Up to this point, we have only discussed how the tension of the polymers gets into the picture but we have not discussed how the interactions between polymers are included. We are considering the polymers to be strongly repelling, so that configurations in which these polymers touch are essentially prohibited, and we must just omit them from the path-integral. Therefore, the functional integration in Eq. (2.3) only considers paths that do not touch each other. We will discuss how to perform this task further below.

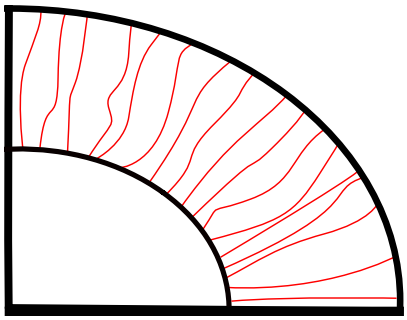

Figure 2.2: Polymers anchored to a curved substrate: Both end of the polymers are attached to elliptic-like substrates.

In this work, we study the following two extensions to the directed polymer problem:

2.1.1 Polymers anchored to curved substrates

As discussed previously in the introduction, one natural realization of our polymer system happens at the pericellular coats of cells. In this setting the system does not look like it does in Figure 2.1, but rather looks like it does in Figure 2.2. It is reasonable to ask then how does this change in geometry affects the free energy and other statistical functions of the system.

In order to solve this question we first, as a warm up, generalize the polymer system to be anchored to concentric circles and being radially directed. In order to do this change, we need to write the functional integral in more appropriate coordinates, namely, polar coordinates. This change, as reported in Ref. [15] can be tricky, and we will have to pay attention to how we perform the time-slicing of the integral as well as to which approximation we are considering.

After this we generalize the system to general convex closed surfaces that differ slightly from a circle such as an ellipse with small eccentricity.

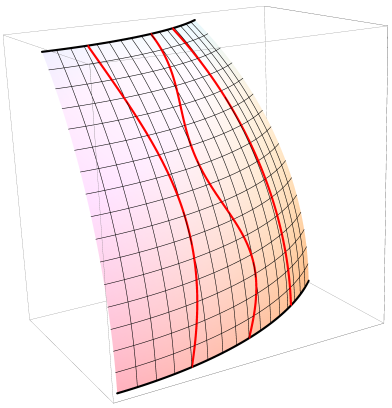

Figure 2.3: Polymers put over tension over a curved surface

2.1.2 Polymers constrained to curved surfaces

Since in the previous extension we consider describing polymers in curvilinear coordinates and in more complicated geometries, it is only natural to want to formulate the problem in a non-flat metric, i.e. to include curvature into the discussion. One natural way in which one could see this being relevant physically is to put polymers under tension over the surface of convex surfaces, such as a sphere or a cylinder. This situation is depicted in Figure 2.3.

The main question is how does this affect the free energy of the system. Does only intrinsic curvature has an effect, or can also extrinsic curvature have a role to play?

In the next section, we review the main tools used to tackle the directed polymer problem and their strong repulsive interaction.

2.2 The quantum analogy

The statistical problem of directed lines is not easy to tackle. The strong repulsion between polymers make a direct computation attempt non-viable, and thus an indirect approach is needed. This approach consist into mapping the problem into a quantum mechanical one. There are various difficulties that must be overcome in order to achieve this feat. In this section we thoroughly review these difficulties, as well as the techniques used to surpass them (see Refs. [4, 24, 26]).

The first difficulty that arises is the form of the energy cost per polymer configuration given by Eq. (2.1); the term $\sqrt{1+\left(\frac{dx}{dy}\right)^2}$ is not an easy term to work with, especially with path-integrals. When computing these kind of mathematical objects we would like to always deal with Gaussian integrals, and therefore, quadratic terms in the action. It is with this in mind that we proceed to use the so-called harmonic approximation, or small fluctuations approximation, in which

$$\sqrt{1+\left(\frac{dx}{dt}\right)^2} \approx 1+\frac{1}{2}\left(\frac{dx}{dt}\right)^2. \tag{2.4}$$

With this approximation we are saying that fluctuations and deviations from the preferred straight direction are small. Obviously this approximation requires some conditions to be satisfied by the tension, the temperature and the density of polymers. The details associated to this approximation will be discussed further ahead.

Note that the first term, 1, in the right side of Eq. (2.4) is the same for all polymers and all polymers configuration and as such it is equivalent to a global shift in the free energy. Therefore, we just ignore it. Then we can rewrite the partition function of a polymer system with fixed initial and final configurations, given by Eq. (2.3), as:

$$Z\left[X_i, X_f\right] \propto \int \prod_{j=1}^{N} \left[dx_j\right] \exp\left(-\beta A \sum_{k=1}^{N} \int_0^L dy \left(\frac{dx_k}{dy}\right)^2\right). \tag{2.5}$$

Now, we can loosen the condition of having exact initial and final configurations on the polymers ends and replace it with *a priori* probability distributions $\Psi_i(X_i)$ and $\Psi_f(X_f)$ for the initial and final ends of the polymers respectively. By doing so, now our partition function reads

$$Z\left[\Psi_i,\Psi_f\right] \propto \int\int dX_i dX_f \Psi_f(X_f) \int \prod_{j=1}^{N} [dx_j] \exp\left(-\beta A \sum_{k=1}^{N} \int_0^L dy \left(\frac{dx_k}{dy}\right)^2\right) \Psi_i(X_i). \tag{2.6}$$

This last expression is extremely suggestive of a link between our two dimensional problem and a one-dimensional quantum mechanical problem. First, notice that in this expression, the path-integral between the two probability distributions is the propagator in imaginary time (just replace $\beta \to \hbar$ and $y \to it$). Therefore we can rewrite

$$\int \prod_{j=1}^{N} [dx_j] \exp\left(-\beta A \sum_{k=1}^{N} \int_0^L dy \left(\frac{dx_k}{dy}\right)^2\right) = \langle X_f | \, e^{-L\beta \hat{H}} \, |X_i\rangle \,, \tag{2.7}$$

where $\hat{H}$ is the many-body quantum Hamiltonian:

$$\hat{H} = \sum_{i=1}^{N} \frac{\hat{p_i}^2}{2A}. \tag{2.8}$$

On the other hand, using bra-ket notation, we can rewrite the probability distributions as $\Psi_i(X_i) = \langle X_i|\Psi_i\rangle$ and $\Psi_f(X_f) = \langle \Psi_f|X_f\rangle$. Replacing these expressions in Eq. (2.6) and integrating over the final and initial configurations we conclude that:

$$Z\left[\Psi_i,\Psi_f\right] \propto \langle \Psi_f | \, e^{-L\beta \hat{H}} \, |\Psi_i\rangle \,. \tag{2.9}$$

That is, the computation of the partition function is equivalent to the computation of the matrix element between the initial and final probability distributions of the imaginary time evolution operator.

It is important to notice then that, in this analogy, $|\Psi_i\rangle$ and $|\Psi_f\rangle$ are not wave functions in the usual way. Indeed, rather that being probability amplitudes, they are probability densities. As such, they are positive and integrate to unity. Moreover, since the polymers dont cross, in principle these functions are only defined in the domain $x_1 < x_2 < x_3 \ldots < x_N$.

In order to extend them to the entire N-dimensional domain and preserving their positivity, we impose that these wavefunctions remain the same when the position of two particles are exchanged. In other words, the statistics of the particles described by these functions is bosonic. However, we must keep in mind that these polymers are actually interacting in such a way that they don't touch. In quantum mechanical language, this means that the probability of having two particles at the same position is zero, and thus we are dealing with hardcore bosons, which are known to behave in the same way as free fermions. The mapping between the fermionic wavefunctions and the bosonic ones is given by: $\Psi_B(X) = \prod_{i<j} \text{sign}(x_j - x_i)\Psi_F(X)$ [28].

Therefore, the polymers are effectively mapped to free fermions in one Dimension. In order to compute the matrix element in Eq. (2.9) it is useful to take advantage of this and use the spectral decomposition of $\exp(-\beta L\hat{H})$:

$$e^{-\beta L\hat{H}} = \sum_{n=1}^{\infty} |\phi_n\rangle e^{-\beta L E_n} \langle\phi_n|, \tag{2.10}$$

where $|\phi_n\rangle$ and E_n are the orthonormal eigenstates and corresponding eigenvalues of $\hat{H}$. Now, notice that, unlike regular quantum mechanics, the time evolution operator is not unitary, but it rather has an exponential decaying behavior. This leads to an useful approximation known as groundstate dominance; As L increases, only the lowest energy states will make a significant contribution in this decomposition, that is, the groundstate dominates this expression. Therefore, for L large enough, we can approximate the last expression and write:

$$e^{-\beta L\hat{H}} \approx |\phi_{gs}\rangle e^{-\beta L E_g s} \langle\phi_{gs}|, \tag{2.11}$$

where $|\phi_{gs}\rangle$ denotes the many particle groundstate of the system and E_{gs} its corresponding energy. Since the quantum particles behave like free fermions, this groundstate is build by

filling the lowest energy one particle states until we have used all of our particles. Then we use our mapping to go to the correct bose wavefunction, which in the case of the ground-state, just corresponds to the absolute value of the free fermion wavefunction.

Using Eq. (2.11) we can finally write:

$$Z\left[\Psi_i, \Psi_f\right] \propto e^{-\beta L E_{gs}} \langle \Psi_i | \phi_{gs} \rangle \langle \phi_{gs} | \Psi_i \rangle. \tag{2.12}$$

This implies that in order to find the contribution to the free energy originated in the constraining of the polymers and their repulsion it is enough to compute the groundstate of the analogous quantum mechanic system.

For example, the fact that our polymers are inside a container of width w maps in the quantum analogy in a system of quantum particles inside a box (i.e., hardcore boundary conditions) of width w. We know that the one particle spectrum of such a system is given by $E_n = \frac{n^2\pi^2}{2A\beta^2w^2}$, and thus, for N large, we have that $E_{gs} \approx \frac{N^3\pi^2}{6A\beta^2w^2}$. By using that $F = -\frac{1}{\beta}\log Z$, we conclude then that the contribution to the free energy of the system is given by [24]:

$$F \approx \frac{N^3\pi^2 L}{6A\beta^2w^2}. \tag{2.13}$$

This would probably be a good time to explain under which conditions does the approximation (2.4) holds. In order for this approximation to be justified, we need that the "velocities" of the polymers to be small, i.e., $\left|\frac{dx}{dy}\right| \ll 1$. Following the argument given by de Gennes [4], we need then the associated momentum $p = A\frac{dx}{dy}$ to satisfy $p \ll A$. Given that when the polymers are inserted into the box and they happen to be in a situation of groundstate dominance, the highest occupied state has a momentum of order $\frac{N}{\beta w}$, we can thus conclude that the harmonic approximation is valid under the condition that:

$$\frac{N}{\beta A w} \ll 1, \tag{2.14}$$

that is, a low density or low temperature limit. This argument however is only qualitatively correct since it does not grants us with an appropriate upper bound. In the next section we will revisit this issue by making a direct link with the microscopics of the polymer chain.

At the same time, we can obtain the conditions under which groundstate dominance takes place: since for high N the difference between energy levels in the box is given by $N\pi^2 L/A\beta^2 w^2$, it is clear that groundstate dominance is achieved for length-scales that satisfy:

$$L \gg \frac{w^2 \beta A}{N}. \tag{2.15}$$

Finally, if $O[\{x_n\}]$ is a generic observable that depends on the specific configurations of the polymer system (i.e., a functional of the polymers paths), then the thermal expectation value of such an observable is given by [24]:

$$\begin{aligned}\langle O \rangle =& \frac{1}{Z[\Psi_f, \Psi_i]} \int\int dX_i dX_f \Psi_f(X_f) \int \prod_{j=1}^{N} [dx_j]\, O[\{x_n(y)\}] \\ & \times \exp\left(-\beta A \sum_{k=1}^{N} \int_0^L dy \left(\frac{dx_k}{dy} \right)^2 \right) \Psi_i(X_i).\end{aligned} \tag{2.16}$$

Although not simple in general, this expression simplifies greatly if the observable depends only on the configuration of the system at a particular height, i.e. $O[\{x_n\}] = O[\{x_n(y_0)\}]$.

$$\begin{aligned}\langle O\rangle =&\frac{1}{Z[\Psi_f,\Psi_i]}\int\int\int dX_i dX_f dX_p \Psi_f(X_f)O(X_p)\\ &\times\left[\sum_i\int_{X(y_0)=X_p}\prod_{j=1}^{N}[dx_j]\exp\left(-\beta A\sum_{k=1}^{N}\int_{y_0}^{L}dy\left(\frac{dx_k}{dy}\right)^2\right)\right]\\ &\times\left[\sum_i\int^{X(y_0)=X_p}\prod_{j=1}^{N}[dx_j]\exp\left(-\beta A\sum_{k=1}^{N}\int_{0}^{y_0}dy\left(\frac{dx_k}{dy}\right)^2\right)\right]\Psi_i(X_i),\end{aligned} \tag{2.17}$$

If we assume that $O(X_p)$ can be written as a matrix element over a quantum operator $\hat{O}$, i.e., $O(X_p)=\langle X_p|\hat{O}|X_p\rangle$, then, by means of the quantum analogy we have that:

$$\begin{aligned}\langle O\rangle = \frac{1}{Z[\Psi_f,\Psi_i]}\int\int\int dX_f dX_i dX_p\langle\Psi_f|X_f\rangle\langle X_f|e^{-\beta L\hat{H}}|X_p\rangle\\ \times\langle X_p|\hat{O}|X_p\rangle\langle X_p|e^{-\beta L\hat{H}}|X_i\rangle\langle X_i|\Psi_i\rangle.\end{aligned} \tag{2.18}$$

If we now assume that y_0 is far from both $y=0$ and $y=L$, then groundstate dominance is valid for both the propagator going from $y=0$ to $y=y_0$ and the propagator going from $y=y_0$ to $y=L$. Then, we can approximate Eq. (2.18) as:

$$\langle O\rangle = \langle\phi_{\text{g.s.}}|\hat{O}|\phi_{\text{g.s.}}\rangle, \tag{2.19}$$

in where the dependence of the numerator of Eq. (2.18) in Ψ_f, Ψ_i and $E_{\text{g.s.}}$ get canceled with the partition function in the denominator. In other words, if groundstate dominance is applicable, the thermal expectation value of an observable corresponds to the expectation value of its analogous quantum operator taken with respect to the groundstate.

A particular example of an observable such as the ones describe above is the polymer density profile, $\rho(x)$, at $y=y_0$, which is given by:

$$\rho[\{x_n(y)\}] = \sum_{i=1}^{N} \delta(x - x_i(y_0)). \tag{2.20}$$

Applying Eq. (2.19) to this operator yields that

$$\langle \rho(x) \rangle = N \int dx_2\, dx_3 \ldots dx_N |\langle \phi_{\text{g.s.}} | x, x_2, x_3, \ldots, x_N \rangle|^2. \tag{2.21}$$

Therefore, we see that the polymer density profile equals the single-particle density of quantum mechanics evaluated in the groundstate. Therefore, as we go forward into the next section, we take notice that, under groundstate dominance, i) the free energy of the system depends only on the energy of the groundstate, while ii) the density profile depends entirely on the groundstate itself.

Finally, we end this section by mentioning that, although this treatment has been presented as being pertinent to polymer systems, as indicated in Ref. [24] they can also be applied to other statistical mechanical problems involving line-like degrees of freedom in two dimensions. Examples of such systems are step edges on crystals surfaces [29], vortex lines in planar type-II superconductors [30] and growing interfaces in the Kardar-Parisi-Zhang universality class [31].

2.3 General remarks

As we mentioned in the introduction, a good portion of this thesis focuses on using path-integrals in curvilinear coordinates to model directed polymers systems in more general setups that the ones described in the previous section. In order to do that, we need to pay attention to certain details that previously did not demand too much attention; in particular, the time slicing of the path-integral and how the harmonic approximation affects it, should be discussed thoroughly. This is also justified by the microscopic nature of the polymers. Describing them as continuous paths, appropriate in mesoscopic and macro scales, is just

the continuum limit of their real behavior, which is discrete. Therefore, there must be a good explanation in this length-scale that justifies the use of the harmonic approximation.

So, just as in Ref. [26], we start by considering a polymer as a long chain of $M-1$ links with typical length of order ϵ. This is a microscopic length-scale, and therefore, much smaller than any other length in the system. As the polymers are under tension, we assume that these links can be stretched and deflected, but always in the preferred direction of the system. The energy of each link is given then by: $A\sqrt{(y_n+y_{n+1})^2+(x_n-x_{n+1})^2}$, where (x_{n-1},y_{n-1}) and (x_n,y_n) are the Cartesian coordinates of the link's initial and final ends. We also assume that the preferred direction is along the y axis and that increments in this direction always have the same length: ϵ, that is, the minimum length for each polymer link is ϵ. This provides each link with an energy cost of $A\epsilon\sqrt{1+\frac{(x_n-x_{n+1})^2}{\epsilon^2}}$ and the partition function of a single chain is obtained by considering all possible values of the intermediate coordinates $\{x_n\}_{n=2}^{M-1}$

$$Z \propto \int \prod_{i=2}^{M-1} dx_i \exp\left(-\beta A \sum_{k=2}^{M} \epsilon\sqrt{1+\frac{(x_n-x_{n-1})^2}{\epsilon^2}}\right). \tag{2.22}$$

The proportionality constant counts how many possible values of the lateral coordinates x are accessible to the system per unit length per link. Notice that this last expression has now started to look like a time sliced path-integral in configuration space, although it is not quite there yet. Since we want to take the harmonic approximation, in which the links' length satisfy Gaussian distributions, we normalize each distribution. So, we rewrite

$$Z \propto \left(\sqrt{\frac{2\pi\epsilon}{\beta A}}\right)^{M-1}\left(\sqrt{\frac{\beta A}{2\pi\epsilon}}\right)^{M-1}\int \prod_{i=2}^{M-1} dx_i \exp\left(-\beta A \sum_{k=2}^{M} \epsilon\sqrt{1+\frac{(x_n-x_{n-1})^2}{\epsilon^2}}\right). \tag{2.23}$$

The first added factor, in the harmonic approximation, yields the expected $MkT/2$ contribution to the energy from the equipartition theorem, and thus it just describes the underlying

microscopic physics. Since we just care about the variations in the free energy originated in the polymer-polymer interaction and their constraining, phenomena that happen at macro length-scales, we don't care about this factor, so we write

$$Z \propto \left(\sqrt{\frac{\beta A}{2\pi\epsilon}}\right)^{M-1} \int \prod_{i=2}^{M-1} dx_i \exp\left(-\beta A \sum_{k=2}^{M} \epsilon \sqrt{1+\frac{(x_n - x_{n-1})^2}{\epsilon^2}}\right). \tag{2.24}$$

From this time-slicing we can then see what the harmonic approximation means physically; it imposes conditions on the temperature and tension such that the thermal fluctuations from the optimal path, i.e. $(x_n - x_{n+1})^2$, are small with respect to ϵ and therefore $\sqrt{1+\frac{(x_n-x_{n+1})^2}{\epsilon^2}} \approx 1 + \frac{1}{2}\frac{(x_n-x_{n+1})^2}{\epsilon^2}$. Which is this condition? To obtain it, it is enough to consider just one link and realize that, under the Gaussian distribution, $\langle((x_n - x_{n+1})/\epsilon)^2\rangle \sim 1/(\beta A\epsilon)$, we require that: $A\beta \gg \epsilon^{-1}$. Thus at its heart, the small fluctuation approximation keeps terms of order $(\delta x)^2/\epsilon^2$ and neglects terms of order $(\delta x)^4/\epsilon^4$ (and eventual terms of order $(\delta x)^3/\epsilon^3$). This amounts to ignore contributions to the energy smaller or equal to $1/(\beta A\epsilon)^2$.

After doing this approximation we finally obtain

$$Z \propto \left(\sqrt{\frac{\beta A}{2\pi\epsilon}}\right)^{M-1} \int \prod_{i=2}^{M-1} dx_i \exp\left(-\beta A \sum_{k=2}^{M} \frac{(x_n - x_{n-1})^2}{2\epsilon}\right), \tag{2.25}$$

which is the time-sliced version of the Feynman path-integral in Euclidean configuration space. This successfully connects the polymers' discrete model with the continuum limit that we considered in the previous sections.

Although by working in this way it may seem that we have completely decouple the long length-scale behavior of the polymers from the microscopic one, this is not quite the case. Indeed, ϵ continues to play an important role, even after taking the continuum

limit. For example, as noticed in Ref. [26], the mean average slope of the polymer depends explicitly on ϵ. Indeed, recall from Eq. (2.6) that:

$$\left\langle \left(\frac{dx}{dt}\right)^2 \right\rangle = -\frac{2}{\beta NL}\partial_A Z. \tag{2.26}$$

An explicit computation leads then to the result:

$$\left\langle \left(\frac{dx}{dt}\right)^2 \right\rangle = \frac{1}{A\beta\epsilon} - \frac{\pi^2}{3}\left(\frac{N}{\beta A w}\right)^2. \tag{2.27}$$

The first term in this expression corresponds to the thermal average fluctuation for a single link, and, as we can see, depends explicitly on the value of ϵ. The second term on the right the corresponds to the corrections originated in the polymer-polymer repulsion. They effectively reduce the typical size of a fluctuation resulting in a smaller average slope. More importantly, we should notice two things: The first is that, since we require the average slope to be small, we need to have $\beta A\epsilon \gg 1$. Thus, de Gennes condition for small fluctuations, $N/(\beta A w) \ll 1$, is not enough. We can not ignore the microscopic scale in this aspect. Because of this, we also conclude that we cannot simply take the limit $\epsilon \to 0$ and therefore, the continuum limit requires more care.

The second thing that we should notice is that for sufficiently dense polymer systems, the average square of the polymer slope, Eq. (2.27), becomes negative, indicating a breaking point of the model. Specifically, this is because the continuum limit is not a good approximation of the system at those densities. Indeed, notice that at the densities that would cause a breakdown we have that the: $w/N \sim \frac{e}{(\beta A w)^{1/2}}$, i.e., we would have that the distance between polymers is comparable to a thermal lateral fluctuation. However, in order for the continuum limit to be a good approximation we require that the wavefunction varies slowly compared to the microscopic length-scales. Since the wavefunction vanishes at points in which two polymers intersect, the typical distance over which the wavefunc-

tion change is the average polymer-polymer distance: w/N. On the other hand, the typical microscopic lateral displacement of a polymer is given by: $\epsilon/(\beta A\epsilon)^{1/2}$. Thus, we require the condition:

$$\frac{\epsilon}{(\beta A\epsilon)^{1/2}}\frac{N}{w} \ll 1, \tag{2.28}$$

which can be rewritten as:

$$\frac{N}{\beta A w} \ll \frac{1}{(\beta A\epsilon)^{1/2}}, \tag{2.29}$$

which essentially is de Gennes' small fluctuations condition, but with an appropriate upper bound given in terms of the microscopic parameters of the system. Moreover, this condition tells us that the model is only accurate when the polymer-polymer distance is considerably bigger than a typical thermal fluctuation. With this condition, the breakdown anticipated by Eq. (2.27) cannot happen.

2.4 Radially directed polymers anchored to a circle

As a first step in solving the problem depicted in Figure 2.2, we consider our polymers to be anchored to a circular substrate and being radially directed. This simplification allows us to obtain a procedure that can be easily generalized to more complex and less symmetrical substrate shapes.

In this situation, Cartesian coordinates do not offer a good description of the system and it is much more natural to use polar coordinates (r, θ). This choice also allows to easily state the polymers' property of being radially directed: polymers (and its constituent links) should always advance in a direction in which r grows, or, said in a more mathematical precise sense, the associated shape of the polymer should be a curve of the form $\theta(r)$. Therefore, r takes the role of y as a parameter (and therefore the role of time in the quantum

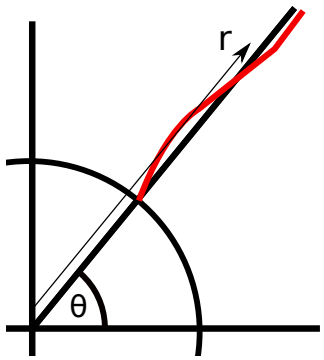

Figure 2.4: Depiction of a polymer anchored to a circular substrate and radially directed. The shape of the possible polymer configurations is described using polar coordinates; each configuration is described by a path $\theta(r)$. Hence, in the quantum analogy, the role of the particle's coordinate is taken by the polar angle and the role of time by the radial distance to the circle.

analogy) and θ replaces the lateral displacements x. See Figure 2.4. Since polar coordinates are orthogonal this change does not affect the situation of a polymer locally. In other words, in a small neighborhood around it, a polymer link does not see the circular geometry behind it. This allows to generalize the polymers' partition function. Finally, polar coordinates are also advantageous because, although when r grows the space available for each polymer also grows, we can easily limit its movement by introducing a constant constraint in θ. This will be very useful at the moment of writing our quantum analogy for this system.

In a more technical comment, while doing the slicing of the path-integral we should consider each link to be a straight line (so we still have flat space). Although this could have unphysical configurations in which a link enters inside of the circle at which its anchored, we can realize that such configurations require a critical deviation in θ of order $\delta\theta_c \sim (\epsilon/R)^{1/2}$, when R is the radius of the substrate. The lateral fluctuation associated with this angle is then: $R\delta\theta_c/\epsilon \sim (R/\epsilon)^{1/2}$. Thus, as $\epsilon/R \to 0$, we see that this problematic configurations require enormous fluctuations and thus negligible statistical weights. Because of this, and in order to also have a good approximation to the continuum, we consider the ratio ϵ/R as the smallest quantities in our system. This is consistent with

considering ϵ as a microscopic length-scale associated with the molecular structure of the polymer and R as a mesoscopic or macroscopic one.

2.4.1 Time-slicing in curvilinear coordinates

Now we explicitly rewrite the individual link length in polar coordinates. For convenience, from now on we incorporate the β factor inside the path's integral "action". To explicitly introduce polar coordinates, notice that the length of one link can be rewritten as:

$$\beta A\sqrt{(y_n+y_{n+1})^2+(x_n-x_{n+1})^2}=\beta A\sqrt{(r_n-r_{n-1})^2+2r_nr_{n-1}(1-\cos(\theta_n-\theta_{n-1}))}. \tag{2.30}$$

Now, we use that $r_n - r_{n-1} = \epsilon$ and the approximation of small deflections to expand $1-\cos(\theta_n-\theta_{n-1})$ in power series

$$\sqrt{(r_n-r_{n-1})^2+2r_nr_{n-1}(1-\cos(\theta_n-\theta_{n-1}))}=\epsilon\sqrt{1+2\frac{r_nr_{n-1}}{\epsilon^2}\left(\frac{\delta_n^2}{2}-\frac{\delta_n^4}{4!}+O(\delta_n^6)\right)}, \tag{2.31}$$

where we have defined $\delta_n \equiv \theta_n - \theta_{n-1}$.

Now, if we were computing the path-integral of a quantum particle in two-dimensions, as recalled in Ref. [15], we would need to be extremely careful with this expansion. In such case we would need to perform integrations not only in θ but also in r and therefore an expansion such as this one is much more harder to justify. Moreover it is not enough to expand only up to second order, since quartic terms can be integrated and reintroduced into the action as contributions of order ϵ. This is one of the main difficulties that arise when trying to use curvilinear coordinates in path-integrals, and it is a topic that has been extensively studied (for a thorough review on the subject, see Ref. [15]). However, this

step ignores the presence of quartic terms in the velocity, which do not happen in quantum mechanics, that arise due to the expansion of the square root. Because of this, in our case, we also need to consider the harmonic approximation; notice that if we expand the square root in powers of δ_n we would obtain:

$$\sqrt{1+2\frac{r_n r_{n-1}}{\epsilon^2}\left(\frac{\delta_n^2}{2}-\frac{\delta_n^4}{4!}+O(\delta_n^6)\right)} \approx 1+\frac{r_n r_{n-1}}{2\epsilon^2}\delta_n^2-\left(\frac{r_n r_{n-1}\delta_n^4}{4!\epsilon^2}+\frac{(r_n r_{n-1})^2\delta_n^4}{8\epsilon^4}\right). \tag{2.32}$$

Pay attention to the quartic terms on the right: On the one hand, the second term, $t_2 = (r_n r_{n-1})^2\delta_n^4/\epsilon^4$ is the term that appeared in the previous section when expanding the square root, and therefore it is the kind of term that we neglect in the harmonic approximation. On the other hand, the first term, $t_1 = (r_n r_{n-1})\delta_n^4/\epsilon^2$, only appears because we are using curvilinear coordinates. It is precisely this term that we should normally have to pay attention to. But, if we compare these two terms we would see that: $t_1/t_2 = \epsilon^2/(r_n r_{n-1})^2 \ll 1$. Therefore, the term that arises as a consequence of the use of curvilinear coordinates is much smaller than the terms we were already neglecting in the harmonic approximation. As such, in our present model, we can just ignore all the quartic terms and write the action of one chain with $M-1$ links as

$$\beta A\sum_{k=2}^{M}\frac{r_k r_{k-1}}{2\epsilon}(\theta_k-\theta_{k-1})^2. \tag{2.33}$$

Soon we will also see that the factor $r_n r_{n-1}$ can be replaced by r_n^2, since the difference between the two is negligible in the continuum limit, approximation that we will take at the end.

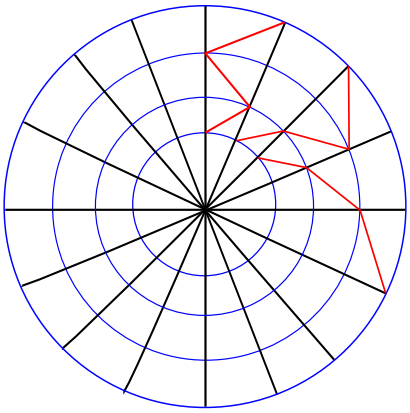

Figure 2.5: Depiction of the cumulative loss of precision produced by the use of a constant angular density in the functional measure. Here, the allowed set of values for θ are depicted by the radially directed black lines, while the blue circles denote equal-time curves. As the radial distance increases, the polymer links, depicted in red, are forced to make abrupt deflections, without being able to explore the neighborhood of its current location

2.4.2 The functional measure

In order to add up over all possible paths, we need to integrate over the intermediate θ_i variables. While doing so, we should be careful to maintain a constant degree of accuracy. The process of integrating over this continuous variable can be seen as the continuous limit of summing over a discrete array of θ values accessible to the polymer link. Therefore, in order to go from the sum to the integral, we should include in the integrand the density of allowed points. In the usual directed polymer problem, the density of points is kept constant as the polymer goes forward. In our present case though, this would yield and ever increasing lack of precision. Indeed, lets think in discrete terms and let the polymer link access a finite array of angles $\{\theta_n\}_n$. Then, as the radial distance grows, the actual distance in the xy-plane between the points associated with these set of angles is constantly increasing. This situation is depicted in Figure 2.5. In other words, as r increases the polymer can no longer visit the neighborhood of its previous point. In order to fix this, we must therefore increase the number of available angles for the polymer. In the continuum, this is equivalent to increase the density of points.

In order to achieve an unbiased way to perform this increase, we impose a constant density of points over the arclength. In other words, we distribute our points at equal distance from each other. In this way, the density of points in the θ variable scales as $\rho_\theta \to r\rho_\theta$. This leads then to the measure $rd\theta$.

A different way to see this is that, locally, the polymers just see a preferred direction and an orthogonal lateral one. To consider all possible values of this lateral direction we integrated the "action" over this variables x_i. To change this to polar coordinates we just need to remember then that locally: $dx_i = rd\theta_i$. With this in mind we can write the sliced version of the path-integral of the system

$$Z \propto \left(\sqrt{\frac{\beta A}{2\pi\epsilon}}\right)^{M-1} \int \prod_{i=2}^{M-1} r_i d\theta_i \exp\left(-\beta A \sum_{k=2}^{M} \frac{r_k r_{k-1}(\theta_k - \theta_{k-1})^2}{2\epsilon}\right), \tag{2.34}$$

The same procedure can then be done for more general situations. Lets suppose that we are using generalized coordinates $(\tilde{t}, \tilde{x})$ to describe our system. Then, for each value of $\tilde{t}$ we have an equal-time curve, $\boldsymbol{r}_{\tilde{t}}(\tilde{x})$, which is parametrized using $\tilde{x}$ as parameter. Associated to this curve is the arclength parameter $s_{\tilde{t}}(\tilde{x})$. In order to keep the slicing precision constant, we impose a constant density of points in the arclength variable. Again, this amounts to dividing the curve in points distributed at equal distances. This leads then to the following measure of integration

$$ds_{\tilde{t}} = d\tilde{x}\frac{ds_{\tilde{t}}}{d\tilde{x}}. \tag{2.35}$$

Equation (2.35) can then be used to tackle more complicated extensions of the problem.

2.4.3 Establishing the quantum analogy

Having tackled the time-slicing and change of measure, we are in good shape to find the analogous quantum system to our problem. First, notice that Eq. (2.34) can be rewritten as:

$$Z \propto \frac{1}{\sqrt{r_M r_1}} \sqrt{\frac{r_M r_{M-1}\beta A}{2\pi\epsilon}} \int \prod_{i=2}^{M-1} d\theta_i \sqrt{\frac{r_i r_{i-1}\beta A}{2\pi\epsilon}} \exp\left(-\beta A \sum_{k=2}^{M} \frac{r_k r_{k-1}(\theta_k - \theta_{k-1})^2}{2\epsilon}\right). \tag{2.36}$$

To obtain this expression we have redistributed the r_n terms between the different integrals and also introduced the first and final values of the parameter r. We will pay attention to the $(r_M r_1)^{-1/2}$ prefactor later. For the moment, notice that we can use the identity

$$\sqrt{\frac{r_i r_{i-1}\beta A}{2\pi\epsilon}} \exp\left(-\beta A \frac{r_i r_{i-1}(\theta_i - \theta_{i-1})^2}{2\epsilon}\right) = \int \frac{dp_i}{2\pi} \exp\left(-\epsilon \frac{p_i^2}{2\beta r_i r_{i-1}} - i p_i(\theta_i - \theta_{i-1})\right), \tag{2.37}$$

to rewrite the partition function as:

$$Z \propto \frac{1}{\sqrt{r_M r_1}} \int \prod_{i=2}^{M-1} d\theta_i \int \prod_{i=2}^{M} \frac{dp_i}{2\pi} e^{\sum_{k=2}^{M}\left[\epsilon \frac{-p_k^2}{2\beta A r_k r_{k-1}} - i p_k(\theta_k - \theta_{k-1})\right]}. \tag{2.38}$$

Now, notice that $\frac{1}{r_k r_{k-1}} = \frac{1}{r_k^2} + O(\epsilon)$, so, as we foretold, up to first order in ϵ:

$$Z \propto \frac{1}{\sqrt{r_M r_1}} \int \prod_{i=2}^{M-1} d\theta_i \int \prod_{i=2}^{M} \frac{dp_i}{2\pi} e^{\sum_{k=2}^{M}\left[\epsilon \frac{-p_k^2}{2\beta A r_k^2} + i p_k(\theta_k - \theta_{k-1})\right]}. \tag{2.39}$$

This means that when we wrote the time-sliced partition function and the length of each link we could have just wrote it as if it was a differential: $ds = \sqrt{\epsilon^2 + r^2 d\theta^2} \approx r(1 + r^2 d\theta^2/2\epsilon^2)$. This is a direct consequence of the small deviations approximation and it is one of the main results that we obtain from this example and we will certainly use it in more complicated scenarios.

Now define quantum operators $\hat{\theta}$ and $\hat{p}_\theta$ that satisfy $[\hat{\theta}, \hat{p}_\theta] = i$. Then, its eigenstates,

$|\theta\rangle$ and $|p\rangle$ satisfy:

$$\langle\theta|p_\theta\rangle = \frac{e^{ip\theta}}{\sqrt{2\pi}}, \tag{2.40}$$

so our partition function can be rewritten as:

$$Z \propto \frac{1}{\sqrt{r_M r_1}} \int \prod_{i=2}^{M-1} d\theta_i \int \prod_{i=2}^{M} dp_i \langle\theta_i| e^{-\epsilon \frac{\hat{p}_\theta^2}{2\beta A r_k^2}} |p_i\rangle\langle p_i|\theta_{i-1}\rangle, \tag{2.41}$$

Integrating over p_i and using completeness we fund then that our partitioned partition function takes the form of a time sliced propagator in imaginary time quantum mechanics

$$Z \propto \frac{1}{\sqrt{r_M r_1}} \int \prod_{i=2}^{M-1} d\theta_i \langle\theta_i| e^{-\epsilon \frac{\hat{p}_\theta^2}{2\beta A r_k^2}} |\theta_{i-1}\rangle, \tag{2.42}$$

Therefore, in the continuum limit we obtain that our partition function would be the propagator in imaginary time of the following quantum Hamiltonian:

$$\hat{H}_\theta(r) = \frac{\hat{p}_\theta^2}{2\beta A r^2}, \tag{2.43}$$

when r is the parameter associated with time: if the polymer starts at a substrate with radius R and finishes at a circle with radius $R + L$, then r goes from R to $R + L$.

As we see from Eq. (2.43), the main difference between the polymer system anchored to the circle and the traditional ones is that the quantum Hamiltonian that describes the system in the continuum limit is now explicitly time-dependent. Although, in general, such time dependance could be a great complication, notice that, in this case, the Hamiltonian commutes with itself at different times, i.e., $[\hat{H}_\theta(r_1), \hat{H}_\theta(r_2)] = 0$. Therefore, the time evolution of the system is simply given by the following operator:

$$\hat{U} = \exp\left(-\int_R^{r_f} dr \hat{H}_\theta(r)\right) = \exp\left(-\frac{1}{2\beta A}\left(\frac{1}{R} - \frac{1}{r_f}\right)\hat{p}_\theta^2\right), \tag{2.44}$$

where r_f is the radial distance of the final ends of the polymers. For the many polymer-system we have then that the analogous time evolution operator is given by:

$$\hat{U} = \exp\left(-\sum_{k=1}^{N} \frac{1}{2\beta A}\left(\frac{1}{R} - \frac{1}{r_f}\right)\hat{p}_{\theta,k}^2\right), \tag{2.45}$$

This is the operator that we need to consider in order to compute the free energy of the system. To start with, note that, since it is hermitian, it has an spectral decomposition in orthonormal states:

$$\hat{U} = \sum_{n} e^{-E_n}|n\rangle\langle n|, \tag{2.46}$$

where E_n are the eigenvalues associated to the eigenstates $|n\rangle$. Recall that these are many-particle eigenvalues and, therefore, they are obtained by taken into consideration the statistics of the system. In our case, just as before, we have fermion-like particles. Then, by assuming groundstate dominance we obtain that:

$$\hat{U} \approx e^{-E_{gs}}|gs\rangle\langle gs|, \tag{2.47}$$

Assuming that the polymers are constrained to an angular sector of spread δ, that is, hard-core boundary conditions at $\theta = 0$ and $\theta = \delta$ (see Figure 2.6), is easy to see that:

$$E_{gs} = \frac{N^3\pi^2}{6\beta A\delta^2}\left(\frac{1}{R} - \frac{1}{r_f}\right), \tag{2.48}$$

which yields the following free energy

$$F = \frac{N^3\pi^2}{6\beta^2 A\delta^2}\left(\frac{1}{R} - \frac{1}{r_f}\right), \tag{2.49}$$

and the following difference between energy levels

$$\delta E = \frac{N\pi^2}{\beta A\delta^2}\left(\frac{1}{R} - \frac{1}{r_f}\right). \tag{2.50}$$

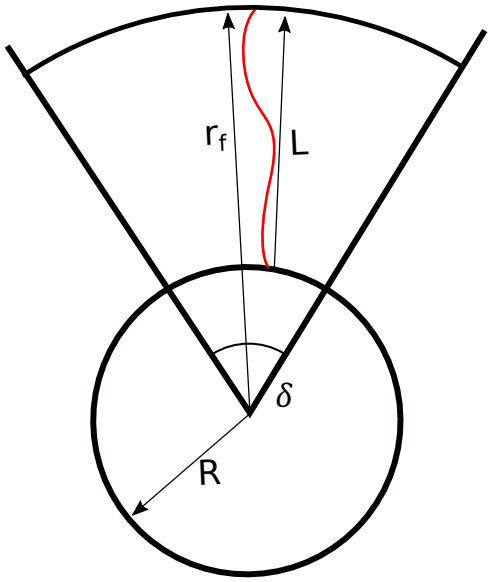

Figure 2.6: Depiction of the boundary conditions for an angular box of size δ. The initial and final radius are R and r_f respectively. Their difference is the natural polymer length L.

This means that as the polymers grow longer we have a saturation process in which the difference between energy levels reaches a constant value (instead of growing to infinity as before). The reason behind this is that as polymers grow they are driven apart and the space available to them increases. This grants the system access to a larger amount of valid configurations. The result is an increment of the entropy, which yields a reduction of the system's free energy. However, under appropriate circumstances groundstate dominance can still be achieved. As we see from Eq. (2.50), in order to have groundstate dominance for $r_f \gg R$ we must have that $\frac{N}{\beta A \delta^2 R} \gg 1$. On the other hand, in order to be able to use the continuum limit, we must bound the initial polymer density: $\frac{N}{\beta A \delta R} \ll \frac{1}{\sqrt{A\beta\epsilon}}$. Combining this two conditions we finally obtain that in order to have groundstate dominance δ must satisfy the following condition

$$\delta \ll \frac{1}{\sqrt{A\beta\epsilon}} \ll 1, \tag{2.51}$$

Therefore our polymers must be constrained to a small sector of the entire circle. If they were not constrained, even though the system would have a finite size, the periodic bound-

ary conditions would make the system similar to an infinite one, situation in which groundstate dominance is no longer valid, even in the simple polymer case (see Eq. (2.15)). Notice that the condition of small δ appears because of groundstate dominance. The continuum limit just bounds the polymer density. Therefore, the small δ is not a phenomenon intrinsic to the model. Therefore, by going beyond groundstate dominance we could, in principle, explore any walled domain, or even the entire circle with periodic boundary conditions. However, such a setup would make the problem extremely dependent on the initial configuration of the system. Since in this problem, polymer that are initially far away from each other trace completely different trajectories, it makes sense for this dependence to be present. Similarly, in order to avoid this dependence, we need to restrict ourselves to sets of polymers that are initially closed to each other.

Our suspicion that polymer repulsion becomes negligible as polymer grow larger can be seen by computing the square of the polymer slope. By using Eq. (2.26), we see that in this case:

$$\left\langle \left(\frac{ds}{dt}\right)^2 \right\rangle = \frac{1}{A\beta\epsilon} - \frac{R}{L}\frac{\pi^2}{3}\left(\frac{N}{\beta AR\delta}\right)^2, \tag{2.52}$$

where we have defined the polymer length $L \equiv r_f - R$. Thus, as the polymer grow much larger than the radius of the circle, $R/L \to 0$, we have that the expected square of the slope goes to $\frac{1}{A\beta\epsilon}$, which is the result for a system of free polymers.

Until now, we have discussed only the regime of long polymers. We can also explore the opposite regime, i.e., short polymers, which we can use to check our results. Indeed, consider $r_F = R + L$ with $L/R \ll 1$. In that case, we can expand Eq. (2.49) in powers of L/R to obtain that:

$$F = \frac{N^3\pi^2}{6\beta^2 A\delta^2 R^2}\left(1 - \frac{L}{R} + O\left(\frac{L}{R}\right)^2\right). \tag{2.53}$$

Thus, by noticing that the width of the system is given by $w = R\delta$, we see that in the limit $L/R \to 0$ we recover the free energy of simple polymers directed in a preferred Cartesian direction (see Eq. (2.13)) plus corrections given by the curvature of the substrate $\kappa = 1/R$. In this case, the conditions for groundstate dominance are the same that in the flat edge polymer problem.

We end this section by commenting the role of the prefactor $(r_f r_i)^{-1/2}$ that appear on the partition function in Eq. (2.42). For fix initial and final angles θ_i and θ_f, the entire expression for the propagator reads

$$Z \propto \frac{1}{\sqrt{r_f}}\langle\theta_f|\hat{U}(r_f, r_i)|\theta_i\rangle\frac{1}{\sqrt{r_i}}. \tag{2.54}$$

Notice then that, since at a given radius the arclength parameter of an equal-time circle is given by $s = r\theta$, we have that

$$\int d\theta|\theta\rangle\langle\theta| = 1, \tag{2.55}$$

which implies

$$\int ds\frac{1}{\sqrt{r}}|\theta(s)\rangle\langle\theta(s)|\frac{1}{\sqrt{r}} = 1 = \int ds|s\rangle\langle s|. \tag{2.56}$$

As such, we see then that:

$$|s\rangle = \frac{1}{\sqrt{r}}|\theta\rangle. \tag{2.57}$$

This can also be verified via

$$\langle s_1|s_2\rangle = \delta(s_2 - s_1) = \frac{1}{r}\delta(\theta_2 - \theta_1) = \frac{1}{r}\langle\theta_1|\theta_2\rangle. \tag{2.58}$$

Using Eq. (2.57) we can then rewrite Eq. (2.54) as:

$$Z \propto \langle s_f|\hat{U}(r_f, r_i)|s_i\rangle. \tag{2.59}$$

Thus, if we have *a priori* probability densities for the initial and final polymer configurations given by $\Psi_i(s_i)$ and $\Psi_f(s_f)$, then the partition function reads:

$$Z \propto \int\int ds_f ds_i \Psi(s_f)\langle s_f|\hat{U}(r_f, r_i)|s_i\rangle\Psi(s_i). \tag{2.60}$$

If we let $\Psi(s) = \langle s|\Psi\rangle$, then we conclude that:

$$Z \propto \langle\Psi_f|\hat{U}(r_f, r_i)|\Psi_i\rangle. \tag{2.61}$$

So, the structure of the partition function is preserved when going to the circle, as long as the initial and final states $|\Psi_i\rangle$ and $|\Psi_f\rangle$ represent probability densities in the arclength variable. Notice that, if this is the case, then this function does not represent a probability density in the θ variable. This feature does not appear in quantum mechanics and is due to the fact that these wavefunctions are not probability amplitudes but rather probability densities. Indeed, notice that:

$$\int ds\langle s|\Psi\rangle = 1, \tag{2.62}$$

implies that:

$$\int d\theta\sqrt{r}\langle\theta|\Psi\rangle = 1. \tag{2.63}$$

As such, we see that the probability density in the θ variable is given by:

$$P(\theta) = \sqrt{r}\langle\theta|\Psi\rangle. \tag{2.64}$$

As a consequence, if we choose $|\tilde{\Psi}\rangle$ to represent the probability density in θ, i.e., $P(\theta) = \langle\theta|\tilde{\Psi}\rangle$,then it is not true that $Z = \langle\tilde{\Psi}_f|\hat{U}|\tilde{\Psi}_i\rangle$. The state that is propagated is not $|\tilde{\Psi}\rangle$ but rather $r^{-1/2}|\tilde{\Psi}\rangle$. This is a direct consequence of the imposed measure in the time-slicing of the path-integral.

As strange as this result may appear, notice that it is consistent: we can then use the expression for $P(\theta)$ to write immediately that:

$$Z \propto \int\int d\theta_f\, d\theta_i\, P(\theta_f) K(\theta_f, r_f; \theta_i, r_i) P(\theta_i), \tag{2.65}$$

where the kernel $K(\theta_f, r_f; \theta_i, r_i)$ tracks the weight of the possible polymer configurations between the initial and final combinations of θ and r, i.e., the sum of paths for this fixed variables. From our previous expression for Z, we see then that this kernel is given by:

$$K(\theta_f, r_f; \theta_i, r_i) = \sqrt{\frac{2\pi\epsilon}{\beta A}} \frac{1}{\sqrt{r_f}} \langle\theta_f|\hat{U}(r_f, r_i)|\theta_i\rangle \frac{1}{\sqrt{r_i}}. \tag{2.66}$$

By using Eqs. (2.66, 2.64) in Eq. (2.65), we recover our previous expression for the partition function.

In the case of the circle, this permutation between the generalized variable and the arclength variable amounts only to a constant, and therefore, we could have just safely ignored it. However, in more complicated situations in which $s(\theta, r) = f(\theta, r)$, for f an arbitrary positive and increasing function of θ, we would have had that:

$$|s\rangle = \frac{1}{\sqrt{\partial_\theta f}}|\theta\rangle. \tag{2.67}$$

Since this modification is position dependent, it has a big impact when deciding which state is being propagated. We conclude then that, in the most general circumstances, the state that gets propagated is the sate that represents the probability density as a function of the arclength. If the system is described in terms of the generalized coordinate θ, one must also include the factor $\frac{1}{\sqrt{\partial_\theta f}}$.

2.5 Polymers anchored to almost-circular substrates

In this section we study polymers that are anchored to substrates that are slightly different from a circle, such as a low eccentricity ellipse. As mentioned before, we expect that the loss of azimuthal symmetry will grant the problem with interesting effects. One of these effects is a qualitative modification of the analogous quantum Hamiltonian: by going back to the circle case and analyzing its Hamiltonian, Eq. (2.43), it is easy to see that it is equivalent to the Hamiltonian of a particle with a time-dependent mass. Once we remove the circular symmetry we can reasonably expect for the mass to no longer depends only on time, but also on the particle's position. This kind of issues is generally difficult to treat in standard quantum mechanics, specially by canonical quantization: inevitably, operator-ordering issues arise. In essence, if we know the classical Hamiltonian, how should the quantized operators be ordered in order to give the correct theory? There are no mathematical prescriptions to favor one special ordering (besides demanding hermiticity), and one can only use phenomenology to choose an specific ordering (see for example Ref. [32]). In our case though, this will not be an issue. The problem arises when one starts with a quantized Hamiltonian, which leads to an appropriate time slice and path-integral. In our case, we start with a time sliced path-integral which we can match to a well ordered Hamiltonian. Moreover, under the small fluctuation approximation differences in operator ordering give rise to terms that yield negligible corrections. This characterizes the small fluctuations approximation as what would be considered a semi-classical approximation in regular quantum mechanics.

In any case, in order to attack this problem we need an appropriate orthogonal coordinate system that matches the necessities of the problem. We consider the situation of polymers attached to curved substrates whose shapes do not differ greatly from a circle. That is, curves that can be parametrized as:

$$(x(\theta), y(\theta)) = R(\cos(\theta) + \alpha f(\theta), \sin(\theta) + \alpha g(\theta)), \tag{2.68}$$

where $\theta : 0 \to 2\pi$, f and g are periodic regular functions with period 2π and α is a dimensionless small parameter that quantifies how different is our substrate from a circle (e.g., in the case of an ellipse, this would be related to the eccentricity) of radius R. It is important to notice that in this case θ is not the polar angle, although it will still serve as a good coordinate for the path-integral.

Now, we demand our polymers to be directed in the direction perpendicular to the substrate at each point. Following the example of the previous section, we define a parameter ρ in such a way that the distance traveled along this direction is given by $\rho - R$. We use this definition in order to have a proper way to compare with the circular problem. Indeed, with this choice we have that $\rho = R$ corresponds to the original substrate.

Mathematically, the coordinate system described above is given by

$$\begin{aligned}(x(\theta,\rho), y(\theta,\rho)) =& R(\cos(\theta) + \alpha f(\theta), \sin(\theta) + \alpha g(\theta)) \\ &+ (\rho - R)\frac{(\cos(\theta) + \alpha g'(\theta), \sin(\theta) - \alpha f'(\theta))}{\sqrt{(\sin(\theta) - \alpha f'(\theta))^2 + (\cos(\theta) + \alpha g'(\theta))^2}},\end{aligned} \tag{2.69}$$

where f' and g' are the derivatives of f and g respectively. See Figure 2.7. Although Eq. (2.69) is explicit, it can hide the true geometrical meaning of our coordinates. We can

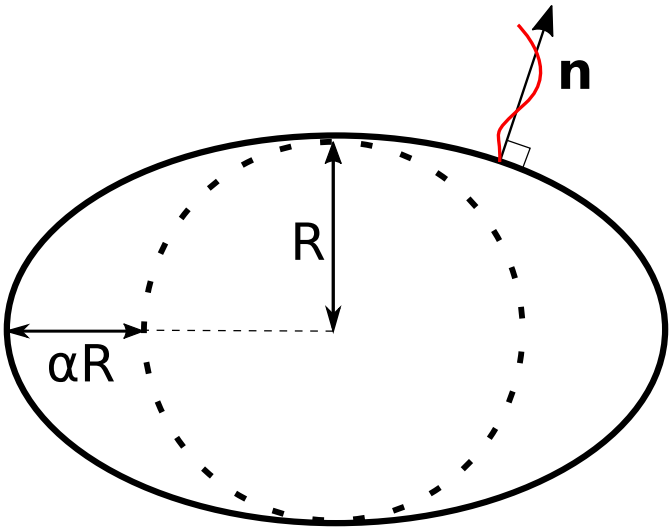

Figure 2.7: Depiction of the generalized coordinate system for non-circular substrates. The shape of the substrate is a deformed circle of radius R, inscribed in the substrate, which is parametrized using a parameter θ. Notice that in this case, this parameter is not the polar angle. The size of the deformation is captured by the a parameter α. Polymers are then directed along the direction normal to the substrate, $\hat{\boldsymbol{n}}(\theta)$. In order to describe the distance traveled by the polymer along this normal, we define the parameter ρ, in terms of which, the previously mentioned distance is given by $\rho - R$. In the quantum analogy, ρ takes the role of time. The coordinate system is set up in such a way that at each different value of ρ we obtain a different "equal-time" convex curve also parametrized by θ. In this coordinates, a curve with a fixed value of θ corresponds to the line perpendicular to the substrate originating from the point specified by θ. The polymers shapes are then described by paths of the form $\theta(\rho)$. The relationship between θ and the polar angle θ_p, is given by $\theta_p(\rho) = \arctan(x(\theta,\rho)/y(\theta,\rho))$.

make this transparent by rewriting this equation as

$$\boldsymbol{r}(\theta,\rho) = \boldsymbol{c}(\theta) + (\rho - R)\hat{\boldsymbol{n}}(\theta), \tag{2.70}$$

in where $\boldsymbol{r}$ denotes the position vector, $\boldsymbol{c}$ the curve traced by the substrate and $\hat{\boldsymbol{n}}$ the outward normal vector to $\boldsymbol{c}$. Note that in order to define our coordinates in this way, it is key for the curve $\boldsymbol{c}$ to be convex. If this condition is satisfied we know that for any point $\boldsymbol{r}$ there is a unique point in $\boldsymbol{c}$ that minimizes the distance between the point and the curve. If the curve is smooth then we can find this point by differentiating

$$\partial_\theta |\boldsymbol{r} - \boldsymbol{c}(\theta)|^2 = 2(\boldsymbol{r} - \boldsymbol{c}(\theta)) \cdot \partial_\theta \boldsymbol{c}(\theta) = 0. \tag{2.71}$$

Since $\partial_\theta \boldsymbol{c}(\theta)$ is the tangent vector to $\boldsymbol{c}$, we must have then that $(\boldsymbol{r} - \boldsymbol{c}(\theta)) \propto \hat{\boldsymbol{n}}(\theta)$, and thus we conclude that for any $\boldsymbol{r}$ there is at least one θ such that $\boldsymbol{r} = \boldsymbol{c}(\theta) + (\rho - R)\hat{\boldsymbol{n}}(\theta)$. Since the curve is convex, this $\theta$is unique. Thus, we can establish an injective map between the space outside the substrate and our coordinates θ and ρ. Thus, these coordinates are single valued and well defined. This is extremely important in order for the quantum analogy to work. Instead of working in the complicated geometry of the xy-plane, we work in the simple $\theta\rho$-plane, in which the problem lives in a rectangle. If the mapping is injective, that means that contact (i.e., zero range) interactions in the xy-plane remain being contact interactions in the $\theta\rho$-plane. This allows us to continue using the Pauli exclusion principle to model the strong repulsion between the polymers. If the curve were not convex, the mapping would be, in general, not single-valued. Under these circumstances, a configuration in which two polymers touch in the xy-plane could be mapped in the $\theta\rho$-plane into polymers being at different values of the parameter θ, thus adding an effective finite-range interaction.

Another quite appealing property of the coordinate system described in Eqs. (2.69, 2.71) is that it is orthogonal. Indeed, notice that:

$$\partial_\theta \boldsymbol{r} = \boldsymbol{t}(\theta) + (\rho - R)\partial_\theta \hat{\boldsymbol{n}}(\theta), \tag{2.72}$$

in where $\boldsymbol{t} = \partial_\theta \boldsymbol{c}$ is the tangent vector to $\boldsymbol{c}$. Now, recall that $\hat{\boldsymbol{n}}$ is a unit vector, and thus it traces a circle as θ evolves. As a consequence, we must have that: $\partial_\theta \hat{\boldsymbol{n}}(\theta) \perp \hat{\boldsymbol{n}}(\theta)$. However, since these curves are constrained to the plane, this must imply that: $\partial_\theta \hat{\boldsymbol{n}}(\theta) \propto \boldsymbol{t}$. Therefore, we conclude that

$$\partial_\theta \boldsymbol{r} \propto \boldsymbol{t}. \tag{2.73}$$

On the other hand, we also have that

$$\partial_\rho \boldsymbol{r} = \hat{\boldsymbol{n}}, \tag{2.74}$$

and thus

$$\partial_\theta \boldsymbol{r} \cdot \partial_\rho \boldsymbol{r} = 0. \tag{2.75}$$

Hence, we have that, by expanding in small deviations in θ and ρ (characterized by δ and ϵ, respectively), we obtain:

$$|\boldsymbol{r}(\theta+\delta,\rho+\epsilon) - \boldsymbol{r}(\theta,\rho)|^2 = |(\partial_\theta \boldsymbol{r})\delta + (\partial_\rho \boldsymbol{r})\epsilon|^2 = (\partial_\theta \boldsymbol{r})^2\delta^2\delta + (\partial_\rho \boldsymbol{r})^2\epsilon^2. \tag{2.76}$$

Indeed, if we compute this expansion explicitly for a small α we obtain that

$$ds = \sqrt{1 + \frac{M(\theta,\rho)}{\beta A}\left(\frac{d\theta}{d\rho}\right)^2}\, d\rho, \tag{2.77}$$

where we have defined

$$\begin{aligned}\frac{M(\theta,\rho)}{\beta A} &\equiv \left(\frac{dx}{d\theta}\right)^2 + \left(\frac{dy}{d\theta}\right)^2 \\ &\approx \rho^2 + 2\alpha\rho(\rho-R)\left[\left(\frac{\rho-2R}{\rho-R}f'(\theta) - g''(\theta)\right)\sin(\theta) + \left(\frac{2R-\rho}{\rho-R}g'(\theta) - f''(\theta)\right)\cos(\theta)\right].\end{aligned} \tag{2.78}$$

Under the small fluctuation approximation and the condition $\epsilon/R \ll 1$ we do not need to consider higher order corrections. This is because once we had taken the ϵ^2 term out of the square root and written the action in terms of slopes, these higher order terms lead to corrections of the form $\rho^2\delta^n/\epsilon^2$ with $n \geq 3$. These terms are much smaller than orders of the form $\rho^n\delta^n/\epsilon^n$, which we neglect under the small fluctuations approximation. There is

an extra term of order $(\epsilon/R)(R^2\delta^2/\epsilon^2)$ which we can also safely neglect if $\epsilon \ll R$.

Thus, we just take into account the differential arclength and proceed to write the path-integral: By taking away the square root and dropping the constant (i.e., 1), term, we can write the time-sliced path-integral for one polymer chain with $M-1$ links with fix ends as

$$Z \propto \frac{(\beta A)^{1/2}}{M(\theta_M,\rho_M)^{1/4}M(\theta_1,\rho_1)^{1/4}} \int \prod_{j=2}^{M-1} d\theta_j \prod_{i=2}^{M} \sqrt{\frac{M(\theta_i,\rho_i)^{1/2}M(\theta_{i-1},\rho_{i-1})^{1/2}}{2\pi\epsilon}} \exp\left(-\sum_{k=2}^{M} \frac{M(\theta_{k-1},\rho_{k-1})(\theta_k-\theta_{k-1})^2}{2\epsilon}\right), \tag{2.79}$$

where, in order to obtain this expression, we have redistributed the $M(\theta,\rho)$ terms in the functional measure among all integrals. Notice that by proceeding in this way, we can already identify the prefactor $\frac{(\beta A)^{1/2}}{M(\theta_M,\rho_M)^{1/4}M(\theta_1,\rho_1)^{1/4}}$ that leads to the modification described in Eq. (2.67).

Having explicitly written the path-integral explicitly, it is tempting to try to proceed as we did in the circular case. However, since now we have terms that depend explicitly on the position, things get trickier. In particular, the step that goes from Eq. (2.39) to Eq. (2.41) is hard to prove since now position and momentum are mixed. As noticed in Ref. [33] , this is the origin behind the operator ordering problem. When doing quantum mechanics thus one requires more precise tools in order to handle these issues. However, we must recall that we are neither doing quantum mechanics nor computing the path-integral exactly. For instance, there is no expectations as how the analog to the Schrödinger equation should look in our theory. This is not the case in quantum mechanics. For example, when dealing with particles under the action of an external magnetic field we know that the correct theory is achieved via minimal coupling. When going to the path-integral formalism, this form of the Schrödinger equation is only achieved under a very particular partition of the action;

the so-called midpoint rule, which is usually attributed to the small time propagation being like an Itô process. In our case though, we do not require to impose an specific partition. On the contrary, we construct our theory by considering the time-slicing of small polymer links, and this is what imposes the appropriate wavefunction formalism in the continuum limit. Nevertheless, under the small fluctuation approximation all these issues do not really mater, since the differences between particular slicings yields negligible terms.

Now, even if the last statement is true, we must find a way to find the proper wave formalism to our theory. A way to do this is to follow Feynman's derivation of the Schrödinger equation [34].

This method goes as follows: if $K(x,t;x_0,t_0)$ is the propagator, then we must have that

$$K(x,t+\epsilon;x_0,t_0)=\int dy K(x,t+\epsilon;y,t)K(y,t;x_0,t_0). \tag{2.80}$$

On the other hand

$$K(x,t+\epsilon;y,t)=\sqrt{\frac{m}{2\pi\epsilon}}e^{-\frac{m}{2}\frac{(x-y)^2}{\epsilon}}, \tag{2.81}$$

that is to say, we are going considering the imaginary time case. Now, instead of integrating in y, we could change variables to $\eta=x-y$. Then, Eq. (2.80) becomes

$$K(x,t+\epsilon;x_0,t_0)=\sqrt{\frac{m}{2\pi\epsilon}}\int d\eta e^{-\frac{m}{2}\frac{\eta^2}{\epsilon}}K(x-\eta,t;x_0,t_0). \tag{2.82}$$

In the continuum limit, the Gaussian distribution becomes highly spiked around the origin and thus an expansion in both ϵ and η is justified. This leads then to

$$K+\epsilon\partial_t K=\sqrt{\frac{m}{2\pi\epsilon}}\int d\eta e^{-\frac{m}{2}\frac{\eta^2}{\epsilon}}\left(K-\eta\partial_x K+\frac{1}{2}\eta^2\partial_x^2 K\right). \tag{2.83}$$

Integrating over η and collecting powers of ϵ yields that the propagator satisfies the equation

$$\partial_t K = \frac{1}{2m}\partial_x^2 K, \tag{2.84}$$

which is just the Schrödinger equation in imaginary time. Since the propagator and the wavefunction satisfy the same equation, this effectively derives the Schrödinger equation.

In our specific case, we must generalize Eq. (2.82) to

$$K(\theta,\rho+\epsilon;\theta_0,\rho_0) = \int d\eta \sqrt{\frac{M^{1/2}(\theta,\rho+\epsilon)M^{1/2}(\theta-\eta,\rho)}{2\pi\epsilon}} e^{-\frac{\epsilon}{2}\frac{M(\theta-\eta,\rho)\eta^2}{\epsilon^2}} K(\theta-\eta,\rho;\theta_0,\rho_0). \tag{2.85}$$

Therefore, when expanding in η and ϵ corrections appear not only as derivatives of K, but also in both the measure and the one-link action. However, notice that:

$$\left[M^{1/2}(\theta,\rho+\epsilon)M^{1/2}(\theta-\eta,\rho)\right]^{1/2} \approx M^{1/2}(\theta,\rho)\left(1+F_1(\theta,\rho)\eta+F_2(\theta,\rho)\eta^2+G(\theta,\rho)\frac{\epsilon}{\rho}\right), \tag{2.86}$$

for some functions F_1, F_2 and G of θ and ρ. These term can be introduced into the action by noticing that:

$$\left(1+F_1\delta+F_2\eta^2+G\frac{\epsilon}{\rho}\right) \approx \exp\left((\beta A\epsilon)\left(F_1\frac{\epsilon/\rho}{\beta A\epsilon}\frac{\eta}{\epsilon}+F_2\frac{\epsilon^2/\rho^2}{\beta A\epsilon}\frac{\eta^2}{\epsilon^2}+G\frac{1}{\beta A\epsilon}\frac{\epsilon}{\rho}\right)\right). \tag{2.87}$$

Then, if we assume that $\epsilon/R \sim 1/(\epsilon\beta A)$, we have that the terms in Eq. (2.87) are smaller than $(\epsilon A\beta)^{-2}$, and thus they are negligible under the small fluctuation approximation.

A similar situation happen when expanding the terms in the exponential. This leads to terms of order $\rho^2\delta^3/\epsilon^2$ and $\rho^2\delta^4/\epsilon^2$ which we have already neglected when we time-sliced

the path-integral. Hence, by keeping only the leading order terms, we obtain that Eq. (2.85) becomes:

$$K(\theta, \rho + \epsilon; \theta_0, \rho_0) = \sqrt{\frac{M(\theta, \rho)}{2\pi\epsilon}} \int d\eta e^{-\frac{\epsilon}{2}\frac{M(\theta,\rho)\eta^2}{\epsilon^2}} K(\theta - \eta, \rho; \theta_0, \rho_0). \tag{2.88}$$

By expanding the propagator in its derivatives, computing the Gaussian integrals and collecting powers of ϵ as in the usual case we obtain then that:

$$\partial_\rho K = \frac{1}{2M(\theta, \rho)} \partial_\theta^2 K, \tag{2.89}$$

and thus we can identify that the quantum analogy to our polymer system is in this case given by the Hamiltonian:

$$\hat{H} = \frac{1}{2M(\theta, \rho)} \hat{p}_\theta^2. \tag{2.90}$$

The first thing that should strike us is that this Hamiltonian is non-hermitian. Although this marks a notorious difference with respect to the previous cases, we should recall that we are not doing quantum mechanics and there is no fundamental principle in the polymer problem that could impose the need of having an hermitian Hamiltonain. In quantum mechanics, this requirement comes from the need of having a unitary time evolution operator. This is needed because we require time evolution to preserve the norm of the quantum states and their interpretation as probability amplitudes. In our present problem however, our time evolution operator is not unitary and does not preserve the norm of our states. The time-evolved initial *a priori* probability density is not a probability density. The only thing we require is for the time-evolved state to continue being real and positive, so the partition function is a real positive number. Our Hamiltonian does preserve these qualities.

Again, however, the actual structure of the Hamiltonian is not important in this case.

Notice that if we had not neglected the correction terms in the measure and the exponential we would have obtained a different operator ordering for our Hamiltonian (this would have been manifested by the appearance of first order derivatives and external potentials). Since these terms were of order $(\beta A\epsilon)^{-2}$ in the action, they must also give raise to corrections to the free energy of this order. Therefore, to leading order, different operator orderings differ in negligible corrections. Hence, in principle, we could also have written

$$2\hat{H}' = \frac{1}{\sqrt{M(\theta,\rho)}}\hat{p}_\theta^2\frac{1}{\sqrt{M(\theta,\rho)}}, \tag{2.91}$$

which is hermitian. The difference will not matter when computing expectation values and thermodynamic quantities. We will come back to this point shortly. Physically though, we van identify the Hamiltonian (2.90) as the Hamiltonian of a particle with a position dependent mass. Since in band theory, a band can lead to an effective position dependent mass, this problem has been extensively studied (see for example Ref. [32]). However, to us, it is sufficient to mention that the breaking of the circular symmetry has introduced position dependent terms, and thus, this could lead to more complicated corrections to quantities such as the polymer density.

However, we now face a big challenge. The real issue regarding the Hamiltonian Eq. (2.90) is not its particular order or the fact that is not hermitian. The big issue is that this Hamiltonian does not commute with itself at different times, and thus we do not have simple time-dependence. Therefore, even if we could compute its exact instantaneous eigenvectors and eigenvalues, feat that in principle could be impossible to achieve, the quantum propagator is not just the exponential of the integral of the eigenvalues. Quite the contrary, the quantum evolution operator has the form

$$\hat{U} = \hat{T}\left(e^{-\int d\rho \hat{H}(\rho)}\right), \tag{2.92}$$

in where $\hat{T}$ is the time-ordering operator. This formal expression hides an infinite expansion of time-ordered integrals of operators that do not commute. As such, in the general case it can be quite complicated.

Given the aforementioned difficulties, it is not the objective of this work to solve the polymer problem in its most general setup. In order to obtain analytical results we restrict ourselves to situations in which the original substrate does not differ to much from a circle. This translates into having a small parameter α. By looking into Eq. (2.78) we see then that we could think in the α term as a small correction over the circle. In terms of the Hamiltonian, we rewrite Eq. (2.90) as

$$\hat{H} = \frac{\hat{p}^2}{2\beta A\rho^2} + \alpha\hat{V}(\hat{p}, \theta, \rho), \tag{2.93}$$

i.e., the modification of the substrate with respect to the circle can be thought as a small external momentum-dependent one-particle potential, which we consider as a perturbation.

In order to move forward we need a way to compute perturbative corrections to the time-evolution operator. In the next section, we develop such a mechanism for a general setup. The idea is that we will be able to apply it not only in this case, polymer anchored to curved convex substrates, but to more general cases as well.

2.6 Perturbation theory

In this section we compute perturbative corrections to the propagator, and therefore, to the partition function. We consider a polymer system with an analog "time-dependent quantum" Hamiltonian given by:

$$\hat{H}(t) = \hat{H}_0(t) + \alpha\hat{V}(t), \tag{2.94}$$

in where t plays the role of time in the analogy, $\hat{H}_0(t)$ is the original unperturbed self-adjoint Hamiltonian, α is a small parameter used to track the order of the corrections and $\alpha\hat{V}(t)$ is the small perturbation to the system. Notice that, unlike time-dependent perturbation theory in quantum mechanics, we allow the unperturbed Hamiltonian to depend on time. However, this must be a simple time-dependence, in the sense that $\hat{H}_0(t)$ commutes with itself at different times and thus its eigenbasis does not change with time. This is exactly the situation that we had with the polymers anchored to a circle.

As we saw in the previous sections, given the above Hamiltonian, we would have that the partition function of the system is given by

$$Z \propto \langle \Psi_f | \hat{U}(t_f, t_i) | \Psi_i \rangle, \tag{2.95}$$

in where, if $\hat{T}$ denotes the time-ordering operator, then

$$\hat{U}(t_f, t_i) = \hat{T}\left(e^{-\int_{t_i}^{t_f} dt \hat{H}(t)} \right), \tag{2.96}$$

is the time evolution operator of the system. As in quantum mechanics, this previous expression is nothing more than a formal expression. In general, an actual computation of $\hat{U}(t_f, t_i)$ is very hard or impossible to achieve. Moreover, unlike in quantum mechanics, this is not a unitary operator or even a normal operator. Therefore, it is not guaranteed to have an spectral decomposition. Because of this, trying to employ standard time-independent perturbation theory in this operator is not a proper way to proceed. Instead, we use that if a state $|\Psi(t)\rangle$ satisfy:

$$|\Psi(t)\rangle = \hat{U}(t, t_i) |\Psi_i\rangle, \tag{2.97}$$

then $|\Psi(t)\rangle$ must be a solution of the imaginary time Schrödinger equation:

$$-\partial_t|\Psi(t)\rangle = \hat{H}(t)|\Psi(t)\rangle = \left(\hat{H}_0(t) + \alpha\hat{V}(t)\right)|\Psi(t)\rangle \tag{2.98}$$

with the initial condition:

$$|\Psi(t_i)\rangle = |\Psi_i\rangle. \tag{2.99}$$

We can then express this states in an appropriate basis. Since we assumed that the unperturbed Hamiltonian was self-adjoint, we can then use its eigenvectors as our basis.

Let $\{|n\rangle\}_n$ be the eigenbasis of the unperturbed Hamiltonian $\hat{H}_0(t)$ and $\{E_n(t)\}_n$ their corresponding eigenvalues. As mentioned before, given the simple time dependence of the original Hamiltonian, the eigenbasis is time-independent. However, their eigenavalues can be time-dependent.

We then now proceed in analogy with quantum time-dependent theory. If the Hilbert space does not change with time, as it is our case, we can then write the following expansion:

$$|\Psi(t_i)\rangle = \sum_n c_n(t)e^{-\omega_n(t)}|n\rangle, \tag{2.100}$$

in where we have defined:

$$\omega_n(t) \equiv \int_{t_i}^{t} dt E_n(t). \tag{2.101}$$

By writing the coefficients of the expansion (2.100) as $c_n(t)e^{-\omega_n(t)}$, we are isolating the contribution of the perturbative potential from the unperturbed time evolution drived by $\hat{H}_0$. The initial condition (2.99) is then imposed by demanding that, for all n:

$$c_n(0) = \langle n|\Psi_i\rangle. \tag{2.102}$$

After expanding the time-evolved state in the eigenbasis, we next demand this state to satisfy the Schrödinger equation, Eq. (2.98). By inserting the expansion in the Eq. (2.98), using that the eigenbasis is time-independent and that $\partial_t \omega_n(t) = E_n(t)$, we obtain

$$-\sum_n \dot{c}_n(t) e^{-\omega_n(t)}|n\rangle = \alpha \sum_n c_n(t) e^{-\omega_n(t)} \hat{V}(t)|n\rangle, \tag{2.103}$$

in where the dot denotes a time derivative. The orthogonality of the eigenstates then leads to the following equation for the n-th coefficient:

$$\dot{c}_n(t) = -\alpha \sum_m c_m(t) e^{-(\omega_m(t)-\omega_n(t))} V_{nm}(t), \tag{2.104}$$

in where we have used the shorthand notation: $V_{nm}(t) = \langle n|\hat{V}(t)|m\rangle$. Equation (2.104) is exact. At first sight it looks like it could blow up for states in which $\omega_m(t) - \omega_n(t) < 0$. However, recall that what enters in the eigenstate expansion is $c_n(t)e^{-\omega_n(t)}$. Thus, each term on the right side of Eq. (2.104) will actually exponentially decay as $e^{-\omega_m(t)}$.

Now, in order to solve Eq. (2.104), we take a perturbative approach. We assume the following expansion for $c_n(t)$:

$$c_n(t) = c_n^0(t) + \alpha c_n^1(t) + \alpha^2 c_n^2(t) \ldots. \tag{2.105}$$

Inserting Eq. (2.105) into Eq. (2.104) and collecting powers of α yields a set of coupled equations, one for each perturbative order. In particular, at leading order we have that

$$\dot{c}_n^0(t) = 0, \tag{2.106}$$

and thus, we can set $c_n^0(t) = c_n(0)$. This implies that for all other orders we have the initial

condition: $c_n^k(0) = 0$. Next, we look for the first order correction. This satisfy

$$\dot{c}_n^1(t) = -\alpha \sum_m c_m(t_i) e^{-(\omega_m(t)-\omega_n(t))} V_{nm}(t), \tag{2.107}$$

and thus, we have that

$$c_n^1(t) = -\alpha \sum_m c_m(t_i) \int_{t_i}^t d\tau e^{-(\omega_m(\tau)-\omega_n(\tau))} V_{nm}(\tau). \tag{2.108}$$

Hence

$$e^{-\omega_n(t)} c_n^1(t) = -\alpha \sum_m c_m(t_i) e^{-\omega_n(t)} \int_{t_i}^t d\tau e^{-(\omega_m(\tau)-\omega_n(\tau))} V_{nm}(\tau). \tag{2.109}$$

Again, this expression looks dangerous as it has contributions for which $\omega_m(\tau) - \omega_n(\tau) < 0$, and thus it could in principle blow up, and therefore, break the perturbative expansion. However, if the time-dependance of the perturbative potential $\hat{V}_{nm}(t)$ is well behaved, as it is in our case, then the exponential behavior of the integrand gets carried outside the integral, where it is countered by the factor $e^{-\omega_n(t)}$. However, it leaves behind a finite contribution due to the lower limit of the integral. This finite contribution will then decay over time as $e^{-\omega_n(t)}$. The upper limit of the integral decays instead as $e^{-\omega_m(t)}$.

Until now we have only assumed that the added potential is small and thus, that a perturbative expansion is possible. We have not stated anything about how fast the term in this expansion decay, which we can also use for our advantage. For example, if we are in a situation in which groundstate dominance can be applied to the unperturbed system, then only terms that decay as $e^{-\omega_0(t)}$ are be relevant contributions.

Therefore, by using groundstate dominance, we see that, for $n \neq 0$, the only terms that contribute, due to the integral's upper limit, are

$$e^{-\omega_n(t)}c_n^1(t) \approx -\alpha c_0(t_i)e^{-\omega_n(t)}\int_{t_i}^{t} d\tau e^{-(\omega_0(\tau)-\omega_n(\tau))}V_{n0}(\tau). \tag{2.110}$$

On the other hand, we have that all terms in the expression for $c_0^1(t)$ contribute due to the integral's lower limit. Hence we write

$$\begin{aligned} e^{-\omega_0(t)}c_0^1(t) \approx -\alpha c_0(t_i)e^{-\omega_0(t)}&\int_{t_i}^{t} d\tau V_{00}(\tau) \\ &- \alpha\sum_{m\geq 1} c_m(t_i)e^{-\omega_0(t)}\int_{t_i}^{t} d\tau e^{-(\omega_m(\tau)-\omega_0(\tau))}V_{0m}(\tau). \end{aligned} \tag{2.111}$$

Thus, to first order, we have that

$$\begin{aligned} |\Psi(t)\rangle \approx & e^{-\omega_0(t)}c_0(t_i)\left(1-\alpha\int_{t_i}^{t} d\tau V_{00}(\tau) - \alpha\sum_{m\geq 1}\frac{c_m(t_i)}{c_0(t_i)}\int_{t_i}^{t} d\tau e^{-(\omega_m(\tau)-\omega_0(\tau))}V_{0m}(\tau)\right)|0\rangle \\ & - e^{-\omega_0(t)}c_0(t_i)\alpha\sum_{n\neq 0}\left(e^{\omega_0(t)}e^{-\omega_n(t)}\int_{t_i}^{t} d\tau e^{-(\omega_0(\tau)-\omega_n(\tau))}V_{n0}(\tau)\right)|n\rangle, \end{aligned} \tag{2.112}$$

which, by using that this is valid up to order α, we rewrite as

$$\begin{aligned} |\Psi(t)\rangle \approx & e^{-\omega_0(t)}c_0(t_i)\left(1-\alpha\int_{t_i}^{t} d\tau V_{00}(\tau) - \alpha\sum_{m\geq 1}\frac{c_m(t_i)}{c_0(t_i)}\int_{t_i}^{t} d\tau e^{-(\omega_m(\tau)-\omega_0(\tau))}V_{0m}(\tau)\right) \\ & \times\left(|0\rangle - \alpha\sum_{n\neq 0} e^{\omega_0(t)}e^{-\omega_n(t)}\int_{t_i}^{t} d\tau e^{-(\omega_0(\tau)-\omega_n(\tau))}V_{n0}(\tau)|n\rangle\right). \end{aligned} \tag{2.113}$$

By the same principle, we can then rewrite

$$|\Psi(t)\rangle \approx \left(|0\rangle - \alpha \sum_{n\neq 0} e^{\omega_0(t)} e^{-\omega_n(t)} \int_{t_i}^{t} d\tau e^{-(\omega_0(\tau)-\omega_n(\tau))} V_{n0}(\tau)|n\rangle\right) e^{-\omega_0(t)}$$
$$\times \left(1 - \alpha \int_{t_i}^{t} d\tau V_{00}(\tau)\right) \left(c_0(ti) - \alpha \sum_{m\geq 1} c_m(t_i) \int_{t_i}^{t} d\tau e^{-(\omega_m(\tau)-\omega_0(\tau))} V_{0m}(\tau)\right). \tag{2.114}$$

Then, recall that

$$1 - \alpha \int_{t_i}^{t} d\tau V_{00}(\tau) \approx e^{-\alpha \int_{t_i}^{t} d\tau V_{00}(\tau)}. \tag{2.115}$$

which can be further justified by the fact that when computing higher corrections, and focusing only on the groundstate, one systematically gets the entire series for the exponential. In addition, note that:

$$c_0(ti) - \alpha \sum_{m\geq 1} c_m(t_i) \int_{t_i}^{t} d\tau e^{-(\omega_m(\tau)-\omega_0(\tau))} V_{0m}(\tau)$$
$$= \left(\langle 0| - \alpha \sum_{m\geq 1} \int_{t_i}^{t} d\tau e^{-(\omega_m(\tau)-\omega_0(\tau))} V_{0m}(\tau)\langle m|\right) |\Psi_i\rangle \tag{2.116}$$

Then, by using Eqs. (2.115, 2.116) in Eq. (2.113), we obtain

$$|\Psi(t)\rangle = \left(|0\rangle - \alpha \sum_{n\neq 0} e^{\omega_0(t)} e^{-\omega_n(t)} \int_{t_i}^{t} d\tau e^{-(\omega_0(\tau)-\omega_n(\tau))} V_{n0}(\tau)|n\rangle\right)$$
$$\times e^{-\int_{t_i}^{t} d\tau (E_0(\tau)+\alpha V_{00}(\tau))} \left(\langle 0| - \alpha \sum_{m\geq 1} \int_{t_i}^{t} d\tau e^{-(\omega_m(\tau)-\omega_0(\tau))} V_{0m}(\tau)\langle m|\right) |\Psi_i\rangle. \tag{2.117}$$

Since the initial state is arbitrary, we can deduct then from (2.117), that, up to first order:

$$\hat{U}(t,t_i) = \left(|0\rangle - \alpha \sum_{n\neq 0} e^{\omega_0(t)} e^{-\omega_n(t)} \int_{t_i}^{t} d\tau e^{-(\omega_0(\tau)-\omega_n(\tau))} V_{n0}(\tau)|n\rangle \right) \times e^{-\int_{t_i}^{t} d\tau (E_0(\tau)+\alpha V_{00}(\tau))} \left(\langle 0| - \alpha \sum_{m\geq 1} \int_{t_i}^{t} d\tau e^{-(\omega_m(\tau)-\omega_0(\tau))} V_{0m}(\tau)\langle m| \right). \tag{2.118}$$

From this expression for the propagator we can learn a few things. Notice that the left and right contributions are not the same as in the unperturbed case. Since the time evolution operator is not hermitian this can be expected. On the one hand, the corrections that apply to initial states, i.e., the left part of the propagator, correspond to contributions coming from the lower limit of the time integral. Therefore, only times close to the beginning contribute. On the other hand, the corrections that apply to final states, i.e., the right part of the propagator, receives their meaningful contributions from the upper limit of the integral. Therefore, if groundstate dominance for the unperturbed system is applicable we have that, up to first order in α, the details of the *a priori* initial and final probability distributions do seem to matter, but the system can only retain a short memory. This is enough, though, to have an effect on the polymer density. Indeed, the corrected right and left sides do modify the unperturbed groundstate, modifying along the way the polymer density (see Eq. (2.18)).

Finally, the free energy of the system also receives a correction. There are two sources for this correction: One coming from the correction of the groundstate itself and one coming to the correction of the groundstate energy. The former though is highly dependent on the specifics of the *a priori* initial and final probabilities. In contrast, the latter is an universal correction. Indeed, from Eq. (2.118) we see that the unperturbed groundstate has been corrected by the expectation value of the perturbation on the groundstate integrated over time. Therefore, we see that, to first order in α

$$\delta F_U = \frac{\alpha}{\beta} \int_{t_i}^{t_f} d\tau \langle 0|\hat{V}(\tau)|0\rangle, \tag{2.119}$$

which can be understood as an spatial average of the perturbation over the plane. Given that the *a priori* probability densities must be positive functions and given that the groundstate is the only eigenstate which is positive definite, we must have that it carries a considerable weight in the eigenstate expansion of the probabilities. As such, the later correction to the groundstate is always present, granting an universal character to this shift in the free energy.

We would like to end this section by mentioning that the eigenbasis used in this derivation is not made of single-particle states, but rather of the many-particle ones. As such, quantities like V_{nm} are, in principle, not simple to compute, and by extension, corrections to the polymer density, are not easy to obtain. However, the correction to the free energy can be easily computed if the perturbation is a single-particle operator. Indeed, for a single particle operator we have that:

$$\langle 0|\hat{V}|0\rangle = \sum_{n=1}^{N} (n|\hat{V}|n), \tag{2.120}$$

in where $|n)$ denotes now single-particle states.

2.7 Polymers anchored to non-circular substrates: corrections

In this section we use the methods of the previous section in order to obtain concrete corrections to the free energy of the polymers anchored to non-circular substrates. We focus on the universal correction given by Eq. (2.118). By comparing Eqs. (2.90, 2.78, 2.93) we see that in this concrete case:

$$\hat{V}(\theta,\rho) = \\ -\frac{2(\rho-R)}{\rho^3}\left[\left(\frac{\rho-2R}{\rho-R}f'(\theta)-g''(\theta)\right)\sin(\theta)+\left(\frac{2R-\rho}{\rho-R}g'(\theta)-f''(\theta)\right)\cos(\theta)\right]\hat{p}_\theta^2. \tag{2.121}$$

Therefore, the universal shift is given by

$$\delta F_U = \frac{\alpha}{\beta}\int_R^{\rho_f} d\rho \langle \Psi_{\rm gs}|\hat{V}(\rho)|\Psi_{\rm gs}\rangle. \tag{2.122}$$

The groundstate appearing in this expression is the groundstate of the bosonic many-particle problem. This is the absolute value of the fermionic groundstate. Given that the potential includes a second power of $\hat{p}_\theta$, and thus a second derivative, this could be problematic. However, if issues arise, they must do so when the groundstate vanishes, i.e., at the boundaries of the wall or when two particles have the same position. At these points though, the wavefunction that is not affected by the derivatives vanishes, and hence, these issues do not affect our integral. Along the same lines, both fermionic wavefunctions have the same sign in the entire region of integration, and thus, we can completely ignore the absolute value and take the expectation value with respect to the fermionic groundstate. This state is achieved by filling the N lower energy individual one-particle eigenstates. The n-th eigenstate is given by:

$$\langle\theta|\Psi_n\rangle = \sqrt{\frac{2}{\delta}}\sin\left(\frac{n\pi\theta}{\delta}\right). \tag{2.123}$$

By taking advantage of Eq. (2.120), we see that:

$$\begin{aligned}\delta F_U = &-2\frac{\alpha}{\beta}\sum_{n=1}^{N}\left(\frac{2n^2\pi^2}{\delta^3}\right)\int_R^{\rho_f} d\rho\rho(\rho-R)\left[\left(\frac{\rho-2R}{\rho-R}f'(\theta)-g''(\theta)\right)\sin(\theta)\right.\\ &\left.+\left(\frac{2R-\rho}{\rho-R}g'(\theta)-f''(\theta)\right)\cos(\theta)\right]\sin\left(\frac{n\pi\theta}{\delta}\right)^2.\end{aligned} \tag{2.124}$$

This expressions can then be simplified by remembering that in order to apply ground-state dominance, which our perturbation theory assumes, $\delta \ll 1$.

Before going to a particular example we can use this perturbative result to exhibit how incorporating operator ordering induced terms into the Hamiltonian would yield negligible corrections.

Given that the mass functions must have a period of 2π, it is enough to work with functions of the form $\cos(m\pi\theta)$ and $\sin(m\pi\theta)$, in where m is an integer. Then, if we were to include the above mentioned corrections, they would manifest as:

$$\frac{2}{\delta}\int_0^{\delta} d\theta\left(\cos(m\pi\theta+\gamma)\sin\left(\frac{n\pi\theta}{\delta}\right)\partial_\theta\sin\left(\frac{n\pi\theta}{\delta}\right)\right), \tag{2.125}$$

and

$$\frac{2}{\delta}\int_0^{\delta} d\theta\left(\cos(m\pi\theta+\gamma)\sin\left(\frac{n\pi\theta}{\delta}\right)^2\right), \tag{2.126}$$

with equivalent expressions for $\sin(m\pi\theta)$. Then, by expanding in δ (which is small because of groundstate dominance), these expression yield corrections of order

$$\frac{NR}{\beta^2AR^2} = (NRA)\left(\frac{N}{\beta AR\delta}\right)^2\delta^2. \tag{2.127}$$

Recalling that the borderline case that we could explore with our theory is $(N/(\beta AR\delta))^2 \sim (A\beta\epsilon)^{-1}$ and $\delta \sim (A\beta\epsilon)^{-1/2}$, we see then this corrections are, as expected, smaller than $(A\beta\epsilon)^{-2}$, and thus, negligible. This confirms that under the small fluctuation approxima-

tion, operator-ordering is not important. In quantum mechanical terms, this approximation can then be thought as a semi-classical expansion.

Next, we consider a specific example: an ellipse.

2.7.1 An elliptic substrate

Consider Eq. (2.69) with the following functions: $g(\theta) = 0$ and $f(\theta) = \cos(\theta)$. This amounts to having an elliptic substrate. With this choice of functions, the perturbation to the circular problem becomes

$$\hat{V}(\theta,\rho) = -\frac{2}{A\beta\rho^3}\left[R\sin^2(\theta) + 2(\rho - R)\left(\cos^2(\theta) - \frac{1}{2}\right)\right]\hat{p}_\theta^2, \tag{2.128}$$

and thus:

$$\int_R^{\rho_f} d\rho\hat{V}(\theta,\rho) = \left(1 - \frac{\rho_f}{R}\right)\frac{(\rho_f - R)\cos^2(\theta) + 2R\sin^2(\theta)}{A\beta\rho_f^2}. \tag{2.129}$$

Therefore, the universal shift associated to this perturbation for a walled domain with spread δ starting from the parameter θ is given by

$$\begin{aligned}\delta F_U = &\left(1 - \frac{\rho_f}{R}\right)\\ &\times \frac{1}{A\beta\rho_f^2}\sum_{n=1}^{N}\frac{2}{\delta}\frac{n^2\pi^2}{\delta^2}\int_\theta^{\theta+\delta} d\theta'(\rho_f - R)\cos^2(\theta') + 2R\sin^2(\theta'))\sin^2\left(\frac{n\pi(\theta' - \theta)}{\delta}\right).\end{aligned} \tag{2.130}$$

Assuming very long polymers, i.e., $\rho_f \to \infty$, this gives the correction:

$$\delta F_U = -\alpha\frac{N^3\pi^2}{3A\beta R\delta^2}\left(\cos^2(\theta) - \delta\cos(\theta)\sin(\theta)\right) \tag{2.131}$$

However, we can not still compare this expression with the unperturbed one. Recall that in the generalized case, θ is not the polar angle and therefore the δ appearing in Eq. (2.131) is not the same one that appears in Eq. (2.49). If we let θ_0 and δ_0 denote the true angle and angular spread respectively, then we have that, up to first order:

$$\theta_0 = \theta - \alpha \sin(\theta)\cos(\theta). \tag{2.132}$$

Thus, at $\theta = 0,\ \pi/2,\ \pi,\ 3\pi/2,$ and 2π the parameter and the angle match. Moreover, we have that a small angular spread δ_0 around θ_0 is related to δ and θ by:

$$\delta = (1 - \alpha(\sin^2(\theta) - \cos^2(\theta)))\delta_0 \tag{2.133}$$

Taking this into consideration, we have that:

$$F = \frac{N^3\pi^2}{6A\beta^2 R\delta_0^2} + \alpha\frac{N^3\pi^2}{3A\beta^2 R\delta_0^2}(\sin^2(\theta) - \cos^2(\theta)) - \alpha\frac{N^3\pi^2}{3A\beta R\delta^2}\left(\cos^2(\theta) - \delta\cos(\theta)\sin(\theta)\right) \tag{2.134}$$

and, thus, the correction is

$$\delta F = \alpha\frac{N^3\pi^2}{3A\beta^2 R\delta_0^2}(\sin^2(\theta) - 2\cos^2(\theta)) + \alpha\frac{N^3\pi^2}{3A\beta R\delta_0}\cos(\theta)\sin(\theta). \tag{2.135}$$

Therefore, we see that the local curvature of the substrate dominates the leading order contribution. At the top or bottom, where the curve is flatter and thus have an effective bigger radius of curvature, the free energy increases since polymers are driven away from each other at a slower rate, thus increasing the entropy of the system. The exact opposite situation happen at $\theta = 0$, where the ellipse reaches its maximum curvature and thus smaller effective local radius. Here, polymers are driven away from each other at a faster rate and thus we observe a lower free energy. The next order correction has to do with how the

direction along which the polymer are directed changes.

Having completed this example, we finish this section by commenting that the greatest difficulty with dealing with this curved substrates is the fact that grundstate dominance is not as useful as it is in the usual polymer case. In order to obtain more interesting results, such as periodic boundary conditions, we would need to go beyond groundstate dominance. This clearly can not done analytically, and it would require the use of computational tools. However, the analytical techniques developed in this section can be used to treat other modifications of the polymer problem in which groundstate dominance is preserved, such as polymers over curved spaces. In the next sections we discuss these instances. Along the way, we also explore how finite size effects can lead to discrepancies between pure quantum theory and the polymer systems. Therefore, before jumping to curved spaces, we cover an intermediate step: moving (or uneven) walls.

2.8 Example of finite-timestep induced corrections: uneven walls

In the previous sections we saw that the mapping between the polymer system and a quantum mechanical one holds under relative simple conditions. For example, we observed that in the case of curved substrates, in addition to require a small fluctuation approximation, it was also key to have an initial radius much bigger than the microscopic cutoff of the polymer system. Indeed, if this condition were not satisfied, an appropriate continuum limit could not be guaranteed and higher order terms, that we would normally neglect, could become important.

The main difference between the polymer system and the quantum problem comes then through the finiteness of this cutoff, ϵ. Indeed, in quantum mechanics we are allowed to genuinely take the limit $\epsilon \to 0$. In the polymer problem though, we must guarantee small

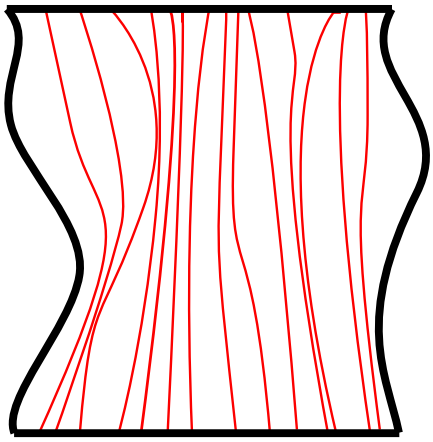

Figure 2.8: Depiction of a polymer system constrained to a box with non-straight walls. In the quantum case, this would correspond to quantum particles enclosed in a one-dimensional box with movable walls, which is well reviewed in the literature (see Refs. [35, 36]). Notice that the walls can either contract or expand. Also, the displacement of both walls is considered to be independent. Thus both the center point of the box, $d(t)$ and its width $\ell(t)$ are time dependent functions. We restrict ourselves to cases with a continuous and smooth variation of the walls. In addition, in order to have a proper continuum theory, we demand the length-scale over which this walls change to be large compared to the microscopic cutoff ϵ.

deviations or fluctuations, and thus we must have that $\beta A\epsilon \gg 1$. Of course, this is at odds with taking the limit $\epsilon \to 0$. It is true though that in order to have an effective continuum limit we require for ϵ to be small compared to the other length-scales of the problem. However, how small is the ratio between the cutoff and these length scales and how it compares with $(\beta A\epsilon)^{-1}$ is not set *a priori*. Hence, in some situations one should not overlook its presence. This leads then to corrections to the quantum problem that are caused by the finiteness of ϵ. One simple setup in which one can see this happens is in the case of a many-polymer system constrained by non-straight walls. See Figure (2.8).

The time slicing of this problem does not have too many modifications with respect to the usual polymer problem. Indeed, Cartesian coordinates are appropriate to describe the system and therefore, there are no correction in the action or the measure. Thus, we can immediately take the small fluctuation approximation as usual. However, the movable wall condition imposes different limits of integration for the x_i variable at each timestep.

Indeed, if we call the coordinate of the center of the box as $d(t)$ and the width of the box $\ell(t)$, then, we have that at the i-th time slice:

$$d(t) - \frac{\ell(t)}{2} \leq x_i \leq d(t) + \frac{\ell(t)}{2}. \tag{2.136}$$

However, we can define a rescaled position variable, $\tilde{x}$, such that

$$\tilde{x} = \frac{1}{\ell(t)}(x - d(t)). \tag{2.137}$$

By using this variable we see that at each timestep the limits of integration shift to the interval $[-1/2, 1/2]$ and thus taking us back to the one-dimensional box problem with fixed wall, which we already know how to handle. The price that one must pay to achieve this is that extra terms appear on the action. Indeed, notice that:

$$\Delta x = x_{i+1} - x_i = \ell(t+\epsilon)\tilde{x}_{i+1} + d(t+\epsilon) - \ell(t)\tilde{x}_i - d(t). \tag{2.138}$$

Since ϵ is small, we can expand this in series. Keeping terms up to first order, we get:

$$\Delta x = (\ell(t) + \dot{\ell}(t)\epsilon)\Delta\tilde{x} + (\dot{d}(t)\epsilon) + \dot{\ell}(t)\epsilon\tilde{x}_i \tag{2.139}$$

Thus, by changing variables, we obtain that the action becomes

$$\frac{\beta A}{2}\left(\frac{\Delta x}{\epsilon}\right)^2 = \frac{\beta A}{2}\left((\ell(t) + \dot{\ell}(t)\epsilon)\left(\frac{\Delta\tilde{x}}{\epsilon}\right) + \dot{d}(t) + \dot{\ell}(t)\tilde{x}_i\right)^2. \tag{2.140}$$

As a consequence, we see that the center of the Gaussian distribution shifts to $(\dot{d}(t) + \dot{\ell}(t)\tilde{x}_i)\epsilon/(\ell(t) + \dot{\ell}(t)\epsilon)$. Among other things, this implies that $\left(\frac{\Delta\tilde{x}}{\epsilon}\right)$ is not required to be small. Only its deviation from $(d(t) + \dot{d}(t)\epsilon)$ is required to be small, which is already guaranteed by the small fluctuation approximation. On the other hand, the measure of integration does not receive major modifications. Indeed, we have that:

$$dx_i = \ell(t_i) d\tilde{x}_i. \tag{2.141}$$

We are now in conditions to obtain the analog of the Schrödinger equation of the system by following Feynman's method. First, we have that:

$$\begin{aligned} K(\tilde{x}, t+\epsilon; \tilde{x}_0, t_0) =& \sqrt{\frac{\beta A \ell(t+\epsilon)^{1/2} \ell(t)^{1/2}}{2\pi\epsilon}} \\ & \times \int d\eta e^{-\frac{\beta A}{2}\left((\ell(t)+\dot{\ell}(t)\epsilon)\left(\frac{\eta}{\epsilon}\right)+\dot{d}(t)+\dot{\ell}(t)(\tilde{x}-\eta)\right)^2} K(\tilde{x}-\eta, t; \tilde{x}_0, t_0). \end{aligned} \tag{2.142}$$

Expanding on ϵ and δ and collecting powers of ϵ, we obtain the following equation

$$\partial_t K = \frac{1}{2\ell^2(t) A\beta} \partial_{\tilde{x}}^2 K + \left(\frac{\dot{\ell}(t)}{\ell(t)} \tilde{x} + \frac{\dot{d}(t)}{\ell(t)} \right) \partial_{\tilde{x}} K + \frac{1}{4} \frac{\dot{\ell}(t)}{\ell(t)} K. \tag{2.143}$$

This can be rewritten as

$$\partial_t K = \frac{1}{2\ell^2(t) A\beta} \partial_{\tilde{x}}^2 K + \left(\frac{\dot{\ell}(t)}{\ell(t)} \frac{1}{2} (\tilde{x}\partial_{\tilde{x}} + \partial_{\tilde{x}}\tilde{x}) + \frac{\dot{d}(t)}{\ell(t)} \partial_{\tilde{x}} \right) K - \left(\frac{1}{4} \frac{\dot{\ell}(t)}{\ell(t)} \right) K, \tag{2.144}$$

or

$$\begin{aligned} -\partial_t K =& -\frac{1}{2\ell^2(t) A\beta} \partial_{\tilde{x}}^2 K - i \left(\frac{\dot{\ell}(t)}{\ell(t)} \frac{1}{2} (\tilde{x}(-i)\partial_{\tilde{x}} + (-i)\partial_{\tilde{x}}\tilde{x}) + \frac{\dot{d}(t)}{\ell(t)} (-i)\partial_{\tilde{x}} \right) K \\ & - \left(\frac{1}{4} \frac{\dot{\ell}(t)}{\ell(t)} \right) K, \end{aligned} \tag{2.145}$$

From here we can easily read the Hamiltonian of the analogous quantum system

$$\hat{H} = \frac{\hat{p}^2}{2A\beta\ell^2(t)} + i \frac{\dot{\ell}(t)}{2\ell(t)} (\tilde{x}\hat{p} + \hat{p}\tilde{x}) + i \frac{\dot{d}(t)}{\ell(t)} \hat{p} - \frac{\dot{\ell}(t)}{4\ell(t)}. \tag{2.146}$$

As we can see, once again we have that the Hamiltonian is explicitly non-hermitian, as we have terms proportional to i. However, it is clear that this factor must be present. Other-

wise, an originally real wave function would become complex under time evolution.

A different approach to obtain this Hamiltonian would have been to start with the quantum Hamiltonian for the original coordinates. As pointed out in Ref. [36], this is a system whose Hilbert space is time dependent. More specifically, $|\Psi(t)\rangle$ and $|\Psi(t+\epsilon)\rangle$ belong to different Hilbert spaces. In order to define the spatial derivative one can embed the time-dependent Hilbert space into a bigger one, and redefine derivatives through tensor operators. Having a well defined Hamiltonian in the original coordinates, we can rescale to $\tilde{x}$ by using the unitary operators associated to re-scalings and translations. Proceeding in this way yields:

$$\hat{H}' = \frac{\hat{p}^2}{2A\beta\ell^2(t)} - i\frac{\dot{\ell}(t)}{2\ell(t)}(\tilde{x}\hat{p} + \hat{p}\tilde{x}) - i\frac{\dot{d}(t)}{\ell(t)}\hat{p}, \tag{2.147}$$

which differs from the one we obtained by explicit computation; it lacks the $-\frac{\dot{\ell}(t)}{4\ell(t)}$ term. Therefore, these two procedures do not yield the same answer. However, notice that if $\dot{\ell}\epsilon$ becomes smaller than $(\beta A\epsilon)^2$, then in principle we could neglect the corrections that lead that extra term. In fact, once that happens, operator ordering again does not matter. Hence we can conclude that quantum mechanics and the polymer system agree completely only when we can take the limit $\epsilon \to 0$, i.e., when we have a true continuum.

In terms of computation, notice that if we write: $\ell(t) = w + \alpha f(t)$ with $\alpha \ll 1$, we can then rewrite our Hamiltonian as:

$$\hat{H} = \frac{\hat{p}^2}{2A\beta w^2} - 2\alpha\frac{f(t)^2}{w^2}\frac{\hat{p}^2}{2A\beta w^2} - i\frac{\dot{f}(t)}{2\ell(t)}(\tilde{x}\hat{p} + \hat{p}\tilde{x}) + i\frac{\dot{d}(t)}{\ell(t)}\hat{p} - \frac{\dot{\ell}(t)}{4\ell(t)}. \tag{2.148}$$

Then, we could consider $\hat{H}$ as $\frac{\hat{p}^2}{2A\beta w^2}$ plus a small perturbation:

$$\hat{V}(\tilde{x},t) = -2\alpha\frac{f(t)^2}{w^2}\frac{\hat{p}^2}{2A\beta w^2} - i\frac{\dot{f}(t)}{2\ell(t)}(\tilde{x}\hat{p}+\hat{p}\tilde{x}) - i\frac{\dot{d}(t)}{\ell(t)}\hat{p} - \frac{\dot{\ell}(t)}{4\ell(t)}. \tag{2.149}$$

This would allow us to use our perturbation theory formalism. However, notice that, since in this case one could, in principle, control how fast the walls change, we could consider the limit of extremely slow time dependence. In this limit, the adiabatic theorem of quantum mechanics becomes a valid approximation and the system would follow its instantaneous eigenstates. If we also consider groundstate dominance, in this case we only require to know the instantaneous groundstate of the system. Although this sounds simple, recall that this is a many particle groundstate, and thus we would require to solve for the excited states of the single particle problem in order to obtain it.

The physical reason behind why the adiabatic theorem becomes a valid approximation is the following; if the length-scale over which the walls change is long compared to the space it takes to the polymer to diffuse in the lateral direction, then the polymer has enough space to explore or retreat from the space being opened or restricted as the walls expand or contract, respectively. As a consequence, the polymers can adjust to this change without being excited.

2.9 Polymers over curved surfaces:

In the previous sections we saw that the use of generalized curvilinear coordinates enabled us to extend the mapping between directed polymer and quantum mechanics to setups with more general, although flat, geometries. Since we were able to successfully handle such coordinates, it is only natural to ask then if we could achieve the same for the case of polymers constrained to non-Euclidean geometries, i.e., curved surfaces. Although this may sound as a merely academic proposition, real experimental realizations of polymers systems are

often in solution with spherical-like colloids which are much bigger than the length of the polymers [37]. The question of polymers extending, or wrapping, over curved surfaces has been explored before [38, 39], but for different polymer models and only considering single polymer chains. Indeed, the problem of strongly-interacting directed polymers (i.e., subjected to tension) over a surface has not been addressed before.

One of the main differences between flat and curved spaces is the fact that the geodesics, i.e., the curves of minimal length, are not straight lines. Therefore, by putting a polymer under tension over a curved surface (that is, constrained to lie within the curved manifold) we find that the configuration of minimal energy naturally acquires a curved shape. What this implies, at the level of an individual polymer link, is that the reflection symmetry along the preferred axis (i.e., the direction of stretching) is broken, and the polymer link prefers going either to the right or to the left. This introduces two new phenomena in the polymer system. The first one is that the local curvature can either push two different polymers against each other or keep them away. In the former case, the number of possible configurations accessible to the system diminishes, reducing the entropy and thus giving raise to an increment to the free energy. On the contrary, the later case has the opposite effect, resulting in a lower free energy. Thinking in terms of a quantum analog, the curvature can introduce an external potential which tries to collect the quantum particles in its local minima and keeps them away from its local maxima. The second phenomena that can arise due to the change in shape of the polymer induced by the geometry is related to the hardcore boundaries of the system. Indeed, curvature could drive our polymer to move toward the boundaries. Since they are impenetrable, this yields a considerable deflection of the polymer path with respect to its optimal configuration. This deflection will inevitably affect the neighboring polymers, yielding an increment in the total free energy.

Notice that, until now, we have mentioned effects produced by non-vanishing intrinsic

curvature. Given that our model penalizes total length, then, in principle, the role of extrinsic curvature, i.e., how the manifold folds in tree dimensional space, should be non-existent. That is to say, if the manifold only has extrinsic curvature, i.e., it is intrinsically flat, it can be mapped isometrically without deformations to the plane. In this way, this map takes the curves representing the polymers shape and puts them in the plane without deforming them. Therefore, this map preserves the energy of each configuration, thus yielding the same partition function. However, the coordinates that describe each curve do not need to be preserved in this map. As a consequence, if we establish the hardcore boundaries of our system at fixed values of these coordinates, the curve that represents the boundary is not mapped to a straight curve. This, then, yields a polymer problem with uneven boundaries, which we discussed in the previous section. Therefore extrinsic curvature can only produce corrections to the free energy due to boundary (or wall) effects.

The above was a qualitatively description of the effect of curvature. In order to compute quantitative results we need to find a way to write the path-integral in coordinates that can describe the curved manifold. This process is again facilitated by the use of the small fluctuation approximation. Similar to the case of polymers anchored to curved edges, this partition should be done in Euclidean space. The difference is that now the Euclidean space is three-dimensional. However, as there are an infinite number of curved surfaces, it is not possible to find a set of coordinates that can be used to cover all cases. In order to gain insight about how successful the extension can be, we start with a simple case.

2.9.1 Polymers over the surface of a sphere

We can start by trying to cover a simple, but important, case. Polymers constrained to the surface of a sphere. Of course, the natural coordinates in this case would be the use of the polar and azimuthal angles of spherical coordinates

$$
\begin{aligned}
x(\theta,\phi) &= R\cos(\phi)\sin(\theta) \\
y(\theta,\phi) &= R\sin(\phi)\sin(\theta)\,, \\
z(\theta,\phi) &= R\cos(\theta)
\end{aligned}
\tag{2.150}
$$

in where R denotes the radius of the sphere. When doing the time slice of the path-integral, we assume that the length of the cutoff (either $\epsilon = R\Delta\theta$ or $\epsilon = R\Delta\phi$ depending on how the polymers are directed) is much smaller than the radius, i.e., $\epsilon/R \ll (A\beta\epsilon)^{-1} \ll 1$. We demand this for two reasons: (i) in order to ensure that the continuum limit provides a good approximation, and (ii) for simplicity; in this case we only need to expand $(\Delta x)^2$, $(\Delta y)^2$ and $(\Delta z)^2$ up to second order. Proceeding in this way, we have that:

$$
\Delta s = \left[(\Delta x)^2 + (\Delta y)^2 + (\Delta z)^2\right]^{1/2} = R\left[\sin^2(\theta)(\Delta\phi)^2 + (\Delta\theta)^2\right]^{1/2}. \tag{2.151}
$$

We can then choose to direct our polymer along θ or along ϕ. See Figure 2.9.

Let us study first the case in which we direct the polymers along θ, i.e., along the curves parametrized by a constant θ (see Figure. 2.9 a). In this case, we have that the role of the coordinate of the analogous quantum particle is taken by ϕ and the role of time is taken by θ. Then, we can write

$$
A\beta\Delta s = A\beta d\theta R\left[1 + \sin^2(\theta)\left(\frac{d\phi}{d\theta}\right)^2\right]^{1/2} \approx A\beta(Rd\theta)\left(1 + \frac{1}{2}\sin^2(\theta)\left(\frac{d\phi}{d\theta}\right)^2\right), \tag{2.152}
$$

in where we have used the small fluctuation approximation. On the other hand, it is clear that the functional measure takes the form

$$
ds_i \to R\sin(\theta_i)d\phi_i, \tag{2.153}
$$

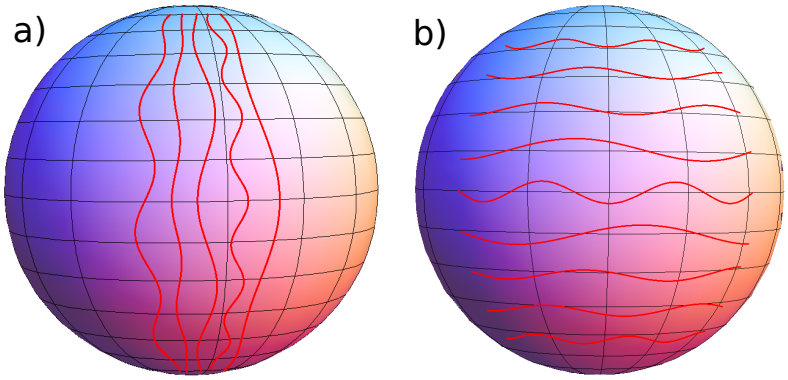

Figure 2.9: Polymers constrained to lie at the surface of a sphere. By using spherical coordinates, it is easy to direct the polymers along two directions: along the meridians (i.e., constant θ) or along latitudes (i.e., constant ϕ). a) Polymers directed along the meridians; the polymer's shape is parametrized as $\theta(\phi)$. In this case, the preferred direction coincides with the geodesic of the spheres. As we see, this alignment send polymers against each other near the poles. b) Polymers directed along the latitudes of the sphere; the polymer's shape is parametrized as $\phi(\theta)$. In this case, the direction of alignment does not coincide with the geodesics of the sphere, except for the equator. As such, a quantum analog can only be achieved for polymers near the equator. Also, polymers starting at different latitudes have different unstretched lengths.

for each time slice. Taking into consideration Eqs. (2.158, 2.153), it is not hard to see that the Hamiltonian of the analogous quantum system is given by

$$\hat{H}_\phi = \frac{1}{\sin^2(\theta)} \frac{\hat{p}_\phi}{A\beta R}, \tag{2.154}$$

in where $\hat{p}_\phi \to -i\partial_\phi$. Then, we bound our polymer system to lie between $\phi = 0$ and $\phi = \delta$ and $\theta = \theta_i$ to $\theta = \theta_f$.

Notice that although it is time dependent, just like in the case of polymers anchored to a circle, it commutes with itself at different times, and thus we have that:

$$\hat{U} = \exp\left(- \int_{\theta_i}^{\theta_f} \frac{1}{\sin^2(\theta)} \frac{\hat{p}_\phi}{A\beta R} \right) \tag{2.155}$$

Then, by using

$$\int_{\theta_i}^{\theta_f} \frac{d\theta}{\sin^2(\theta)} = \frac{\sin(\theta_f - \theta_i)}{2\sin(\theta_f)\sin(\theta_i)}, \tag{2.156}$$

and by assuming groundstate dominance, we obtain the following expression for the free energy of the system

$$F = \left(\frac{\sin(\theta_f - \theta_i)}{2\sin(\theta_f)\sin(\theta_i)}\right) \frac{N^3\pi^2}{6\beta^2 AR\delta^2}. \tag{2.157}$$

Notice that the bigger the sphere's radius (R) is, the better approximation groundstate dominance becomes. Indeed, the prefactor in Eq. (2.157) behaves linearly for initial or final conditions that lay away from the poles and diverges when they approach them. This divergence is the result of having the walls approaching each other near the poles. Although one may think that this divergence is enough to grant groundstate dominance to the system, recall that the continuum approximation requires an upper bound on the polymer density. Since this density increases as we approach the poles, we are not allowed to come very close to them, countering in this way the effect of the divergence. Of course, the key to groundstate dominance resides in the linear regime away from the poles. The bigger the sphere radius is, the longer we can in at this regime. Thus, if the typical width of the system (controlled by δ) is much smaller than the polymer length, we can have groundstate dominance.

Notice also that, besides this wall induced effect, the situation between the polymers on the sphere directed along θ is not very different to polymers in a plane. The reason behind this is that in this case we have chosen to direct the polymers along the geodesics of our manifold. Indeed, constant values of ϕ map on the sphere to big arcs, and thus to the geodesics of the sphere. Therefore, as the polymers grow, the right/left symmetry is maintained, leading to something very similar to flat polymers. This contrasts greatly with what happens if we choose to direct our polymers along ϕ instead (see Figure.2.9 b)). In

this case, the role of position is taken by θ while ϕ takes the role of time. Then the action of the system becomes

$$\Delta s = d\phi \sin(\theta) R \left[1 + \frac{1}{\sin^2(\theta)} \left(\frac{d\theta}{d\phi}\right)^2\right]^{1/2} \approx (Rd\theta) \left(\sin(\theta) + \frac{1}{2\sin(\theta)} \left(\frac{d\theta}{d\phi}\right)^2\right), \tag{2.158}$$

where again we assume that the small fluctuation approximation is valid.

The first big difference that we can notice is that an external potential, $\sin(\theta)$, has appeared in the action. This term shows up because, in this case, polymers that start at different θ and travel the same angular spread in ϕ cover different distances over the surface of the sphere. Indeed, the ratio between the two unstretched lengths (namely, the length of the path traversed for a fixed value of θ) is given by $\sin(\theta_1)/\sin(\theta_2)$. Ideally, we would like to cover systems of polymers that are unbiased in this regard, i.e., polymers whose unstretched length is independent of its initial point. We can achieve this by changing variables: $\phi \to \phi'/\sin(\theta)$. In this new coordinate system the distance traversed by each polymer, for a fixed value of θ, is given by $R\Delta\phi'$. The price that one must pay for doing this change is that now the equal-time curves are no longer meridians, but rather a more complicated curve over the surface of the sphere. A direct consequence of this is that our coordinates are no longer orthogonal, and therefore terms linear in $\Delta\theta$ appear in the action. Indeed, we have that the transformed action is given by:

$$\beta A \epsilon ds_i = \beta AR \left[\epsilon^2 - 2\cot(\theta)\phi'\epsilon\delta + (1 + \cot^2(\theta)\phi'^2)\delta^2\right]^{1/2}, \tag{2.159}$$

in where $\epsilon \equiv \phi'_{i+1} - \phi'_i$ is a constant timestep, and $\delta \equiv \theta_{i+1} - \theta_i$. We then rewrite Eq. (2.159) as:

$$\beta A\epsilon ds_i = \beta AR\epsilon \left[1 - 2\cot(\theta)\phi' \left(\frac{\delta}{\epsilon}\right) + (1 + \cot^2(\theta)\phi'^2) \left(\frac{\delta}{\epsilon}\right)^2\right]^{1/2}. \tag{2.160}$$

The presence of the linear term in δ effectively shifts the center of the gaussian distribution, breaking the mirror symmetry at each timestep. This happens in this case because the curves described by a constant value of θ are not geodesics of the sphere, and thus, they are not the natural shape that the polymers would like to acquire. We can make this fact explicit by rewriting:

$$\beta A\epsilon ds_i = \beta AR\epsilon \left[1 + (1 + \cot^2(\theta)\phi'^2) \left(\frac{\delta}{\epsilon} - \frac{\cot(\theta)\phi'}{1 + \cot^2(\theta)\phi'^2}\right) - \frac{\cot^2(\theta)\phi'^2}{1 + \cot^2(\theta)\phi'^2}\right]^{1/2}. \tag{2.161}$$

From Eq. (2.161) it is clear that the configuration with minimum energy is not achieved at $\delta = 0$, but rather at $\delta/\epsilon = \cot(\theta)\phi'/(1 + \cot^2(\theta)\phi'^2)$. What the small fluctuation approximation yields in this case is thus small deviations around this preferred displacement. This makes the expansion of the square root very tricky. To start with, it is not always achievable. Indeed, near the poles the last term inside the square root approaches one, situation that leads to a non-Gaussian distribution. Away from the poles though, an expansion to second order in the deviation from the preferred displacement yields a Gaussian action which is not properly normalized with respect to the measure of the path-integral. This has severe consequences, as it makes a continuum quantum analog non-viable. Indeed, when applying Feynman's method to find the proper Hamiltonian, we realize that the leading order term in the expansion is not the wavefunction itself, but rather a multiple of it, which breaks the continuum limit. Thus, we see that in this case, we can only achieve a proper quantum analog if the last term inside the square root is small. In fact, it needs to be small enough so that one can neglect its product with the square of the deflection. Under this assumption, one obtains that

$$\beta A\epsilon ds_i = \frac{\beta AR\epsilon}{2}\left[\left(\frac{\delta}{\epsilon}\right)^2 - 2\cot(\theta)\phi'\left(\frac{\delta}{\epsilon}\right)\right], \tag{2.162}$$

in where we have ignored the constant first term. On the other hand, the path-integral measure becomes

$$Rd\theta_i\sqrt{1+\cot^2(\theta)\phi'^2} \approx Rd\theta_i. \tag{2.163}$$

We justify this last approximation by noticing that we are assuming that $\cot(\theta)\phi'$ is small. Hence, $\sqrt{1+\cot^2(\theta)\phi'^2} \approx \exp(\cot^2(\theta)\phi'^2/2)$. In this way we can reintroduce this as a correction to the action which would be proportional to $(\beta A\epsilon)^{-1}\cot^2(\theta)\phi'^2$, and thus comparable to $(\delta/\epsilon)^2\cot^2(\theta)\phi'^2$, which we consider negligible.

Combining Eqs (2.162, 2.163) we can proceed to employ Feynman's trick, which yields the following quantum Hamiltonian:

$$\hat{H} = \frac{\hat{p}_\theta^2}{2\beta AR} + i\cot(\theta)\phi'\hat{p}_\theta - \frac{\beta A\cot^2(\theta)\phi'^2}{2}. \tag{2.164}$$

As we see, by simply directing our polymers in a direction that does not match the geodesics of the surface, the process of finding a quantum analog became much more intricate. In fact, we saw that in the most general case this mapping was not achievable, and this is because the expansion of the square root did not provide properly normalized Gaussian distributions. In this particular case, we were forced to consider a sector of the sphere near the equator, which is itself a geodesic of the sphere. When we deviate from this big arc, we obtain that the geodesic of the system can be quite different to a curve of constant θ (for example, if the initial and final points of the polymer are at opposite sides, the geodesic is a curve that cuts through the poles of the sphere). This implies that in the most general setting, the small fluctuation approximation is not a good approximation. Since the mapping to quantum mechanics seems to be linked to this approximation, this

would imply the failure of the method. Reinforcing this idea is the fact that none of the difficulties discussed in this case appeared in the previous problem, in which we directed our polymers along the geodesic of the system. Thus, when dealing with curved spaces, we should limit ourselves to problems with small curvature in which the geodesics do not deviate too much from the directions along which we are directing the polymers. This is the objective of the upcoming sections.

2.9.2 Appropriate metric for slightly curved surfaces: The Monge patch

As we mentioned before, the total amount of possible manifolds and parametrization cannot be covered by a general set of coordinates. We also saw that the direction in which we direct our polymers, as a result of the induced shifts in the distributions of fluctuations, greatly affects the applicability of the quantum analogy. Thus, in order to form some form of consistent theory, we propose to explore the regime of slightly curved surfaces. This facilitates the use of the quantum analogy as well as allows us to compare the problem on the manifold to the flat polymer problem via perturbation theory; this comparison may facilitate the isolation of the effects produced by the curvature. Moreover, this regime has a good intersection with manifolds that admit a parametrization of the form $z = f(x, y)$, also known as Monge patches. The clear advantage of studying this kind of parametrization is that it allows to cover a wide range of different manifolds, one for each function $f(x, y)$, without the need of redefining the set of coordinates in the quantum analogy. Indeed, we can always choose to direct our polymers along the y coordinate and use x as the coordinate of the quantum particles. In addition to demand small curvature, we also demand the manifold to be smooth manifolds (i.e., differentiable), and to be characterized by typical length-scales that are much larger than the cutoff of the polymer chain. This last requirement of course is needed in order to have a proper continuum approximation. Mathematically, we can combine this requirements (smoothness, small curvature, long typical length-scales) by demanding that:

$$\frac{\partial f}{\partial x},\ \frac{\partial f}{\partial y} \ll 1. \tag{2.165}$$

On the technical side, this requirement also allows us to only keep up to second order terms when performing the time-slicing of the path-integral.

Thus, we have that for one polymer link, the length covered under a fluctuation is given by

$$\Delta s = \epsilon \left[1 + (1 + f_x^2) \left(\frac{\Delta x}{\epsilon} \right)^2 + 2 f_x f_y \left(\frac{\Delta x}{\epsilon} \right) + f_y^2 \right]^{1/2}, \tag{2.166}$$

in where the subscripts are a shorthand notation for partial derivatives.

2.9.3 Extrinsic curvature: Flat patches

One of the advantages of this parametrization is that it allows us to explicitly check our qualitative predictions regarding the effects of extrinsic curvature on the polymer system. In this section we focus then in manifolds without intrinsic curvature.

Recall that a measure of the intrinsic curvature is the Gaussian curvature: κ_G. For a Monge patch, this curvature is given by:

$$\kappa_G = \frac{f_{xx} f_{yy} - f_{xy}^2}{(1 + f_x^2 + f_y^2)^2}. \tag{2.167}$$

Thus we look for patches that satisfy $\kappa_G = 0$. For simplicity we cover three cases that satisfy this condition. These are

- $f(x, y) = g(x)$,
- $f(x, y) = g(y)$,
- and $f(x, y) = cx + g(y)$,

in where g is an arbitrary smooth function.

In the first case, notice that: $\Delta s = \epsilon \left[1 + (1 + g_x^2)\left(\frac{\Delta x}{\epsilon}\right)^2\right]^{1/2}$, while the path-integral measure is generated by $dx\sqrt{1 + g_x^2}$. Although this will give a quantum analog with a position dependent mass, which may be difficult to solve, notice that this arises only because x is not the optimal variable for this problem. Indeed, if we use the equal-time arclenth variable $s_e \equiv \int_{x_0}^{x} \sqrt{1 + g_x^2}$, we have that: $\Delta s = \left[1 + \left(\frac{\Delta s_0}{\epsilon}\right)^2\right]^{1/2}$, while the measure is just ds_e. Since under this change of variables the boundaries of the system go from constant x to constant s_e (i.e., straight lines in both coordinates), we see then that we can exactly map the problem on the manifold to a polymer problem in a plane. Therefore, there are no contributions from extrinsic curvature in this case.

In the second case, we have that:

$$\Delta s = \epsilon \left[1 + \left(\frac{\Delta x}{\epsilon}\right)^2 + g_y^2\right]^{1/2}, \tag{2.168}$$

which we can rewrite as:

$$\Delta s = \sqrt{1 + g_y^2}\epsilon \left[1 + \frac{1}{1 + g_y^2}\left(\frac{\Delta x}{\epsilon}\right)^2\right]^{1/2}. \tag{2.169}$$

Thus, this just corresponds to the case of a variable time-step length. Indeed, by defining $\epsilon(t) = \epsilon\sqrt{1 + g_y^2}$ we have that:

$$\Delta s = \epsilon(t) \left[1 + \left(\frac{\Delta x}{\epsilon(t)}\right)^2\right]^{1/2}. \tag{2.170}$$

The partition function is then obtained by simply replacing ϵ by $\epsilon(t)$ everywhere, including the measure and overall factor that multiplies the propagator. By doing this we reach again a polymer problem on the plane, were now the total polymer length has changed to:

$$L = \int_0^{L_0} dy\sqrt{1 + g_y^2}, \tag{2.171}$$

as expected. Thus, again, the extrinsic curvature does not bring any modifications to the polymer problem.

Finally, for the third case we have that:

$$\Delta s = \epsilon \left[1 + (1+c^2) \left(\frac{\Delta x}{\epsilon} \right)^2 + 2 c g_y \left(\frac{\Delta x}{\epsilon} \right) + g_y^2 \right]^{1/2}. \tag{2.172}$$

Notice that this is genuinely different from the previous two cases. The new linear term that has appeared does not allow us to make the change of variables to the same-time arclengths or rescaling the time that mapped the problem back to a plane. Moreover, it shifts the center of our distributions, and thus it provides corrections to the free energy of the system. This contribution, as we mentioned at the beginning of this section, can only come from a wall or boundary effect. Indeed, for this kind of parametrization the polymer problem in the plane and on the manifold do not share straight boundaries. As we saw in the previous section, having uneven walls contributes with a linear term in the action. In order to show this explicitly, notice first that we can rewrite Eq. (2.172) as:

$$\Delta s = \sqrt{1+g_y^2}\epsilon \left[1 + \frac{1+c^2}{1+g_y^2} \left(\frac{\Delta x}{\epsilon} \right)^2 + \frac{2 c g_y}{1+g_y^2} \left(\frac{\Delta x}{\epsilon} \right) \right]^{1/2}. \tag{2.173}$$

Then, we can go into coordinates defined along the manifold. In this change of coordinates, y remains intact while the lateral coordinates transform as:

$$x' = \sqrt{1+c^2} x + \frac{c}{\sqrt{1+c^2}} g(y). \tag{2.174}$$

Inverting this mapping and considering a small deviation we see then that:

$$\frac{\Delta x}{\epsilon} = \frac{1}{\sqrt{1+c^2}} \frac{\Delta x'}{\epsilon} - \frac{c g_y}{1+c^2}. \tag{2.175}$$

Rewriting our action, Eq. (2.173) in these new coordinates we obtain that:

$$\Delta s = \sqrt{1+g_y^2}\epsilon\left[1+\frac{1}{1+g_y^2}\left(\left(\frac{\Delta x'}{\epsilon}\right)^2-\frac{c^2 g_y^2}{(1+c^2)}\right)\right]^{1/2}, \tag{2.176}$$

or:

$$\Delta s = \epsilon\left[1+\left(\frac{g_y}{\sqrt{1+c^2}}\right)^2+\left(\frac{\Delta x'}{\epsilon}\right)^2\right]^{1/2}. \tag{2.177}$$

On the other hand, the measure of the path-integral transforms as: $\sqrt{1+c^2}dx_i \rightarrow dx_i'$. Now, notice that the height achieved by the manifold, measured from the tilted plane $z = cx$, is precisely $g/\sqrt{1+c^2}$. Using this, we can see that, through the change of coordinates, we have reached exactly the previously discussed case, which can be addressed by a rescaling of ϵ. The important thing to notice though is that our initial boundary conditions where hardcore walls at $x = 0$ and $x = L$. Under our mapping, these go into: $x' = cg(y)/\sqrt{1+c^2}$ and $x' = (L+cg(y))/\sqrt{1+c^2}$, which are clearly non-straight lines. As discussed previously this is the source of the corrections to the free energy.

Thus, recapitulating, a locally flat manifold (i.e., without intrinsic curvature), but with non-zero extrinsic curvature, can only contribute through boundary effects. The extrinsic curvature by itself does not provide any changes to the partition function of the system.

2.9.4 Manifolds with non-zero intrinsic curvature

In this section we focus on the problem of Monge patches with non-zero intrinsic curvature. Recall that for a single time slice the action was given by

$$\Delta s = \left[(\Delta y)^2+(1+f_x^2)(\Delta x)^2+2f_x f_y \Delta x(\Delta y)+f_y^2(\Delta y^2)\right]^{1/2}. \tag{2.178}$$

The first thing that we may notice is that, in the general case, and just as in the case of the sphere, polymers at different positions will have different unstretched lengths. In order to isolate the effects of curvature, we need to change our coordinate system to a different one in which all the paths described by a constant x end up having the same length, which we can use as the new time parameter. Calling this length t, we see then that the relationship between y, t and x is obtained by solving

$$t = \int_0^{y(x,t)} dy' \sqrt{1 + f_y(x, y')} \tag{2.179}$$

for $y(x,t)$. Although this cannot be done in general, notice that

$$\Delta y = \frac{\partial y}{\partial x}\Delta x + \frac{\partial y}{\partial t}\Delta t, \tag{2.180}$$

and so, in principle, we only require the partial derivatives of y with respect to x and t. We can obtain these by differentiating Eq. (2.179). Indeed, by differentiating with respect to x, we obtain that

$$\frac{\partial y}{\partial x} = -\frac{1}{\sqrt{1 + f_y(x, y(x,t))^2}} \int_0^{y(x,t)} dy' \frac{f_y(x, y') f_{xy}(x, y')}{\sqrt{1 + f_y(x, y')^2}}, \tag{2.181}$$

and

$$\frac{\partial y}{\partial t} = \frac{1}{\sqrt{1 + f_y(x, y(x,t))^2}}. \tag{2.182}$$

Thus, by defining

$$\Omega(x,t) \equiv -\int_0^{y(x,t)} dy' \frac{f_y(x, y') f_{xy}(x, y')}{\sqrt{1 + f_y(x, y')^2}},\ \Lambda(x,t) \equiv \sqrt{1 + f_y(x, y(x,t))^2} \tag{2.183}$$

we have that

$$\Delta y = \frac{1}{\Lambda(x,t)} \left(\Omega(x,t)\Delta x + \Delta t\right). \tag{2.184}$$

Using this in Eq. (2.178), we obtain then that

$$\Delta s = \left[(\Delta t)^2 + \frac{(\Lambda f_x + \Omega f_y)^2 + \Lambda^2 + \Omega^2}{\Lambda^2}(\Delta x)^2 + 2\left(\Omega + \frac{f_y f_x}{\lambda}\right)(\Delta x \Delta t)\right]^{1/2}, \tag{2.185}$$

which we rewrite as

$$\Delta s = \epsilon \left[1 + \frac{(\Lambda f_x + \Omega f_y)^2 + \Lambda^2 + \Omega^2}{\Lambda^2}\left(\frac{\Delta x}{\epsilon}\right)^2 + 2\left(\Omega + \frac{f_y f_x}{\Lambda}\right)\frac{\Delta x}{\epsilon}\right]^{1/2}, \tag{2.186}$$

where we have redefined the cutoff as $\epsilon \equiv \Delta t$. The path-integral measure matching the new equal-time curves is then given by

$$\left[\frac{(\Lambda f_x + \Omega f_y)^2 + \Lambda^2 + \Omega^2}{\Lambda^2}\right]^{1/2} dx \tag{2.187}$$

Now, recall that we have assumed smoothness, small curvature and a slow variation of the manifold, conditions that we translated mathematically into $f_x, f_y \ll 1$. This also translates to Ω, i.e., $\Omega \sim f_y^2 \ll 1$. However, we have not compared how small these quantities are with respect to the pure scale: $(\beta A \epsilon)$. In order to proceed and have an appropriate small deflection approximation that matches the measure of the path-integral, we assume that these quantities are such that: $f_x^2 f_y^2 (\Delta x)^2/\epsilon^2$ and $\Omega f_x f_t (\Delta x)^2/\epsilon^2$ and $\Omega^2(\Delta x)^2/\epsilon^2$ are smaller that $(A\beta\epsilon)^2$, and thus negligible. In this case, we can safely expand the square root and ignore the constant term, obtaining

$$A\beta\Delta s = \frac{A\beta\epsilon}{2}\left[\frac{(\Lambda f_x + \Omega f_y)^2 + \Lambda^2 + \Omega^2}{\Lambda^2}\left(\frac{\Delta x}{\epsilon}\right)^2 + 2\left(\Omega + \frac{f_y f_x}{\Lambda}\right)\frac{\Delta x}{\epsilon}\right]. \tag{2.188}$$

With this, we are now in condition to obtain the analog to the Schrödinger equation. We again do this by following Feynman's method. As usual, recall that, under the assumptions of the small fluctuations approximation and that ϵ is much smaller than the typical length-scales over which the manifold changes, all of the corrective terms that will give rise to changes in operator ordering are negligible. Thus we immediately write the expansion for the propagator:

$$(1+\epsilon\partial_t)K(x,t;x_0,t_0) = \left[\frac{\beta A((\Lambda f_x+\Omega f_y)^2+\Lambda^2+\Omega^2)}{2\pi\Lambda^2\epsilon}\right]^{1/2} \times \int d\eta e^{-\frac{\beta A\epsilon}{2}\left[\frac{(\Lambda f_x+\Omega f_y)^2+\Lambda^2+\Omega^2}{\Lambda^2}\left(\frac{\eta^2}{\epsilon}\right)^2+2\left(\Omega+\frac{f_y f_x}{\Lambda}\right)\frac{\eta}{\epsilon}\right]}\left(1-\eta\partial_x+\frac{1}{2}\eta^2\partial_x^2\right)K(x,t;x_0,t_0). \tag{2.189}$$

After integrating over η we obtain that

$$(1+\epsilon\partial_t)K(x,t;x_0,t_0) = e^{\frac{\beta A\epsilon/2(\Lambda\Omega+f_y f_x)^2}{\Lambda f_x+\Omega f_y)^2+\Lambda^2+\Omega^2}} \times \left(1+\epsilon\Lambda^2\frac{\Omega+f_y f_x/\Lambda}{(\Lambda f_x+\Omega f_y)^2+\Lambda^2+\Omega^2}\partial_x + \frac{\epsilon\Lambda^2}{2\beta A((\Lambda f_x+\Omega f_y)^2+\Lambda^2+\Omega^2)}\partial_x^2+\ldots\right)K(x,t;x_0,t_0). \tag{2.190}$$

Under our set of approximations and conditions, the term in the exponential is small. Expanding in ϵ and collecting its powers we reach then the following Schrödinger equation

$$\partial_t\Psi = \frac{\Lambda^2}{(\Lambda f_x+\Omega f_y)^2+\Lambda^2+\Omega^2)}\left[\frac{1}{2\beta A}\partial_x^2+\left(\Omega+\frac{f_y f_x}{\Lambda}\right)\partial_x+\frac{\beta A}{2}\left(\Omega+\frac{f_y f_x}{\Lambda}\right)^2\right]\Psi, \tag{2.191}$$

and so we identify the Hamiltonian of the system as

$$\hat{H} = \frac{\Lambda^2}{(\Lambda f_x + \Omega f_y)^2 + \Lambda^2 + \Omega^2)} \left[\frac{\hat{p}^2}{2\beta A} - i \left(\Omega + \frac{f_y f_x}{\Lambda} \right) \hat{p} - \frac{\beta A}{2} \left(\Omega + \frac{f_y f_x}{\Lambda} \right)^2 \right]. \tag{2.192}$$

Physically, this resembles a particle with a time and position dependent mass subjected to an electromagnetic field, although with a complex vector potential. This is of course due to the imaginary time formalism. It does not, though, have the form of a Hamiltonian with minimal coupling. Indeed, this is because of the small fluctuation approximation that allows us to neglect terms that would change the order of the operators. So, in principle, we could also write the Hamiltonian as with a minimal coupling, as the extra terms will yield negligible corrections. Notice that the first derivatives in this case arise because of the breaking of the mirror symmetry along the preferred direction due to curvature and thus it cannot be neglected *a priori*.

Now, since the curvature is small, the Hamiltonian can clearly be written as a perturbation over the flat polymer problem. The perturbative potential in this case is given by

$$\hat{V} = -\frac{\Omega^2 + (\Lambda f_x^2 + \Omega f_y^2)^2}{\Lambda^2} \left[\frac{\hat{p}^2}{2\beta A} - i \left(\Omega + \frac{f_y f_x}{\Lambda} \right) \hat{p} - \frac{\beta A}{2} \left(\Omega + \frac{f_y f_x}{\Lambda} \right)^2 \right], \tag{2.193}$$

and as usual, up to first order in the curvature, we have that the universal correction to the free energy is given by:

$$\delta F_U = \int_0^L dt \langle \text{g.s.} | V | \text{g.s.} \rangle. \tag{2.194}$$

In general, this is quite a complicated expression, as it requires to explicitly compute y as a function of t and then integrate it in order to obtain Ω. However, there is a situation in which everything simplifies. Indeed, if we assume that

$$f(x,y) = h(x) + g(y), \tag{2.195}$$

in where h and g are arbitrary functions, then we have that $\Omega = 0$ and y does not depend on x anymore. Indeed in this case, we have that the unstretched length of each polymer does not depend on its position and therefore the change of variables in longer needed. Thus, we could have just continued using y as our time.

Indeed, since

$$\frac{\partial}{\partial t} = \frac{\partial y}{\partial t}\frac{\partial}{\partial y} = \frac{1}{\sqrt{1+g_y^2}}\partial_y \tag{2.196}$$

we obtain then the following modified Hamiltonian

$$\hat{H} = \frac{\sqrt{1+g_y^2}}{1+h_x^2}\left[\frac{\hat{p}^2}{2\beta A} - i\left(\frac{g_y h_x}{\sqrt{1+g_y^2}}\right)\hat{p} - \frac{\beta A}{2}\left(\frac{h_y g_x}{\sqrt{1+g_y^2}}\right)^2\right]. \tag{2.197}$$

and thus, we have the quantum perturbation

$$\hat{V} = -\left(h_x^2 - \frac{1}{2}g_y^2\right)\left[\frac{\hat{p}^2}{2\beta A} - i\left(g_y h_x\right)\hat{p} - \frac{\beta A}{2}\left(g_y h_x\right)^2\right], \tag{2.198}$$

in where we used that g_y is small. Finally, note that although the last term seems to be a second order correction, it yields terms that are bigger than a true second order corrections coming from the momentum terms. Thus, we can safely compute its contribution using firs order perturbation theory.

2.10 Final remarks

In this work we have successfully extended the formalism of quantum analogs to treat systems of strongly repulsive directed polymers in complicated geometries. First, by using path-integrals in curvilinear coordinates and using the small fluctuation approximation, we

were able to extend the problem to polymers anchored to curved edges), directed along the normal direction to this edge. We found that, although we could craft formal theory and find proper quantum analogs (usable for any such convex edge, analytical corrections can only be found in the limit of almost circular shapes. In order to compute this corrections we developed, in close analogy with time dependent perturbation theory in quantum mechanics, an appropriate perturbation scheme. We also found that the increasing amount of space available to the polymers (as a consequence of a bigger radial distance) conspire against the use of groundstate dominance, and thus, in order to obtain analytical results, we are restricted to cover only small sectors of the substrate. More general setups would require to work with a large number of excited states of many-particle systems, and thus are best suited for numerical computations.

Although the loss of groundstate dominance constrains the regime of applicability of our results, the techniques used to craft the extension are general enough to be used in different setups in which groundstate dominance is not lost, such as uneven walls and polymers over curved surfaces, extensions that we also forged. In the latter case, we saw that, in general, quantum analogs are hard to obtain and can only be achieved under a very mild curvature. In particular, the direction of alignment plays an important role. If this direction is close to a direction that the polymer would take by following a geodesics of the substrate, then a proper quantum analog can be achieved. However, more extreme situations lead to the breaking of the small fluctuation approximation, and therefore, to distributions that differ from the distributions appearing in quantum path-integrals. Indeed, the expansion of the square root of the action in the polymer system is tricky and should be handled with care, especially when using non-orthogonal coordinates.

Finally, we close this chapter by remarking that the process of using quantum analogs is exact almost exclusively in the flat original system. By doing a formal analysis of the

small fluctuation and continuum approximations, which the existing literature does not pay too much attention to, we have learned that in contrast to quantum mechanics, the polymer system requires a finite timestep or cutoff. This condition can lead to big differences between the two systems, such as the appearance of new terms in the Hamiltonian, which do not appear in a quantum system. Another big difference between the two systems, that arises due to the finite size of the timestep, is the issue of operator ordering. While in quantum mechanics this is a severe issue, the small fluctuation approximation employed in the problem of directed polymers makes this problem irrelevant, as different orders contribute with negligible terms.

CHAPTER 3
FLOCKING AND THE QUANTUM ANALOGY

The study of active or self propelled particles has received an increasing attention over the years. We use this term to refer to agents or particles that either have an energy reservoir or consume energy from the environment in order to achieve systematic motion [40]. The most basic example would be a particle with an engine that produces constant thrust. As such, real examples are abundant in biological systems in a wide spectrum of length-scales: from molecules [41], to systems of microorganisms such as cells or bacteria [42], to collections of live animals [43, 44, 45]. However, living systems are not the only ones that can be described as active; since the unifying characteristic is systematic motion, we can also have non-living systems such as colloids [46] or robots [47].

Complementing this wide spectrum of realizations is the fact that systems of these particles are by themselves physically interesting. The energy consumption processes associated to these systems breaks time-reversal symmetry and drives them out of equilibrium. In addition, interactions between these particles are not bound to conserve energy or momentum. This intrinsic non-equilibrium nature can yield striking emergent phenomena which cannot exist in equilibrium systems, and that greatly differ from the behavior of their individual constituents, such as pattern formations, wave propagation and order-disorder transitions. Among these, one important case is orientational order. In general, active particles, such as bacteria or birds, have elongated shapes, which result in interactions which foster this kind of order [48].

The prime example of an orientational phase transition is the flocking transition. Here, we consider systems of self-propelled particles that try to align the orientations of their

movement. The transition is achieved when the average orientation of the system reaches a non-zero value and long-range correlations. The seminal model of such system is the Vicsek model [49]. In this model, self-propelled particles constrained to a two-dimensional plane travel at constant speed, but with a variable direction. The way in which these particles decide where to move is a combination of stochastic effects and interactions: at each time step, the particle's direction of movement is taken to be the average of the direction of its neighbors falling inside a given radius, plus some random deviation produced by a gaussian white noise with no time correlation. Hence, the system is Markovian. In these terms, if one thinks in the orientation of the particles as a spin degree of freedom, this model is very similar to the XY model of equilibrium statistical mechanics. The substantial difference is the self-propulsion of the particles. Indeed, numerical simulations showed that, in a certain parameter regime, the particles aligned in a given direction, hence spontaneously breaking the rotational symmetry of the system. Variations of this model, such as Refs. [50, 51, 52] also show a similar result.

From the physical point of view, this is striking since this cannot happen in a two-dimensional system in thermal equilibrium. Indeed, the Mermin-Wagner theorem [53] states that continuous symmetries, such as the rotational one, cannot be spontaneously broken in systems with dimension equal or lesser than two. However, theorems, in addition to conclusions, have also conditions, and one important condition for the Mermin-Wagner theorem is that the system must be in thermal equilibrium. Thus, the self-propulsion of the particles, which is the only difference with an equilibrium system, must be the responsible factor behind this long-range order.

The link between the appearance of this two-dimensional long-range order and the self-propulsion was successfully explained by Toner and Tu in Ref. [54]. Indeed, in a very similar way to the Ginzburg-Landau theory of phase transitions, these authors write, using

only symmetry restrictions, a general stochastic hydrodynamic equation for the velocity field of the particles

$$\begin{aligned}
&\partial_t \boldsymbol{v} + (\boldsymbol{v}\cdot\nabla)\boldsymbol{v} = \alpha\boldsymbol{v} - \beta|\boldsymbol{v}|^2 - \nabla P_r + D_L\nabla(\nabla\cdot\boldsymbol{v}) + D_1\nabla^2\boldsymbol{v} + D_2(\boldsymbol{v}\cdot\nabla)^2\boldsymbol{v} + \boldsymbol{f},\\
&P_r = \sum_{n=1}^{\infty}\sigma_n(\rho-\rho_0)^n,\\
&\partial_t\rho + \nabla\cdot(\rho\boldsymbol{v}) = 0.
\end{aligned} \tag{3.1}$$

Here $\boldsymbol{v}$ is the velocity field, ρ is the density (see the lower equation), P_r the pressure, assumed to be density dependent (see the middle equation), and in where β, D_1, D_2 and D_L are positive coefficients, possibly density dependent. Finally, $\boldsymbol{f}$ is a random stochastic force.

A linear stability analysis of an ordered solution of this equation shows the appearance of instabilities. However, by rescaling the system and using renormalization group methods, Toner and Tu show that the linearized equation breaks down as the transition is taking place. Hence, the non-linear terms of the system, which originate due to the self-propulsion, must be included in the analysis. By doing so, the system is shown to have long-range order, even in two-dimensions, in which case the critical exponents can be computed exactly. The interested reader can find a review of the Toner-Tu theory in Ref. [55].

Although the Toner-Tu approach allows the acquisition of general results about active media systems, it has the disadvantage that the hydrodynamic coefficients are unknown. Indeed, a microscopic, model dependent approach [56, 57, 58, 46] is needed to see the connection between the coefficients and the microscopic parameters. This connection can lead to interesting applications. For example, in experimental realizations of active fluids [46, 41], this connection between microscopics and hydrodynamics can be used to construct design principles targeting the realization of novel materials and devices. Recent work has

focused on the robustness of active liquids against disorder [59], the design of flow patterns in confined active fluids [60, 61, 62, 63, 64], and the use of such channel networks for the design of topological metamaterials [65] and logic gates [66].

One specific challenge is that the coarse graining of a microscopic model of self-propelled particles is, in general, technically difficult. As a result, specific counter-intuitive phenomena associated with active-liquid hydrodynamics are difficult to describe in generic, model-independent terms. In this pursuit, the introduction of additional minimal models of self-propelled particles, along with their coarse-grained hydrodynamics, can strengthen the connection between small- and large-scale phenomena in active systems.

In this work [6], we introduce a particularly simple, minimal model of self-propelled particles and explore their individual and collective statistics in order to arrive at a hydrodynamic description. This two-dimensional model is particularly tractable due to its connection to the Schrödinger equation that describes the statistics of a quantum particle. As such, we use basic results from quantum mechanics to develop physical intuition for active-fluid phenomena. For example, we describe active-liquid analogs for such well-known quantum-mechanical concepts as spin, spin-orbit coupling, and the Heisenberg uncertainty principle. We discuss how the analog of a spinor can be used to introduce a propulsion direction via spin-orbit coupling. We then construct a probabilistic, Fokker-Planck interpretation for the dynamics of a single self-propelled particle in the presence of positional Brownian noise, see Figure 3.1. We show that the microscopic model we consider includes feedback between rotational and translational (or positional) noise, which we interpret as an analog of the Heisenberg uncertainty relation within our model. Crucially, we use this single-particle model to construct a hydrodynamic description of many self-propelled particles. We thus obtain simple relations between the coefficients in the Toner-Tu model [54] and the microscopic parameters of individual particles we consider, including their interactions. We can

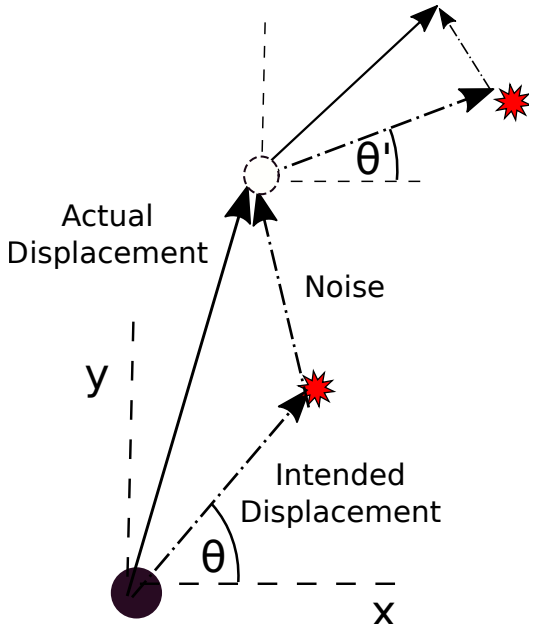

Figure 3.1: Sketch of the single-particle dynamics in the model we consider. The particle has an intended direction of displacement in which it propels at a constant rate, but, along the way,the external positional Brownian noise kicks in, altering the final trajectory of the particle. This noise comes from an external over-damped medium, such as a low Reynolds number fluid, which makes the particle's inertia negligible. At each step, the particles chooses a new angle of displacement, process in which the external noise also has an influence.

then conclude that as for any model in the Toner-Tu universality class, the many-particle system we consider exhibits long-range orientational order in two dimensions [54].

3.1 Model of self-propelled particles

We begin with a well-known connection between non-relativistic quantum mechanics (described via the Schrödinger equation) and statistical mechanics (described via the diffusion equation). Consider the Schrödinger equation

$$i\hbar\partial_t\Psi = \hat{H}\Psi. \tag{3.2}$$

For the free-particle Hamiltonian operator $\hat{H} = \hat{p}^2/2m = -\hbar^2\nabla^2/2m$ upon a rotation of time into the imaginary axis via $t \to -it$, this Schrödinger equation transforms into the

diffusion equation

$$\partial_t \Psi = \frac{\hbar}{2m} \nabla^2 \Psi. \tag{3.3}$$

In the diffusion equation, Ψ can be identified with a particle density ρ and $\frac{\hbar}{2m}$ with a diffusion constant D. This bridge allows us to use tools from quantum mechanics to characterize classical stochastic phenomena. However, this approach does not capture self-propulsion or spontaneous active flow, which cannot be described via the diffusion equation.

In order to capture self-propulsion, each particle ought to carry information about its direction of motion, for which we need to introduce additional degrees of freedom. On the quantum side of the analogy, this additional information encodes a quantum spin state. For a system with spin, Ψ is an n-component spinor, and has additional symmetries with respect to spin rotation, which we consider in the next section. Significantly, a quantum system with *spin-orbit coupling* has a momentum operator that depends on its spin state. We consider the two-dimensional Hamiltonian (with $\hbar = 1$ from now on)

$$\hat{\mathcal{H}} = \frac{1}{2} \left[\boldsymbol{\sigma} \cdot \nabla + m(I - \sigma_z) - \frac{1}{\kappa} \nabla^2 \right], \tag{3.4}$$

where $\boldsymbol{\sigma} \cdot \nabla \equiv \sigma_x \partial_x + \sigma_y \partial_y$ is the spin-orbit coupling term and

$$\sigma_x \equiv \begin{pmatrix} 0 & 1 \\ 1 & 0 \end{pmatrix}, \sigma_y \equiv \begin{pmatrix} 0 & -i \\ i & 0 \end{pmatrix}, \sigma_z \equiv \begin{pmatrix} 1 & 0 \\ 0 & -1 \end{pmatrix}.$$

are the Pauli spin matrices. Of these, (σ_x, σ_y) represent a two-dimensional coordinate frame. In the quantum system if $\kappa \to \infty$, $\hat{\mathcal{H}}$ becomes the two-dimensional Dirac Hamiltonian in the Weyl representation (with a global energy shift).

Dimensionality plays an important role in this description: the one-dimensional Dirac equation is given by $\hat{\mathcal{H}}$ with $\kappa \to \infty$ and for Ψ independent of y. Rotated into imaginary

time, the one-dimensional case yields a description for the time-dependent probability distribution of a persistent random walker. The stochastic process that corresponds to such a walker is called a Poisson process, and the one-dimensional Dirac equation in imaginary time can be restated as telegrapher's equations describing this process. Such walkers move along a line at constant speed and with a turning rate (i.e., rate for changing direction) given by m. This analogy has its origin in Feynman's checkerboard path integral for the one-dimensional Dirac equation [34], which was analyzed in imaginary time in Refs. [67, 68, 69].

Although we develop intuition by considering the quantum side of the analogy, we focus on the mathematical description of self-propelled particles by performing a rotation of time into the imaginary axis via $t \to it$. One of our main results is to show that the (imaginary-time) Schrödinger equation in two dimensions

$$-\partial_t \Psi = \hat{\mathcal{H}} \Psi \tag{3.5}$$

with $\hat{\mathcal{H}}$ given by Eq. (3.4) describes the time-evolution for the probability distribution $\Psi(\boldsymbol{r}, t)$ of a self-propelled particle, with two sources of noise: Positional Brownian noise controlled by the strength of the diffusion constant $1/\kappa$, as well as orientational noise in the polarization angle controlled by the parameter m in the term $m(I - \sigma_z)$. This latter term describes the ability of active particles to change their direction of motion, as it does in the one-dimensional Dirac equation. Another one of our results is that, unlike the one-dimensional case, the two-dimensional Dirac Hamiltonian cannot consistently describe the probability density of a single self-propelled particle: to ensure a physical description, κ must be constrained to be less than $8m$. We now proceed to derive these results.

3.2 Spin, rotation, and velocity

There are several considerations that motivate using spins as carriers of information about the direction of propulsion. We use the spinorial representation of the rotation group in which rotation by an angle θ around an axis $\hat{\mathbf{n}}$ is generated by the unitary operator $\hat{U}_{\hat{\boldsymbol{n}},\theta} = \exp(-i\theta\hat{\mathbf{n}}\cdot\boldsymbol{\sigma}_3/2)$, where we have used the spin vector $\boldsymbol{\sigma}_3$, defined by $\boldsymbol{\sigma}_3 \equiv (\sigma_x, \sigma_y, \sigma_z)$. In our specific case, we are considering particles constrained to live in the xy-plane, and therefore, all rotations are rotations around the z-axis: σ_z generates this abelian two-dimensional rotation group. These rotation operators are given by

$$\hat{U}_\theta = \exp(-i\theta\sigma_z/2) = e^{-i\theta/2}\begin{pmatrix} 1 & 0 \\ 0 & e^{i\theta} \end{pmatrix}. \tag{3.6}$$

As a global phase does not change the physical state, we redefine the operator as

$$\hat{U}_\theta = \begin{pmatrix} 1 & 0 \\ 0 & e^{i\theta} \end{pmatrix}. \tag{3.7}$$

The actions of a rotation on a spinor (a, b) transforms it into $(a, be^{i\theta})$. Note that the phase of the second component of the spinor encodes information about its direction. This reduction to a $U(1)$ type of object is expected, since the group is abelian. Without loss of generality, we choose a frame such that the first component of the spinor is real. Then, the spinor describing a particle with oriented along $\hat{\boldsymbol{n}} = (\cos\theta, \sin\theta)$ is given by

$$\xi = \begin{pmatrix} s_1 \\ s_2 = |s_2|e^{i\theta} \end{pmatrix}, \tag{3.8}$$

with $s_1 \in \mathbb{R}$. The particle orientation is then given by $|s_2|\hat{\boldsymbol{n}} \equiv (\Re s_2, \Im s_2)$, i.e., in terms of real ($\Re$) and imaginary ($\Im$) parts.

We use a spinor to describe the stochastic nature of the orientation. The spinor encodes the orientation of the particle and, in addition, the probability current $|\boldsymbol{j}|$ as well as the probability ρ of finding the particle in a certain position $\boldsymbol{r}$ regardless of its orientation. We show that the spinor encodes this information via $s_1 = \rho$ and $|s_2| = |\boldsymbol{j}|$, and can represent a probability density $P(\boldsymbol{r}, \theta)$ to find the particle at position $\boldsymbol{r}$ oriented along angle θ given by

$$P(\boldsymbol{r}, \theta) = s_1 + \boldsymbol{v}(\theta) \cdot \boldsymbol{s_2}, \tag{3.9}$$

where $\boldsymbol{v}(\theta) = (\cos\theta, \sin\theta)$ and $\boldsymbol{s_2} = (\Re s_2, \Im s_2)$.

The eigenvectors of the x- and y-components of the operator $\boldsymbol{\sigma} = (\sigma_x, \sigma_y)$ correspond to particles oriented along the x- and y-directions, respectively. We then note that $\boldsymbol{\sigma} \cdot \nabla \sim \boldsymbol{v} \cdot \nabla$ is a representation of a convective derivative: $\boldsymbol{\sigma} \cdot \nabla$ propagates the probability density in the direction in which the spinor points. This relation between $\boldsymbol{\sigma}$ and the velocity operator can be gathered directly from a Heisenberg equation of motion. If we consider the simplified Hamiltonian $\mathcal{H} = \boldsymbol{\sigma} \cdot \nabla$, we can express the time derivative of the position operator $\boldsymbol{r}$ (i.e., the velocity operator) as $\boldsymbol{\sigma}$

$$\frac{d\boldsymbol{r}}{dt} = [H, \boldsymbol{r}] = \boldsymbol{\sigma} \cdot [\nabla, \boldsymbol{r}] = \boldsymbol{\sigma}, \tag{3.10}$$

Due to additional terms in the Hamiltonian (3.4), in the model we consider the positional Brownian noise contributes alongside $\boldsymbol{\sigma}$ to the velocity operator.

3.3 Probabilistic interpretation

In order to demonstrate the link between Eq. (3.5) and the motion of self-propelled particles, which can be written in terms of probability densities and currents, we decompose the

spinor Ψ into real and imaginary parts:

$$\Psi = \begin{pmatrix} \rho + i\chi \\ j_x + ij_y \end{pmatrix}, \tag{3.11}$$

where ρ, χ, j_x, and j_y are real functions of the position vector $\boldsymbol{r}$ and time t (and are independent of θ). In this notation, Eq. (3.5) becomes

$$-2\partial_t \rho = \nabla \cdot \boldsymbol{j} - \frac{1}{\kappa}\nabla^2 \rho, \tag{3.12}$$

$$-2\partial_t \chi = -\nabla_\perp \cdot \boldsymbol{j} - \frac{1}{\kappa}\nabla^2 \chi, \tag{3.13}$$

$$-2\partial_t \boldsymbol{j} = \nabla\rho - \nabla_\perp \chi + 2m\boldsymbol{j} - \frac{1}{\kappa}\nabla^2 \boldsymbol{j}. \tag{3.14}$$

where we introduce $\boldsymbol{j} \equiv (j_x, j_y)$ and, for any vector $\boldsymbol{a}$, $\boldsymbol{a}_\perp = (a_y, -a_x)$. Notice that the first of these equations can be interpreted as a continuity equation, with ρ taking the role of a density and $\boldsymbol{j}$ making a contribution to the current.

Under this interpretation, χ is a gauge degree of freedom for the orientation of the local coordinate frame. We make the simplest choice of gauge: $\chi = 0$. Substituting this condition into Eqs. (3.12-3.14), we find

$$-2\partial_t \rho = \nabla \cdot \boldsymbol{j} - \frac{1}{\kappa}\nabla^2 \rho, \tag{3.15}$$

$$\nabla_\perp \cdot \boldsymbol{j} = 0, \tag{3.16}$$

$$-2\partial_t \boldsymbol{j} = \nabla\rho + 2m\boldsymbol{j} - \frac{1}{\kappa}\nabla^2 \boldsymbol{j}. \tag{3.17}$$

We check the consistency of our gauge choice by noting that if Eq. (3.16) is satisfied initially, the evolution given by Eqs. (3.15, 3.17) is consistent with Eq. (3.16). By applying

$\nabla_\perp$ to Eq. (3.17), we indeed find this to hold

$$-2\partial_t(\nabla_\perp \cdot \boldsymbol{j}) = 2m(\nabla_\perp \cdot \boldsymbol{j}) - \frac{1}{\kappa}\nabla^2(\nabla_\perp \cdot \boldsymbol{j}). \tag{3.18}$$

In what follows we define $\boldsymbol{v}(\theta) = (\cos\theta, \sin\theta)$, and use Eq. (3.15) to show that the system of Eqs. (3.15-3.17) is equivalent to a Fokker-Planck equation for the probability density $P(\boldsymbol{r}, \theta) \equiv \rho + \boldsymbol{v}(\theta) \cdot \boldsymbol{j}$, which describes the probability of having a particle between $\boldsymbol{r}$ and $\boldsymbol{r} + d\boldsymbol{r}$ and oriented at an angle between θ and $\theta + d\theta$.

First, we use $\boldsymbol{j} = (\boldsymbol{v} \cdot \boldsymbol{j})\boldsymbol{v} + (\boldsymbol{v}_\perp \cdot \boldsymbol{j})\boldsymbol{v}_\perp$ in Eq. (3.15), multiply Eq. (3.17) by $\boldsymbol{v}$, and add them together to find:

$$-2\partial_t P = (\boldsymbol{v} \cdot \nabla)P + (\boldsymbol{v}_\perp \cdot \nabla)(\boldsymbol{v}_\perp \cdot \boldsymbol{j}) + 2m(\boldsymbol{v} \cdot \boldsymbol{j}) - \frac{1}{\kappa}\nabla^2 P. \tag{3.19}$$

The two remaining terms that have not been expressed in terms of P can be handled in the following way: first, note that $\partial_\theta^2 \boldsymbol{v} = -\boldsymbol{v}$ and thus

$$\boldsymbol{v} \cdot \boldsymbol{j} = -\partial_\theta^2(\boldsymbol{v} \cdot \boldsymbol{j}) = -\partial_\theta^2 P. \tag{3.20}$$

Second, note that $\boldsymbol{v}_\perp \cdot \boldsymbol{j} = -\partial_\theta P$, therefore

$$(\boldsymbol{v}_\perp \cdot \nabla)(\boldsymbol{v}_\perp \cdot \boldsymbol{j}) = (\boldsymbol{v} \cdot \nabla)P - \partial_{\theta,x}^2(P\sin\theta) + \partial_{\theta,y}^2(P\cos\theta). \tag{3.21}$$

Combining Eqs.(3.19-3.21), we arrive at the Fokker-Planck equation

$$\partial_t P = -(\boldsymbol{v} \cdot \nabla)P + \frac{1}{2}\left[\partial_{\theta,x}^2(P\sin\theta) + \partial_{\theta,y}^2(-P\cos\theta) + 2m\partial_\theta^2 P + \frac{1}{\kappa}\nabla^2 P\right]. \tag{3.22}$$

From this expression, we note that m plays the role of a diffusion constant in the orientation θ, whereas κ^{-1} plays that role for the position $\boldsymbol{r}$.

3.4 Microscopic Langevin equation

Not all Fokker-Planck equations can represent random microscopic models. In order to do so, the equations' diffusion matrix must be positive-definite. In this section, we derive and analyze the drift vector and diffusion matrix for the model defined by Eqs. (3.4-3.5) and derive the conditions for which an underlying microscopic model exists.

To begin this analysis, we first replace θ by $z = a\theta$, in where a is a particle length scale, in order to rescale the dimensions in the diffusion matrix. We compare Eq. (3.22) with the usual Fokker-Planck equation:

$$\partial_t P = -\sum_{i=1}^{3} \partial_i(\boldsymbol{\mu}_i P) + \frac{1}{2}\sum_{i,j=1}^{3} \partial_{i,j}^2(D_{ij}P), \tag{3.23}$$

where $\boldsymbol{\mu}$ is called the drift vector and D is called the diffusion matrix. We then read off

$$\mu = (\boldsymbol{v}, 0) = (\cos\theta, \sin\theta, 0), \tag{3.24}$$

using a vector notation in which the third component is the z-variable, and

$$D = \begin{pmatrix} 1/\kappa & 0 & a\sin(\theta)/2 \\ 0 & 1/\kappa & -a\cos(\theta)/2 \\ a\sin(\theta)/2 & -a\cos(\theta)/2 & 2ma^2 \end{pmatrix}. \tag{3.25}$$

As mentioned before, in order to construct a particle-based model for Eq. (3.22), we require that D must be a positive-definite matrix. To check, we find its eigenvalues λ_1, λ_+, and λ_-:

$$\lambda_1 = 1/\kappa \tag{3.26}$$

$$\lambda_\pm = \frac{1}{2}\left(2ma^2 + \frac{1}{\kappa}\right) \pm \frac{1}{2}\left[\left(2ma^2 - \frac{1}{\kappa}\right)^2 + a^2\right]^{1/2}. \tag{3.27}$$

From the expression for λ_-, we conclude that D is positive-definite if and only if

$$8m > \kappa. \tag{3.28}$$

Thus, in order for Eq. (3.22) with $m > 0$ to correspond to a microscopic model, positional Brownian noise must be present, because condition (3.28) cannot hold in the limit $\kappa \to \infty$. This implies that in two-dimensions, the Dirac equation cannot describe a self-propelled particle, in contrast to the one-dimensional case.

Further insight about the relationship between m and κ and their physical interpretation can be gained by deriving the connection between Eq. (3.22) and the underlying microscopic process, i.e., the Langevin equation

$$d\boldsymbol{R}_t = \boldsymbol{\mu}(\boldsymbol{R}_t, t)dt + \Sigma(\boldsymbol{R}_t, t)d\boldsymbol{W}_t, \tag{3.29}$$

in which $\boldsymbol{R}_t$ is a N-dimensional vector representing the random variables, $\boldsymbol{\mu}$ is the associated drift vector (also N-dimensional), $\Sigma(\boldsymbol{R}_t, t)$ is a $N \times M$ matrix and $\boldsymbol{W}_t$ is an M-dimensional Wiener process interpreted either in the Itô or Stratonovich sense [70, 71].

If for the moment we consider an Itô process, then the diffusion matrix D satisfies: $D = \Sigma\Sigma^T$. Notice that if one such Σ_0 satisfies this decomposition, then for any orthogonal matrix R, $\Sigma' = \Sigma_0 R$ also satisfies it, so there are many different Langevin equations that yield the exact same Fokker-Planck equation. Using a Cholesky decomposition, we find a particular solution with $M = 3$

$$\Sigma = \begin{pmatrix} \kappa^{-1/2} & 0 & 0 \\ 0 & \kappa^{-1/2} & 0 \\ \frac{a\kappa^{1/2}}{2}\sin(\theta) & -\frac{a\kappa^{1/2}}{2}\cos(\theta) & 2^{1/2}a\left[m - \frac{\kappa}{8}\right]^{1/2} \end{pmatrix}, \tag{3.30}$$

which yields the following Langevin equation for $\boldsymbol{R} = (x, y)$ and θ:

$$d\boldsymbol{R} = \boldsymbol{v}(\theta)dt + \kappa^{-1/2}\boldsymbol{\xi}dt \tag{3.31}$$

$$d\theta = \frac{\kappa^{1/2}}{2}(\boldsymbol{v}_{\perp}(\theta)\cdot\boldsymbol{\xi})dt + \sqrt{2}\left[m - \frac{\kappa}{8}\right]^{1/2}\xi_3 dt \tag{3.32}$$

Here $\boldsymbol{\xi} = (\xi_1, \xi_2)$ is the two-dimensional positional Brownian noise (i.e., affecting the position of the particle), while ξ_3 is an internal noise altering the pointing angle. Notice that to identify this process we assumed that this was an Itô stochastic differential equation. Generally, this differs from a Stratonovich process by an extra noise-induced drift vector

$$\boldsymbol{\mu}_i = \frac{1}{2}\sum_{k,j=1}^{3}(\partial_j \Sigma_{ik})\Sigma_{jk}. \tag{3.33}$$

In our case though, this term is identically zero, and thus Eqs. (3.31-3.32) can also be seen as an Stratonovich stochastic differential equation.

3.5 Noise and the uncertainty principle

Let us now discuss the physical picture of single-particles dynamics described by Eqs. (3.31-3.32). This microscopic model has similarities to models of active particles used, for example in Refs. [49, 72]. At each instant in time, a particle is oriented at an angle θ and makes an attempt to propagate in the associated direction at a constant speed. However, positional Brownian noise can change the direction of propagation relative to the particle's polarization (the direction of their intended displacement). As a unique feature, the model we consider has a feedback between the positional Brownian and rotational noises: The larger the positional Brownian noise, the weaker the rotational noise. Quantitatively, if we define α_ξ to be the angle for the positional Brownian noise $\boldsymbol{\xi} = (\xi_1, \xi_2)$, we can rewrite the

rotational noise term $\kappa^{1/2}(\boldsymbol{v}_\perp(\theta)\cdot\boldsymbol{\xi})/2$ from Eq. (3.32) as

$$\frac{\kappa^{1/2}|\boldsymbol{\xi}|}{2}\sin(\theta-\alpha_\xi). \tag{3.34}$$

From Eq. (3.34), we note that particles try to oppose the external noise, and prefer to align opposite to the direction of each Brownian kick. This coupling acts as a guidance system: in the absence of external noise, the particle does not know where to point. This is a consequence of how κ enters Eq. (3.32): positional Brownian noise strength is *inversely* proportional to $\kappa^{1/2}$, whereas rotational noise strength is proportional to $\kappa^{1/2}$. Thus, a particle depends on feedback from external noise to decide where to go. A curious analogy emerges from the physics of hair cells in the inner ear, which depend on the presence of external noise to complete their function [73].

To further examine this feature, consider the extreme case when m is just slightly bigger than the lower-bound $\kappa/8$, i.e., $m=\kappa/8+\epsilon$, with $\epsilon/\kappa\ll 1$. If ϵ is sufficiently small, then rotational noise will become irrelevant compared to the positional Brownian noise's contribution and Eq. (3.32) becomes

$$d\theta=\frac{\kappa^{1/2}|\boldsymbol{\xi}|}{2}\sin(\theta-\alpha_\xi)dt. \tag{3.35}$$

In this regime, noise dominates over the self-propelled component of particle motion. The strength of this noise, quantified by $\kappa^{-1/2}$, is not subjected to any restrictions and both the large- and small-noise regimes are physically accessible.

Curiously, the interplay between the strength of the positional Brownian noise and its effect on the polarization are an expression of an uncertainty principle in this model. To see this, disregard the drift and consider the feedback on the angle as simple additive noise. Then one would have that $\langle[\boldsymbol{R}(t)-\boldsymbol{R}(0)]^2\rangle\sim 4t/\kappa$ and $\langle[\theta(t)-\theta(0)]^2\rangle\sim t\kappa/2$, which

leads to the relation

$$\frac{1}{t^2}\langle[\boldsymbol{R}(t)-\boldsymbol{R}(0)]^2\rangle\langle[\theta(t)-\theta(0)]^2\rangle \sim 2. \tag{3.36}$$

Since θ is directly related with direction of propagation, this is a direct analog of the Heisenberg uncertainty principle which relates the uncertainty between the position and velocity of a quantum particle.

Examples of systems with external positional Brownian noise include systems of self-propelled hard rods [74, 75, 76]. These systems have been studied with and without inertia, but in general, the angular and external noises are assumed to be uncorrelated. A situation more similar to ours is explored in [77], in which external noise, called active noise, affects both the angular and positional degrees of freedom. However, this has been done with inertia and yields a different Fokker-Planck equation and a different physical interpretation: instead of having the external noise altering the direction of movement, is the actual direction of movement that alters the fluctuations that the system can exhibit.

To conclude this section, let us generalize this interplay between positional Brownian and rotational noise and give it an arbitrary strength. In that case, Eq. (3.32) acquires an extra arbitrary (real) parameter λ via

$$d\theta = \frac{\kappa^{1/2}\lambda|\boldsymbol{\xi}|}{2}\sin(\theta-\alpha_\xi)dt + \sqrt{2}\left[m-\frac{\kappa\lambda^2}{8}\right]^{1/2}\xi_3 dt \tag{3.37}$$

(with $m > \kappa\lambda^2/8$). The parameter λ controls the response of a self-propelled particle to positional Brownian noise. The sign of λ determines the type of response: for $\lambda < 0$, the particle turns in the direction of a Brownian kick, whereas for $\lambda > 0$ as in the case above, the particle opposes the kick. The Fokker-Planck equation associated with the Langevin

dynamics of Eqs. (3.31, 3.37) is given by

$$\partial_t P = -(\boldsymbol{v}\cdot\nabla)P + \frac{\lambda}{2}\left[\partial^2_{\theta,x}(\sin(\theta)P) + \partial^2_{\theta,y}(-\cos(\theta)P)\right] + m\partial^2_\theta P + \frac{1}{2\kappa}\nabla^2 P. \quad (3.38)$$

Although the extra parameter λ introduces more flexibility into the model, it destroys the bridge with the Schrödinger equation with the current spin degree of freedom. However, the uncertainty principle (3.36) still stands, but with a strength modified by λ.

3.6 Hydrodynamics of active spins

Until now we have concluded that the Schrödinger equation with an spin orbit coupling term can be interpreted as an equation for the probability density of a self-propelled particle. Therefore, it is also clear that the many-body Schrödinger equation can be used to describe a system of many such particles, at least in the non-interacting case; for N particles the Hamiltonian takes the form

$$\hat{\mathcal{H}}_N = \frac{1}{2}\sum_{i=1}^{N}\left[\boldsymbol{\sigma_i}\cdot\nabla_i + m(I_i - \sigma_{z,i}) - \frac{1}{\kappa}\nabla_i^2\right]. \quad (3.39)$$

The structure of the spinor can then be inferred the from the probabilistic interpretation. Since we are dealing with non-interacting particles we expect to have that the probability density for the N particles satisfies $P_N(\boldsymbol{r}_1,\theta_1;\ldots;\boldsymbol{r}_N,\theta_N) = \prod_{i=1}^N P(\boldsymbol{r_i},\theta_i)$, where P_i describes the i-th particle. From this we can then extract

$$\begin{aligned}\rho_i(\boldsymbol{r}_i) &= \tfrac{1}{2\pi}\textstyle\int_0^{2\pi} d\theta_i P_i(\boldsymbol{r}_i,\theta_i)\\ &\qquad\qquad ,\\ \boldsymbol{j}_i(\boldsymbol{r}_i) &= \tfrac{1}{\pi}\textstyle\int_0^{2\pi} d\theta_i \boldsymbol{v}(\theta_i) P_i(\boldsymbol{r}_i,\theta_i)\end{aligned} \quad (3.40)$$

and construct the individual spinors: $\Psi_i(\boldsymbol{r}_i)$ just as in the one-particle case. The many-body spinor will then have 2^N components and the following structure: $\Psi^N_{\sigma_1,\ldots,\sigma_2}(\boldsymbol{r}_1,\ldots,\boldsymbol{r}_N) = \prod_{i=i}^N \Psi_{\sigma_i}(\boldsymbol{r}_i)$, very similar to what one has in many-body quantum mechanics.

Notice though that the procedure of obtaining P from Ψ is always possible, the inverse situation is not. The spinorial description assumes that only the first two Fourier modes (in θ) of the probability distribution are non-zero or relevant and disregards all the others. Thus, in order to be able to describe the dynamical situation with the spinorial description it is important that the initial configuration for P satisfies for all $n \geq 2$, $\int_0^{2\pi} d\theta \exp(in\theta)P(\theta) \approx 0$, in the sense that they are much smaller than the typical value obtained for $n = 0$ or 1.

Having identified the structure of the spinor, the Fokker-Planck equation analogous to (3.39) follows through easily:

$$\begin{aligned}\partial_t P_N = &-\sum_{i=1}^{N}(\boldsymbol{v}_i \cdot \nabla_i)P_N \\ &+ \frac{1}{2}\sum_{i=1}^{N}\left[\partial^2_{\theta_i,x_i}(\sin(\theta_i)P_N) + \partial^2_{\theta_i,y_i}(-\cos(\theta_i)P_N) + 2m\partial^2_{\theta_i}P_N + \frac{1}{\kappa}\nabla_i^2 P_N\right]\end{aligned} \tag{3.41}$$

At its core this means that we are simply dealing with N copies of the single-particle problem. The inclusion of interactions then becomes necessary if we want to uncover new phenomena. Since we are dealing with self-propelled particles, an standard choice is the alignment interaction of the XY-model, which enters through a potential in the Langevin equation

$$d\theta_i = V_i(\{\boldsymbol{r}, \theta\})dt + \frac{\kappa^{1/2}}{2}(\boldsymbol{v}_\perp(\theta) \cdot \boldsymbol{\xi})dt + \sqrt{2}\left[m - \frac{\kappa}{8}\right]^{1/2}\xi_3 dt. \tag{3.42}$$

This potential is explicitly given by

$$V_i(\{\boldsymbol{r}, \theta\}) = g\sum_{j(\neq i)} R(\boldsymbol{r}_i - \boldsymbol{r}_j)\sin(\theta_j - \theta_i), \tag{3.43}$$

in where g is the interaction strength and R describes the spatial range of the interaction,

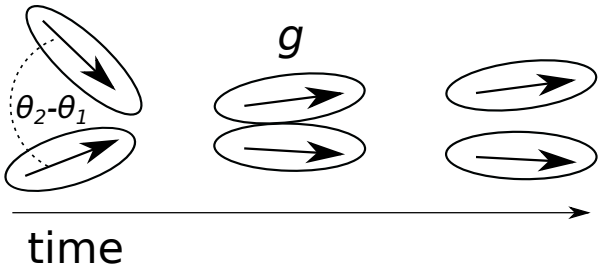

Figure 3.2: Sketch of the process behind the alignment interaction. Elongated active particles interact by trying to align the direction of their polarization, i.e., the orientation of their long semi-axis. Although in this model particles self-propelled along this direction, the presence of the external positional Brownian noise makes the real velocity of the particle to point in a different direction.

i.e., how far apart the interacting particles can see each other. In other words, when two particles are close by, they exchange the information of their intended or pointing angle, and try to align themselves. By close analogy into biology, we can also think in the intended direction as a polarization. As mentioned before, in biological systems such as systems of bacteria, active particles have elongated shapes, which can be thought as an internal polarization. Thus, in order to describe a particle's state we would require the coordinates of its center of mass and the polarization's orientation. In this sense, the potential introduced here then is an alignment between polarizations rather than velocities. See Figure 3.2.

In any case, the inclusion of this two-particle interaction modifies Eq. (3.41) in the following way

$$\begin{aligned}\partial_t P_N = &-\sum_{i=1}^{N}\left[(\boldsymbol{v}_i\cdot\nabla_i)P_N + \partial_{\theta_i}\left(V_i(\{\boldsymbol{r},\theta\})P_N\right)\right] \\ &+\frac{1}{2}\sum_{i=1}^{N}\left[\partial^2_{\theta_i,x_i}(\sin(\theta_i)P_N) + \partial^2_{\theta_i,y_i}(-\cos(\theta_i)P_N) + 2m\partial^2_{\theta_i}P_N + \frac{1}{\kappa}\nabla_i^2 P_N\right].\end{aligned} \tag{3.44}$$

This equation is very difficult to treat exactly, ans thus we will use a self-consistent approximation.

3.7 Self-consistent approximation

In this section we will discuss the introduction of the self-consistent approximation in Eq. (3.44), which is similar to the one considered in Ref. [78]. First, notice that one can rewrite the potential as

$$V_i(\{\boldsymbol{r},\theta\}) = g\Im\left(h(\boldsymbol{r}_i)e^{i\alpha(\boldsymbol{r}_i)}e^{-i\theta_i}\right), \tag{3.45}$$

in were we have defined

$$h(\boldsymbol{r}_i)e^{i\alpha(\boldsymbol{r}_i)} = \sum_{j(\neq i)} R(\boldsymbol{r}_i - \boldsymbol{r}_j)e^{i\theta_j}. \tag{3.46}$$

Then, we approximate by stating that

$$h(\boldsymbol{r}_i)e^{i\alpha(\boldsymbol{r}_i)} \approx \langle h(\boldsymbol{r}_i)e^{i\alpha(\boldsymbol{r}_i)}\rangle_C, \tag{3.47}$$

in where the average $\langle\ \rangle_C$ is taken with respect to the conditional probability of having a particle at $\boldsymbol{r}_i$ and with an orientation θ_i:

$$P(\{\boldsymbol{r}_j,\theta_j\}_{j\neq i}|\boldsymbol{r}_i,\theta_i) = \prod_{\ell(\neq i)} P_\ell(\boldsymbol{r}_\ell,\theta_\ell). \tag{3.48}$$

That is, we think in the interaction as an average external potential. By taking the average we obtain that

$$\langle h(\boldsymbol{r}_i)e^{i\alpha(\boldsymbol{r}_i)}\rangle_C = \sum_{j(\neq i)} \int_0^{2\pi} d\theta_j e^{i\theta_j}\langle R(\boldsymbol{r}_i - \boldsymbol{r}_j)\rangle_{\theta_j}, \tag{3.49}$$

in where

$$\langle R(\boldsymbol{r}_i - \boldsymbol{r}_j)\rangle_{\theta_j} = \int_A d\boldsymbol{r}_j R(\boldsymbol{r}_i - \boldsymbol{r}_j)P_j(\boldsymbol{r}_j,\theta_j). \tag{3.50}$$

For simplicity, we will now consider just a purely contact (zero range) interaction. We achieve this by taking $R(\boldsymbol{r}_i - \boldsymbol{r}_j) = \delta(\boldsymbol{r}_i - \boldsymbol{r}_j)$, which yields

$$\langle h(\boldsymbol{r}_i) e^{i\alpha(\boldsymbol{r}_i)} \rangle_C = \sum_{j(\neq i)} \int_0^{2\pi} d\theta_j e^{i\theta_j} P_j(\boldsymbol{r}_i, \theta_j). \tag{3.51}$$

Thus, within the self-consistent approximation, all of the particles are identical and experience the same forcing. This forcing, in turn, is determined by considering the effect of a particle on its neighbors. Essentially, when studying the bulk of the particles there is nothing that makes one particle more special than the others and in particular, the knowledge that we have of them, regarding their probability densities, can only be inferred from the particle density. Therefore, in terms of probabilities, we consider $P_j(\boldsymbol{r}, \theta) = P(\boldsymbol{r}, \theta)$ for all j. Using this in Eq. (3.51) and taking the $N \gg 1$ limit, we obtain that

$$\langle h(\boldsymbol{r}_i) e^{i\alpha(\boldsymbol{r}_i)} \rangle_C = N \int_0^{2\pi} d\theta e^{i\theta} P_j(\boldsymbol{r}_i, \theta), \tag{3.52}$$

which leads to the following form for a self-consistent potential

$$V_{SC}(\boldsymbol{r}_i, \theta_i) = g h(\boldsymbol{r}_i) \sin(\alpha(\boldsymbol{r}_i) - \theta_i). \tag{3.53}$$

For convenience, we rewrite this expression using an alignment field defined as

$$\boldsymbol{h}(\boldsymbol{r}) = h(\boldsymbol{r}) \boldsymbol{v}(\alpha(\boldsymbol{r})), \tag{3.54}$$

In terms of $\boldsymbol{h}$, we have that

$$V_{SC}(\boldsymbol{r}_i, \theta_i) = g \left(\boldsymbol{h}_\perp(\boldsymbol{r}_i) \cdot \boldsymbol{v}(\theta) \right). \tag{3.55}$$

Notice that the alignment field satisfies $|\boldsymbol{h}(\boldsymbol{r})| = h(\boldsymbol{r})$ and $\boldsymbol{h}(\boldsymbol{r}) = \pi N \boldsymbol{j}$, and thus it is a true measure of an spontaneous alignment between the particles.

Thus, the advantage of this self-consistent approximation is that the many-body Fokker-Planck equation reduces to an effective one-particle non-linear Fokker-Planck equation:

$$\begin{aligned}\partial_t P =& -(\boldsymbol{v}\cdot\nabla)P - g\partial_\theta[(\boldsymbol{h}_\perp\cdot\boldsymbol{v})P] \\ &+\frac{1}{2}\left[\partial^2_{\theta,x}(\sin(\theta)P)+\partial^2_{\theta,y}(-\cos(\theta)P)+2m\partial^2_\theta P+\frac{1}{\kappa}\nabla^2 P\right].\end{aligned} \tag{3.56}$$

Is it possible to introduce a potential term in Eq. (3.4) that could replicate the potential term in the Fokker-Planck equation? By remembering that the spin operator $\boldsymbol{\sigma}$ has a behavior reminiscent of the velocity, we could suggest that a variation of $\boldsymbol{h}_\perp\cdot\sigma$ could do the job. However, there are two issues: (i) The inclusion of such a term, or a variation of it, inevitably leads to a non-zero χ (the imaginary part of the spinor's first component). Recall that throughout the derivation of the probabilistic interpretation it was key to hold this quantity constant ($\chi = 0$). This issue can be surpassed if one is willing to extend the spinor to four components, with the structure $\Psi = (\phi, \bar{\phi})$, and to include additional terms in the Hamiltonian (3.4). (ii) More significantly, the inclusion of the alignment potential in Eq. (3.56) binds together the first two Fourier modes of the distribution with all the rest. As a result, a description based only in the first two modes, as the spinorial one, is insufficient to successfully describe the system, as it does not form a closed system of equations. Therefore, the Schrödinger equation in imaginary time with an spin-orbit coupling term and two-component spinors can describe exactly only non-interacting systems. However an approximate description of the problem with just the first Fourier modes is achievable and leads to a linear stability analysis of the problem. In this sense, the Schrödinger equation can still be used to determine under which conditions the system is stable to perturbations. As we will see later, an extension of the theory considering higher spin numbers allows for a better approximation of the system.

3.8 Onset of alignment

Via the quantum analogy we were able to discover a particular model of self-propelled particles whose sense of direction incorporated feedback from the external positional Brownian noise, obtaining along the way an appropriate Fokker-Planck equation. In this section, we use this equation and a standard approach, based on the dynamics of the angular Fourier modes of P, see Ref.[57], to examine the stability of the isotropic active gas.

As we mentioned in the previous section, a full description of the interacting problem is not achievable by restricting the system to just the first Fourier modes. Therefore, we now proceed to consider the full expansion

$$P(\boldsymbol{r},\theta) = \rho + \boldsymbol{j}\cdot\boldsymbol{v} + \sum_{n\geq 2} \boldsymbol{j}_n \cdot \boldsymbol{v}_n, \tag{3.57}$$

in where $\boldsymbol{v}_n = (\cos(n\theta), \sin(n\theta))$ and $\boldsymbol{j}_n$ are the vectors whose components are the distinct Fourier modes of P, i.e.,

$$\begin{aligned} j_{n,x}(\boldsymbol{r}) &= \frac{1}{\pi}\int_0^{2\pi} d\theta \cos(n\theta) P(\boldsymbol{r},\theta), \\ j_{n,y}(\boldsymbol{r}) &= \frac{1}{\pi}\int_0^{2\pi} d\theta \sin(n\theta) P(\boldsymbol{r},\theta). \end{aligned} \tag{3.58}$$

This expansion is similar to the one introduced in Ref. [57], although this has been done with real Fourier coefficients. Substituting Eq. (3.58) into Eq. (3.56) and taking advantage of the linear independence of the Fourier components leads to the following set of coupled dynamical equations for the Fourier modes

$$
\begin{aligned}
&\partial_t \rho = -\frac{1}{2}\nabla\cdot\left(\boldsymbol{j} - \frac{1}{\kappa}\nabla\rho\right),\\
&\partial_t j_x = \left(\frac{1}{2\kappa}\nabla^2 - m\right) j_x - \frac{1}{2}\partial_x\rho - \frac{3}{4}\nabla\cdot\boldsymbol{j}_2 + g\left(h_x\rho - \frac{1}{2}\boldsymbol{h}\cdot\boldsymbol{j}_2\right),\\
&\partial_t j_y = \left(\frac{1}{2\kappa}\nabla^2 - m\right) j_y - \frac{1}{2}\partial_y\rho - \frac{3}{4}\nabla\cdot\boldsymbol{j}_{2\perp} + g\left(h_x\rho - \frac{1}{2}\boldsymbol{h}\cdot\boldsymbol{j}_{2\perp}\right),\\
&\partial_t j_{2,x} = \left(\frac{1}{2\kappa}\nabla^2 - 4m\right) j_{2,x} - \nabla\cdot\boldsymbol{j}_3 + g\boldsymbol{h}*\boldsymbol{j} - g\boldsymbol{h}\cdot\boldsymbol{j}_3,\\
&\partial_t j_{2,y} = \left(\frac{1}{2\kappa}\nabla^2 - 4m\right) j_{2,y} - \nabla\cdot\boldsymbol{j}_{3\perp} + g\boldsymbol{h}*\boldsymbol{j}_\perp - g\boldsymbol{h}\cdot\boldsymbol{j}_{3\perp},\\
&\vdots
\end{aligned}
\tag{3.59}
$$

where, for compactness, we have defined the $*$ inner product of two vectors as $\boldsymbol{a}*\boldsymbol{b} = a_x b_x - a_y b_y$. As we can see from these equations, it is possible to make higher Fourier modes vanish only if $g = 0$. When we have a non-vanishing interaction, the second Fourier mode feeds the third one. Nevertheless, notice that the dependence of $\boldsymbol{j}_2$ on $\boldsymbol{j}$ is quadratic since $\boldsymbol{h} \propto \boldsymbol{j}$. Thus if we assume that we are in a nearly isotropic state in which $\boldsymbol{j}$ is small compared to ρ, we can also neglect $\boldsymbol{j}_2$. This leads to the linearized theory. This linearization is performed around the disordered phase $\rho = 1/(2\pi A)$, where A is the area of the system. As this approach neglects all stabilizing nonlinear terms, it does not yield a description of the polar active phase. We leave this task for the next section.

The linearized equations are

$$
\begin{aligned}
&\partial_t \rho = -\frac{1}{2}\nabla\cdot\left(\boldsymbol{j} - \frac{1}{\kappa}\nabla\rho\right)\\
&\partial_t \boldsymbol{j} = \left(\frac{1}{2\kappa}\nabla^2 - m\right)\boldsymbol{j} - \frac{1}{2}\nabla\rho + \frac{gN}{2A}\boldsymbol{j}
\end{aligned}
\tag{3.60}
$$

We look for solutions of the form $\rho = \rho_0 e^{\lambda t}$ and $\boldsymbol{j} = \boldsymbol{j}_0 e^{\lambda t}$ and take the spatial Fourier transform. This last step re-expresses gradient terms through the wavevector $\boldsymbol{k} = (k_x, k_y)$. Then, we found that the eigenvalues associated to the system (3.60) are given by

$$\lambda_1 = -\frac{k^2}{2\kappa} - \left(m - \frac{gN}{2A}\right),$$
$$\lambda_{\pm} = -\frac{k^2}{2\kappa} - \frac{1}{2}\left(m - \frac{gN}{2A}\right) \pm \frac{1}{2}\left[\left(m - \frac{gN}{2A}\right)^2 - k^2\right]^{1/2}, \tag{3.61}$$

where $k = |\boldsymbol{k}|$. From Eq. (3.61) we note that, for large wavenumbers (equivalent to short wavelengths) we always get negative real parts for these eigenvalues. This means that short fluctuations in the density can always make the disordered phase stable. Nevertheless, notice that for short wavenumbers (i.e., long wavelengths), these eigenvalues will have a negative real part (thus making the disordered state stable), only if $m > gN/2A$. Given that the spatial density of the system is given by $\rho_d = N/A$, we can rewrite this condition as:

$$m > g\frac{\rho_d}{2}, \tag{3.62}$$

which is the same condition that one finds in the XY and Kuramoto models, of, respectively, two-dimensional spins and synchronizing oscillators (see e.g., Refs. [79, 80]). In the extreme case in which $m \to \kappa/8$, this condition implies that:

$$\frac{1}{4g\rho_d} > \kappa^{-1}, \tag{3.63}$$

which establishes an upper bound for the external positional noise. That is to say, in order to achieve an aligned or ordered state, the external positional noise must overcome a threshold determined by the density and the strength of the interaction. Although this may appear counter intuitive, recall that these particles depend on the external input in order to determine their intended angle of displacement.

The fact that for long wavelengths the system can still exhibit an unstable disordered phase means that, even under the presence of the external positional Brownian noise, the system can still reach an ordered state. This is due to the fact that this noise contributes

with a current that depends on fluctuations of the density. An stable aligned homogeneous states (i.e., independent from position), will not have a contribution of this sort. Therefore, a small deviation from that ideal case will continue to be ordered, as long as the fluctuations are long.

3.9 The polar active liquid

In the previous section we showed that a disordered homogeneous state is not stable for certain values of the system's parameters. In this section we will show that, under the same conditions, the system does present an ordered spatially homogeneous state. This configuration is therefore characterized by a translational symmetry, and thus all spatial derivatives in the Fokker-Planck equation vanish. This leads then to the simplified Fokker-Planck Equation:

$$\partial_t P = g\partial_\theta[(\boldsymbol{h}_\perp \cdot \boldsymbol{v})P] + m\partial_\theta^2 P, \tag{3.64}$$

which has the same form of the Fokker-Planck equation for a stationary XY model, or Kuramoto oscillators with a zero natural frequency. In this homogeneous regime, pressure, or external positional noise, does not explicitly play a role and everything is determined by the orientational noise. It is then not surprising that an aligned phase exists. The exact solution is not hard to obtain and it takes the form $P = \frac{1}{VZ}\exp(-\frac{g}{m}\boldsymbol{h}\cdot\boldsymbol{v})$, in where Z is a normalization constant. Although this is an exact solution, we are interested into exploring the boundary of the phase transition, and thus, it is enough to study the regime in which $\boldsymbol{j}$ is small. It is more illustrative though to operate in terms of a Landau theory; In this regime, we may consider only up to the first three Fourier modes, which yields the following set of

equations:

$$\begin{aligned}
&\partial_t \rho = 0 \\
&\partial_t j_x = -m j_x + g\left(h_x \rho - \frac{1}{2}\boldsymbol{h}\cdot\boldsymbol{j}_2\right) \\
&\partial_t j_y = -m j_y + g\left(h_x \rho - \frac{1}{2}\boldsymbol{h}\cdot\boldsymbol{j}_{2\perp}\right) \\
&\partial_t j_{2,x} = -4m j_{2,x} + g\boldsymbol{h} * \boldsymbol{j} \\
&\partial_t j_{2,y} = -4m j_{2,y} + g\boldsymbol{h} * \boldsymbol{j}_\perp \\
&\vdots
\end{aligned} \tag{3.65}$$

Solving this equations and remembering that $\boldsymbol{h} = \pi N \boldsymbol{j}$ leads then to the following self-consistent equation for the alignment vector $\boldsymbol{h}$

$$\boldsymbol{h} = \frac{\rho_d}{2}\left[\frac{g}{m} - \frac{1}{8}\left(\frac{g}{m}\right)^3 h^2\right]\boldsymbol{h}, \tag{3.66}$$

in where $h = |\boldsymbol{h}|$, and whose non-trivial solution is given by

$$h = 4\left(\frac{m^3}{\rho_d g^3}\right)^{1/2}\sqrt{\frac{\rho_d g}{2m} - 1}. \tag{3.67}$$

Clearly, this solution only exists if $\frac{g\rho_d}{2} \geq m$, which is exactly the same regime in which the disordered phase becomes unstable. Using this, we plot the boundary between the disordered fluid phase and the ordered polar fluid phase in Figure 3.3. Moreover, notice that the self-consistent equation, as well as the equations of motion, can be derived from the following Landau "free energy": $F[\boldsymbol{h}] = \frac{1}{2}\left(m - \frac{\rho_d g}{2}\right)h^2 + \frac{1}{64}\frac{\rho_d g^3}{m^2}h^4 + \ldots$. This just remarks that in states with translational invariance these two models are the same, the difference comes through the displacement of the particles. Finally, note that in order to obtain the ordered polar phase it is crucial that we included the contributions of the higher Fourier modes in the orientational angle, i.e., $\boldsymbol{j}_2$. The coupling of this mode to the lower Fourier modes introduces nonlinearity in the system, which is necessary to stabilize the ordered polar phase.

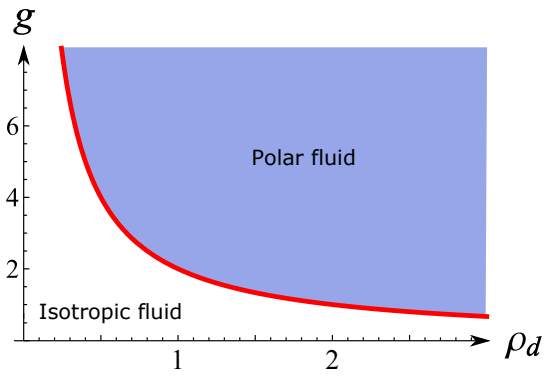

Figure 3.3: Sketch of the flocking phase diagram with $m = 1$. The solid line represents the boundary between the two phases: under the line there is disorder and under the line there is order.

3.10 Hydrodynamic equations: coarse-graining to Toner-Tu theory

Let us now go beyond the assumption of homogeneity and examine the effects of slow, long-wavelength fluctuations in the density and the current for the case of a polar active fluid. This yields the hydrodynamic theory, which, as for any polar active liquid, reduces to a form of Toner-Tu theory [54]. We proceed via the method introduced in [57].

The starting point are the equations of motion, Eq. (3.59). We will assume that the systems is in its ordered state, although only shallowly. Then, up to first approximation $P(\boldsymbol{r}, \theta)$ is almost isotropic (i.e., a weakly ordered regime, with a slight dependence on θ). Physically, this is the same as to say that the hydrodynamic velocity of the system is much smaller than the microscopic velocity of the individual particles. Consequently, we will neglect all Fourier modes higher than $\boldsymbol{j}_2$. For the sake of generality, we will also incorporate the parameter λ from Eqs. (3.37, 3.38), which controls the feedback between the external positional noise and the orientation of the particle. The Schrödinger particles are recovered with $\lambda = 1$. Then, our equations become

$$
\begin{aligned}
&\partial_t \rho = -\frac{1}{2}\nabla\cdot\left(\boldsymbol{j} - \frac{1}{\kappa}\nabla\rho\right),\\
&\partial_t j_x = \left(\frac{1}{2\kappa}\nabla^2 - m\right) j_x + \left(\frac{\lambda-2}{2}\right)\partial_x\rho - \left(\frac{\lambda+2}{4}\right)\nabla\cdot\boldsymbol{j}_2 + g\left(h_x\rho - \frac{1}{2}\boldsymbol{h}\cdot\boldsymbol{j}_2\right),\\
&\partial_t j_y = \left(\frac{1}{2\kappa}\nabla^2 - m\right) j_y + \left(\frac{\lambda-2}{2}\right)\partial_y\rho - \left(\frac{\lambda+2}{4}\right)\nabla\cdot\boldsymbol{j}_{2\perp} + g\left(h_x\rho - \frac{1}{2}\boldsymbol{h}\cdot\boldsymbol{j}_{2\perp}\right),\\
&\partial_t j_{2,x} = \left(\frac{1}{2\kappa}\nabla^2 - 4m\right) j_{2,x} + \left(\frac{\lambda-1}{2}\right)\nabla * \boldsymbol{j} + g\boldsymbol{h} * \boldsymbol{j},\\
&\partial_t j_{2,y} = \left(\frac{1}{2\kappa}\nabla^2 - 4m\right) j_{2,y} + \left(\frac{\lambda-1}{2}\right)\nabla * \boldsymbol{j}_\perp + g\boldsymbol{h} * \boldsymbol{j}_\perp.
\end{aligned}
\tag{3.68}
$$

There are two important aspects in this approximation: First, $|\boldsymbol{j}_2|$ is much smaller than $|\boldsymbol{j}|$ and second, because we are considering the long wavelength approximation, we assume that these quantities change only in length-scales and time-scales much bigger than the microscopic ones. Therefore, we consider the regime

$$
\partial_t \boldsymbol{j}_{2,x}, \partial_t \boldsymbol{j}_{2,y} \ll m\boldsymbol{j}_{2,x}, m\boldsymbol{j}_{2,y}, \tag{3.69}
$$

ans thus we can neglect the time derivatives. In the same way we also neglect the $\frac{1}{\kappa}\nabla^2\boldsymbol{j}_2$ term. Then, by leaving the system in terms of $\boldsymbol{j}$ and remembering that $\boldsymbol{j} = \boldsymbol{h}/\pi N$ and $\rho_d = 2\pi N\rho$, we can rewrite our equations as

$$
\partial_t \rho_d = -\nabla\cdot\left(\boldsymbol{h} - \frac{1}{2\kappa}\nabla\rho_d\right), \tag{3.70}
$$

and

$$\partial_t \boldsymbol{h} = \left[\left(\frac{\rho_d g}{2} - m\right) - \frac{g^2}{8m}h^2\right]\boldsymbol{h} + \left(\frac{\lambda-2}{4}\right)\nabla\rho_d - (\lambda-1)\frac{g}{16m}\left[(\boldsymbol{h}\cdot\nabla)\boldsymbol{h} + (\boldsymbol{h}_\perp\cdot\nabla)\boldsymbol{h}_\perp\right] - (\lambda+2)\frac{g}{8m}\left[\boldsymbol{h}(\nabla\cdot\boldsymbol{h}) - \boldsymbol{h}_\perp(\nabla\cdot\boldsymbol{h}_\perp)\right] + \left[\frac{1}{2\kappa} + \frac{2-\lambda-\lambda^2}{32m}\right]\nabla^2\boldsymbol{h} \quad . \tag{3.71}$$

Finally, the $\boldsymbol{h}_\perp$ terms can be rewritten in a familiar way via

$$\begin{aligned} \boldsymbol{h}_\perp(\nabla\cdot\boldsymbol{h}_\perp) &= \frac{1}{2}\nabla h^2 - (\boldsymbol{h}\cdot\nabla)\boldsymbol{h} \\ (\boldsymbol{h}_\perp\cdot\nabla)\boldsymbol{h}_\perp &= \frac{1}{2}\nabla h^2 - \boldsymbol{h}(\nabla\cdot\boldsymbol{h}) \end{aligned} \quad , \tag{3.72}$$

in where $h = |\boldsymbol{h}|$. The resulting hydrodynamic equation reads

$$\partial_t\boldsymbol{h} + (\lambda+1)\frac{3g}{16m}(\boldsymbol{h}\cdot\nabla)\boldsymbol{h} = \left[\left(\frac{\rho_d g}{2} - m\right) - \frac{g^2}{8m}h^2\right]\boldsymbol{h} + \left(\frac{\lambda-2}{4}\right)\nabla\rho_d + (\lambda+5)\frac{g}{16m}\left[\frac{1}{2}\nabla h^2 - \boldsymbol{h}(\nabla\cdot\boldsymbol{h})\right] + \left[\frac{1}{2\kappa} + \frac{2-\lambda-\lambda^2}{32m}\right]\nabla^2\boldsymbol{h} \quad . \tag{3.73}$$

On the one hand, Eq. (3.70) is the continuity equation associated to the conservation of the number of self-propelled particles. Notice then that $\boldsymbol{h}$, as mentioned before, is not the momentum current of the system. The true momentum current receives an extra contribution from the inhomogeneity of the density which arises due to the presence of external positional Brownian noise.

On the other hand, Eq. (3.73) is the dynamical equation for $\boldsymbol{h}$. The second term on the left-hand side is the equivalent of an advection term. That its prefactor is not one is simply a consequence of the breaking of Galilean invariance (there is only one specific reference frame in which the particles travel with equal speed regardless of their direction of movement). On the right-hand side, the first term is the one responsible for the spontaneous breaking of the rotational symmetry in the polar phase. The second term and third terms

can be thought as pressure like terms. The fourth one can be seen as non-linear feedback from the compressibility while the fifth one can be seen as the usual viscous damping in the Navier-Stokes equations, originated by a mixture of both the external positional noise and its coupling with the orientational one. It is interesting to see that the parameter λ can have interesting effects in the hydrodynamic coefficients. For example, notice that for $\lambda = -1$, i.e., particles that follow the positional noise, the advection term vanishes. In a similar way, taking $\lambda = 2$ makes the pressure feedback independent of spatial density fluctuations. Finally, regarding the effective viscosity of the system, notice that for $\lambda = 1$, that is, our original model, the viscosity reduces to simply $\frac{1}{2\kappa}$, and thus it depends exclusively on the external positional Brownian noise.

Now, this final term may look suspicious given that for large λ it may take negative values (and therefore, unphysical). This is not the case. Recall that we also had the condition: $m \geq \kappa\lambda^2/8$. This is satisfied by writing $m = \kappa(\epsilon + \lambda^2/8)$ $(\epsilon > 0)$. Thus we can write

$$\nu_{\text{eff}} = \frac{1}{2\kappa}\left[1 + \frac{2 - \lambda - \lambda^2}{16(\epsilon + \lambda^2/8)}\right], \tag{3.74}$$

On the one hand we have that, when $2 - \lambda - \lambda^2 < 0$, taking the limit $\epsilon \to 0$ of Eq. (3.74) yields the minimal possible value that the effective viscosity can achieve for each λ. Notice that this it is always positive and converges to $1/4\kappa$ as $\lambda \to \infty$. On the other hand, when $2 - \lambda - \lambda^2 > 0$, we have that the minimum value that the effective viscosity can achieve is $1/2\kappa$. A plot of this coefficient can be found in Figure 3.4.

It is worth mentioning that the previous hydrodynamic equations are compatible with the hydrodynamic equations of Toner and Tu [54], which are based on symmetry considerations. By contrast, we obtain these equations based on the microscopic single-particle model that we introduce in the previous sections along with interparticle interactions. The

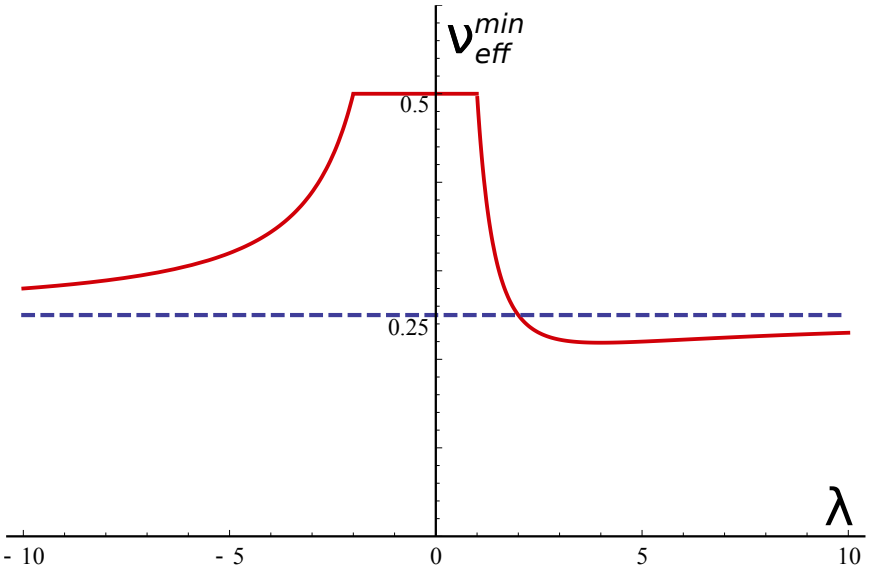

Figure 3.4: Plot of the minimum effective viscosity accessible to the model for a given λ, in units of $1/\kappa$, as a function of the parameter λ, which controls the correlation between the orientational and positional Brownian noise. Notice that this viscosity is always positive. For $-2 \leq \lambda \leq 1$, it presents a plateau at $1/2$. However, when $|\lambda| \gg 1$, it approaches $1/4$. For positive λ this limit is reached from below, while for negatives values the limit is reached from above. As a conclusion, the correlation between the orientational and positional Brownian noise can be used to lower the viscosity of the active fluid.

coefficients that we obtained thus explicitly depend on the microscopic parameters of the model, which allows not only for the form but also for the precise numerical evaluation for the hydrodynamic coefficients in the Toner-Tu equations. Finally, we would also like to mention that in the limit $\kappa \to \infty$, $\lambda \to 0$ with $\lambda^2\kappa \to 0$, our hydrodynamic equations coincide exactly with the ones derived in Ref. [72].

3.11 Generalization to higher spin numbers

Until now we have assumed that the spin degree of freedom in our model is $1/2$, or equivalently, a two component spinor. This choice was made in the interest of simplicity, since in principle the system does not present any fundamental restriction in this regard. Indeed, the only requirement is for the system to be rotationally invariant and, as we know, there are representations of the rotation group for spinors with any number of components. Given this, one could be tempted to try to make this extension by simply replacing the

Pauli matrices with their equivalent spin matrices S_x, S_y and S_z, which satisfy the algebra $[S_i, S_j] = i\epsilon_{ijk}S_k$. However, such an attempt would not work, as the resulting equations will not yield a probabilistic interpretation. The matter of fact is that the spin matrices, S_x, S_y and S_z, are obtained by imposing the entire three-dimensional rotation group symmetry. However, given that our system is two-dimensional, we only require the two-dimensional rotation group. The latter is much more simpler than the former, which gets reflected in the fact that it is abelian, and thus we have much more leeway regarding its representations.

The key observation is that our generalization must be able to yield a probabilistic interpretation. Given the success that we had with truncating the probability density to its first Fourier modes, i.e., $P(\boldsymbol{r}, \theta) = \rho + \boldsymbol{v}(\theta) \cdot \boldsymbol{j}(\boldsymbol{r})$, we can then suggest that truncating the same expression to its first N Fourier modes will gave us the extension we are looking for. Thus, we write

$$P(\boldsymbol{r}, \theta) = \rho + \sum_{n=1}^{N-1} \boldsymbol{v}_n(\theta) \cdot \boldsymbol{j}(\boldsymbol{r}), \tag{3.75}$$

in where $\boldsymbol{v}_n(\theta) = (\cos(n\theta), \sin(n\theta))$. By suggesting this we are implying that the structure of our N-th component spin is given by

$$\Psi_N = \begin{pmatrix} \rho \\ j_x + ij_y \\ j_{2,x} + ij_{2,y} \\ \vdots \\ j_{N-1,x} + ij_{N-1,y} \end{pmatrix}, \tag{3.76}$$

and the rotational operator is given by the matrix

$$R(\theta) = \begin{pmatrix} 1 & 0 & \dots & & & 0 \\ 0 & e^{i\theta} & 0 & & & 0 \\ 0 & 0 & e^{2i\theta} & 0 & \dots & 0 \\ \vdots & \vdots & 0 & \ddots & & \vdots \\ & & \vdots & & \ddots & \\ 0 & 0 & \dots & & & e^{(N-1)i\theta} \end{pmatrix}. \tag{3.77}$$

Having determined the structure of the spinor, we now need to determine the "spin" or velocity matrices that will take the role of the Pauli matrices in Eq. (3.4). Again, the key is to find an operator that would allow us to have a probabilistic interpretation. That is to say, we need a theory that allows for and exact truncation of the probability density to a finite number of Fourier modes. Since the number of possible operators is too big and it is not clear *a priori* if they will lead to a probabilistic interpretation, we follow the inverse route: First, take the Fokker-Planck of our original model, generalized with the parameter λ of Eq. (3.38). By expanding $P(\boldsymbol{r}, \theta)$ in its Fourier modes and only focusing in the dynamical part of the equation, that is, terms with spatial partial derivatives, we see that $\boldsymbol{j}_{N+1}$ satisfy the following equations

$$\begin{aligned} \partial_t j_{N+1,x} &\sim -\left(\frac{(N+1)\lambda + 2}{4}\right) \nabla \cdot \boldsymbol{j}_{N+2} + \left(\frac{(N+1)\lambda - 2}{4}\right) \nabla * \boldsymbol{j}_N, \\ \partial_t j_{N+1,y} &\sim -\left(\frac{(N+1)\lambda + 2}{4}\right) \nabla \cdot \boldsymbol{j}_{N+2\perp} + \left(\frac{(N+1)\lambda - 2}{4}\right) \nabla * \boldsymbol{j}_{N\perp}. \end{aligned} \tag{3.78}$$

By examining Eq. (3.78) we see that if λ takes the specific value

$$\lambda_N = \frac{2}{N+1}, \tag{3.79}$$

then, the equation for $\boldsymbol{j}_{N+1}$ does not depend on the previous Fourier mode $\boldsymbol{j}_N$. Following the structure of Eq. (3.78) we also can see that higher Fourier modes will not depend on

this mode either. Then, solutions with $\boldsymbol{j}_k = 0$, $k \geq N+1$, at $t = 0$, remain being zero throughout the time evolution, and thus we only need a finite number of Fourier modes to describe the theory. Since this Fokker-Planck equation is already linked to a microscopic process, and thus carries a probabilistic interpretation, this is exactly what we are looking for our spinorial theory.

Having identified our theory, we only need to find the coefficients for our "spin" matrices Σ_x and Σ_y. We do this by simply demanding that the equations for the Fourier modes obtained from the Fokker-Planck equation be the same as the ones derived from the spinorial theory. In this way, we obtain that, if

$$-\partial_t \Psi_N \sim (\Sigma_x \partial_x + \Sigma_y \partial_y)\Psi_N, \tag{3.80}$$

then, for $\lambda = \lambda_N$

$$\Sigma_{N,x} = \frac{1}{2}\begin{pmatrix} 0 & 1 & 0 & 0 & \dots & & 0 \\ \frac{2N}{N+1} & 0 & \frac{N+2}{N+1} & \ddots & \ddots & & \vdots \\ 0 & \frac{N-1}{N+1} & 0 & \frac{N+3}{N+1} & \ddots & & \\ \vdots & 0 & \frac{N-2}{N+1} & 0 & \ddots & \ddots & \\ & \ddots & 0 & \ddots & \ddots & \ddots & 0 \\ & & \ddots & \ddots & \ddots & 0 & \frac{2N+1}{N+1} \\ 0 & \dots & & & 0 & \frac{1}{N+1} & 0 \end{pmatrix}, \tag{3.81}$$

and

$$\Sigma_{N,y} = \frac{1}{2}\begin{pmatrix} 0 & -i & 0 & 0 & \dots & & 0 \\ \frac{2N}{N+1}i & 0 & -\frac{N+2}{N+1}i & \ddots & \ddots & & \vdots \\ 0 & \frac{N-1}{N+1}i & 0 & -\frac{N+3}{N+1}i & \ddots & & \\ \vdots & 0 & \frac{N-2}{N+1}i & 0 & \ddots & \ddots & \\ & \ddots & 0 & \ddots & \ddots & \ddots & 0 \\ & & \ddots & \ddots & \ddots & 0 & -\frac{2N+1}{N+1}i \\ 0 & \dots & & & 0 & \frac{1}{N+1}i & 0 \end{pmatrix}. \tag{3.82}$$

Notice that these matrices transform under $R(\theta)$ as a vector, i.e.,

$$R(-\theta)\begin{pmatrix} \Sigma_{N,x} \\ \Sigma_{N,y} \end{pmatrix} R(\theta) = \begin{pmatrix} \Sigma_{N,x}\cos(\theta) - \Sigma_{N,y}\sin(\theta) \\ \Sigma_{N,x}\sin(\theta) + \Sigma_{N,y}\cos(\theta) \end{pmatrix}, \tag{3.83}$$

and thus we continue having rotational symmetry. Now, the reader might object that these matrices are not hermitian. Although this is true, they are similar to an hermitian matrix. Indeed, by defining

$$\alpha_n^N \equiv \left[\frac{N+n}{N+1-n}\right]^{1/2}\alpha_{n-1}, \quad \alpha_1^N \equiv \left[\frac{N+1}{2N}\right]^{1/2}, \tag{3.84}$$

$$Z \equiv \begin{pmatrix} 1 & 0 & \dots & & & 0 \\ 0 & \alpha_1^N & 0 & & & 0 \\ 0 & 0 & \alpha_2^N & 0 & \dots & 0 \\ \vdots & \vdots & 0 & \ddots & & \vdots \\ & & \vdots & & \ddots & \\ 0 & 0 & \dots & & & \alpha_N^N \end{pmatrix}, \tag{3.85}$$

and

$$a_1^N \equiv \left[\frac{N}{2(N+1)}\right]^{1/2}, \quad a_n^N \equiv \frac{1}{2(N+1)}\left[(N+n)(N+1-n)\right]^{1/2}\ (n \geq 2), \tag{3.86}$$

we have that

$$\Sigma_{N,x} = Z^{-1}\begin{pmatrix} 0 & a_1^N & 0 & 0 & \dots & & 0 \\ a_1^N & 0 & a_2^N & \ddots & \ddots & & \vdots \\ 0 & a_2^N & 0 & a_3^N & \ddots & & \\ \vdots & 0 & a_3^N & 0 & \ddots & \ddots & \\ & \ddots & 0 & \ddots & \ddots & \ddots & 0 \\ & & \ddots & \ddots & \ddots & 0 & a_N^N \\ 0 & \dots & & & 0 & a_N^N & 0 \end{pmatrix} Z, \tag{3.87}$$

and

$$\Sigma_{N,y} = Z^{-1}\begin{pmatrix} 0 & -a_1^N i & 0 & 0 & \dots & & 0 \\ a_1^N i & 0 & -a_2^N i & \ddots & \ddots & & \vdots \\ 0 & a_2^N i & 0 & -a_3^N i & \ddots & & \\ \vdots & 0 & a_3^N i & 0 & \ddots & \ddots & \\ & \ddots & 0 & \ddots & \ddots & \ddots & 0 \\ & & \ddots & \ddots & \ddots & 0 & -a_N^N i \\ 0 & \dots & & & 0 & a_N^N i & 0 \end{pmatrix} Z. \tag{3.88}$$

Since matrices in a similarity relationship have the same eigenvalues, and since the Σ's are related to hermitian matrices, we conclude that Σ_x and Σ_y have real eigenvalues. Notice that in order for these quantities to be properly defined (i.e., α_n, Z, and a_n), it was necessary to truncate at the $N+1$-Fourier term with the correct value of λ_N. Otherwise, we would have obtained an undefined or complex α_N, destroying the similarity relationship.

Now, let $\boldsymbol{v}_x$ be an eigenvector of Σ_x with eigenvalue μ. As mentioned before, given the similarity relationship, λ must be real. Additionally, we can always normalize $\boldsymbol{v}_x$ so its first component is one. Given the structure of the spinors, this is compatible with having a real, positive density. Then, the eigenvector equation

$$\Sigma_x \boldsymbol{v}_x = \mu \boldsymbol{v}_x, \tag{3.89}$$

implies the following equation for the second component of $\boldsymbol{v}_x$

$$\frac{1}{2} v_{2x} = \mu. \tag{3.90}$$

Thus, when μ is positive, v_{2x} is positive, when μ is zero, v_{2x} is zero and when μ is negative, v_{2x} is negative. By comparing this with the structure of our spinors, these cases correspond, respectively, to a particle moving to the right, not moving or moving to the left. By a similar argument, we have that if $\boldsymbol{v}_y$ is an eigenvector of Σ_y with eigenvalue μ, then $v_{2y} = 2i\mu$. Therefore, a positive μ matches with a particle moving upwards, a negative μ matches with a particle moving downwards and a zero eigenvalue matches to no movement at all. As such, there is an agreement between the eigenvalues of our spin matrices and the direction of the velocity of the particle under the probability interpretation. This fact, together with a proper transformation under rotations, make Σ_x and Σ_y valid choices for velocity operators, just as σ_x and σ_y were in our two-component theory.

The only piece missing is the extension of the mass term in Eq. (3.4). It is not difficult to see that this term generalizes to

$$M_N = \begin{pmatrix} 0 & 0 & \dots & & & 0 \\ 0 & m & 0 & & & 0 \\ 0 & 0 & 4m & 0 & \dots & 0 \\ \vdots & \vdots & 0 & \ddots & & \vdots \\ & & \vdots & & \ddots & \\ 0 & 0 & \dots & & & N^2 m \end{pmatrix}. \tag{3.91}$$

Then, the Hamiltonian for the system would be:

$$H_N = \boldsymbol{\Sigma}_N \cdot \nabla + M_N - \frac{1}{2\kappa}\nabla^2. \tag{3.92}$$

However, there is a caveat. Recall that when dealing with the two-component theory we found that, in order to maintain the first component of the spinor real, we needed $\nabla_\perp \cdot \boldsymbol{j} = 0$. In this case, we observed that if this condition was satisfied initially, it would also be satisfied for all later times. Therefore, the link to the probabilistic interpretation was held. When extending the spinor to more components though, it is not clear that this situation will hold. As more and more equations are added, this condition becomes more and more intricate. In order to get rid of this problem we can tweak our equations.

Indeed, the problem arises because in our equations of motion there is a non-zero contribution to the time derivative of the imaginary part of the first component of our spinor. Thus, in order to solve the issue, we need to cancel this contribution. In order to achieve this we need to do a few changes.

The first change is to double the size of the spinor, but with the intention of making both halves carry the exact same information. This is achieved by demanding the following structure for the extended $2N$ component spinor Ψ_N^E

$$\Psi_N^E = \begin{pmatrix} \Psi_N \\ \overline{\Psi}_N \end{pmatrix}, \tag{3.93}$$

in where $\bar{z}$ denotes the complex conjugate of z. Next, we will need to modify the spin matrices Σ_x and Σ_y; We define

$$\Sigma'_{N,x} \equiv \frac{1}{2} \begin{pmatrix} 0 & \frac{1}{2} & 0 & 0 & \dots & & 0 \\ \frac{2N}{N+1} & 0 & \frac{N+2}{N+1} & \ddots & \ddots & & \vdots \\ 0 & \frac{N-1}{N+1} & 0 & \frac{N+3}{N+1} & \ddots & & \\ \vdots & 0 & \frac{N-2}{N+1} & 0 & \ddots & \ddots & \\ & \ddots & 0 & \ddots & \ddots & \ddots & 0 \\ & & \ddots & \ddots & \ddots & 0 & \frac{2N+1}{N+1} \\ 0 & \dots & & & 0 & \frac{1}{N+1} & 0 \end{pmatrix}, \tag{3.94}$$

and

$$\Sigma'_{N,y} \equiv \frac{1}{2} \begin{pmatrix} 0 & -\frac{1}{2}i & 0 & 0 & \dots & & 0 \\ \frac{2N}{N+1}i & 0 & -\frac{N+2}{N+1}i & \ddots & \ddots & & \vdots \\ 0 & \frac{N-1}{N+1}i & 0 & -\frac{N+3}{N+1}i & \ddots & & \\ \vdots & 0 & \frac{N-2}{N+1}i & 0 & \ddots & \ddots & \\ & \ddots & 0 & \ddots & \ddots & \ddots & 0 \\ & & \ddots & \ddots & \ddots & 0 & -\frac{2N+1}{N+1}i \\ 0 & \dots & & & 0 & \frac{1}{N+1}i & 0 \end{pmatrix}. \tag{3.95}$$

Therefore, the only modification is to cut the second component of the first row in half. Next, we define correction matrices

$$C_{N,x} \equiv \frac{1}{2} \begin{pmatrix} 0 & \frac{1}{2} & 0 & 0 & \dots & & 0 \\ 0 & 0 & 0 & \ddots & \ddots & & \vdots \\ 0 & 0 & 0 & 0 & \ddots & & \\ \vdots & 0 & 0 & 0 & \ddots & \ddots & \\ & \ddots & 0 & \ddots & \ddots & \ddots & 0 \\ & & \ddots & \ddots & \ddots & 0 & 0 \\ 0 & \dots & & & 0 & 0 & 0 \end{pmatrix}, \tag{3.96}$$

and

$$C_{N,y} \equiv \frac{1}{2} \begin{pmatrix} 0 & \frac{1}{2}i & 0 & 0 & \dots & & 0 \\ 0 & 0 & 0 & \ddots & \ddots & & \vdots \\ 0 & 0 & 0 & 0 & \ddots & & \\ \vdots & 0 & 0 & 0 & \ddots & \ddots & \\ & \ddots & 0 & \ddots & \ddots & \ddots & 0 \\ & & \ddots & \ddots & \ddots & 0 & 0 \\ 0 & \dots & & & 0 & 0 & 0 \end{pmatrix}. \tag{3.97}$$

With this, we can then define new spin matrices for the extended spinor $\Sigma^E_{N,x}$ and $\Sigma^E_{N,y}$

$$\Sigma^E_{N,x} \equiv \begin{pmatrix} \Sigma'_{N,x} & C_{N,x} \\ C_{N,x} & \Sigma'_{N,x} \end{pmatrix}, \tag{3.98}$$

and

$$\Sigma^E_{N,y} \equiv \begin{pmatrix} \Sigma'_{N,x} & C_{N,y} \\ \bar{C}_{N,x} & \bar{\Sigma}'_{N,x} \end{pmatrix}. \tag{3.99}$$

In the same way, we write an extended mass term

$$M_N^E \equiv \begin{pmatrix} M_N & 0 \\ 0 & M_N \end{pmatrix}. \tag{3.100}$$

With these changes, the spinorial equation

$$-\partial \Psi_N^E = \left(\boldsymbol{\Sigma}_N^E \cdot \nabla + M_N^E - \frac{1}{2\kappa} \nabla^2 \right) \Psi_N^E, \tag{3.101}$$

leads to the same equations as before, except for the equation for the imaginary part of the spinor's first component. This will now read $-\partial_t \Im(\Psi_1) = 0$, and thus, it preserves the probabilistic interpretation for all possible initial conditions. This was achieved because the equation for the first component was modified to

$$-\partial_t \Psi_1 = \frac{1}{4}(\partial_x - i\partial_y)\Psi_2 + \frac{1}{4}(\partial_x + i\partial_y)\overline{\Psi_2}, \tag{3.102}$$

which can be rewritten as

$$-\partial_t \Psi_1 = \frac{1}{4}(\partial_x - i\partial_y)\Psi_2 + \overline{\frac{1}{4}(\partial_x - i\partial_y)\Psi_2} = \frac{1}{2}\Re((\partial_x - i\partial_y)\Psi_2), \tag{3.103}$$

leaving in this way only the contribution from the real part.

Now, in order for this fix to work, we need the structure of the spinor $\Psi_N^E = (\Psi_N, \overline{\Psi}_N)$ to be preserved under time evolution. It is easy to see that this is indeed the case. Let us write rewrite Eq. (3.101) for a general spinor $\Psi_N^E = (\phi_1, \phi_2)$

$$\begin{aligned} \partial_t \phi_1 + \left(\boldsymbol{\Sigma}'_N \cdot \nabla + M_N - \frac{1}{2\kappa} \nabla^2 \right) \phi_1 + \boldsymbol{C}_N \cdot \nabla \phi_2 = 0, \\ \partial_t \phi_2 + \left(\overline{\boldsymbol{\Sigma}'}_N \cdot \nabla + \overline{M}_N - \overline{\frac{1}{2\kappa}} \nabla^2 \right) \phi_2 + \overline{\boldsymbol{C}}_N \cdot \nabla \phi_1 = 0, \end{aligned} \tag{3.104}$$

which can be restated as

$$\partial_t \phi_1 + \left(\boldsymbol{\Sigma}'_N \cdot \nabla + M_N - \frac{1}{2\kappa} \nabla^2 \right) \phi_1 + \boldsymbol{C}_N \cdot \nabla \phi_2 = 0, \tag{3.105}$$

and

$$\partial_t \bar{\phi}_2 + \left(\boldsymbol{\Sigma}'_N \cdot \nabla + M_N - \frac{1}{2\kappa} \nabla^2 \right) \bar{\phi}_2 + \boldsymbol{C}_N \cdot \nabla \bar{\phi}_1 = 0. \tag{3.106}$$

If we complement this with the initial condition: $\phi_1(0) = \Psi_N(0)$ and $\phi_2(0) = \overline{\Psi_N(0)}$, we see then that Eqs. (3.105, 3.106) become the exact same equation with the same initial condition. Since the solution is unique, we must therefore have that $\phi_2(t) = \phi_1(t)$ for all later times.

Finally, we could ask if this modification breaks the rotational invariance of our spin matrices or the relationship between their eigenvalues and the velocity? The answer is no. To see this, notice that, after the modification, the rotation operator is given by

$$R_N^E(\theta) = \begin{pmatrix} R_N(\theta) & 0 \\ 0 & R_N(-\theta) \end{pmatrix}. \tag{3.107}$$

By using this rotation operator we see that the extended spin operators, $\Sigma_{N,x}^E$ and $\Sigma_{N,y}^E$, still transform as vectors:

$$R^E(-\theta) \begin{pmatrix} \Sigma_{N,x}^E \\ \Sigma_{N,y}^E \end{pmatrix} R^E(\theta) = \begin{pmatrix} \Sigma_{N,x}^E \cos(\theta) - \Sigma_{N,y}^E \sin(\theta) \\ \Sigma_{N,x}^E \sin(\theta) + \Sigma_{N,y}^E \cos(\theta) \end{pmatrix}. \tag{3.108}$$

Regarding the eigenvectors; if $\boldsymbol{v}_x$ was an eigenvector of $\Sigma_{N,x}$, then $\boldsymbol{v}_x^E = (\boldsymbol{v}_x, \bar{\boldsymbol{v}}_x)$ is also an eigenvector of $\Sigma_{N,x}^E$ (with the same eigenvalue). The same happens for $\Sigma_{N,y}^E$. This is easy to see by choosing a normalization in which the spinor's first component is one. Indeed, in this normalization the second component is either purely real or purely imaginary. Since

the correction terms also have this structure, the product is a real number and the conjugation does not have any effect. For these eigenvectors, the relationship between eigenvalues and the direction of the velocity prevails. Nevertheless, since now we have a bigger matrix we will also have extra eigenvectors. However, these extra eigenvectors have a zero first component, and thus they do not represent physical states in our problem.

3.12 The classical limit

In the previous section we extended our formalism to higher spin numbers. In quantum mechanics, this corresponds to a more classical spin degree of freedom. Indeed, with higher components, the spin observable is allowed to take more different values, eventually leading to a continuum and a classical observable. Does this have an effect in the probabilistic interpretation of our theory? The answer is yes.

Recall that in order to obtain a valid spinorial theory that led to a probabilistic interpretation we needed to have specific values of the parameter λ. For a spinorial description with $N+1$ components, we needed to pick

$$\lambda_N = \frac{2}{N+1}. \tag{3.109}$$

In the probabilistic interpretation, the parameter λ controls the correlation between the external positional Brownian noise and the angular one. As we see, as we increase the number of components, the strength of this feedback becomes smaller and smaller. Thus, our interpretation of this correlation as an expression of the uncertainty principle was an accurate one. By letting the spinor take more components, it becomes an increasingly more classical object and the strength of the uncertainty principle decays. In the limit $N \to 0$, we have that $\lambda \to 0$ and the correlation between the angular and external noise vanishes.

Eventually, this allows us to drop the external positional Brownian noise. In this limit, the spin becomes a classical vector

$$\boldsymbol{\Sigma} \to \boldsymbol{s}(\theta), \tag{3.110}$$

and its degree of freedom enters the wavefunction as an angular variable, θ. Mathematically

$$\Psi_N(\boldsymbol{r}) \to \Psi(\boldsymbol{r}, \theta), \tag{3.111}$$

and thus, our equation of motion becomes

$$-\partial_t \Psi(\boldsymbol{r}, \theta) = \boldsymbol{s}(\theta) \cdot \nabla \Psi(\boldsymbol{r}, \theta) - \frac{\partial^2 \Psi}{\partial \theta^2}, \tag{3.112}$$

which is just the Fokker Planck equation for the probability density $P(\boldsymbol{r}, \theta)$. An equilibrium version of this model has been studied in [81].

3.13 Final remarks

Because the model we consider falls within the Toner-Tu universality class, we can immediately conclude that the polar active particles that we consider do exhibit long-range order [54]. This is in contrast to equilibrium two-dimensional systems which cannot break a continuous symmetry, such as the rotational symmetry of the XY-model, due the Mermin-Wagner theorem [53]. Therefore, the hydrodynamic theory that we obtain, described by Eqs. (3.73), differs from the regular Navier-Stokes equations in two crucial ways: (i) due to the breaking of Galilean invariance via activity and momentum exchange characteristic of dry active matter, the hydrodynamic theory includes terms prohibited in the Navier-Stokes equations, and (ii) as a result of these additional terms, interacting self-propelled particles exhibit long-range polar order.

To summarize, we have introduced a model of active particles based on an analogy with

the Schrödinger equation that describes the propagation of an electron with spin-orbit coupling. We show that this model has a standard description as a stochastic process obeying both a Fokker-Planck and a Langevin equation, which we both derive. We note that within this stochastic interpretation, the orientational and positional Brownian noise of the active particles we consider are coupled via a relation reminiscent of the Heisenberg uncertainty principle. Based on this single-particle physics, we derive a description for a polar active liquid in which the particles preferentially align their velocities. Within this description, we characterize the transition from a disordered to an ordered state via a hydrodynamic Toner-Tu theory. Finally, we extend our theory to a spinor of an arbitrary size, which allows us to approximately incorporate alignment interactions. We finally show how a bigger, and hence more classical spin, leads to the disappearance of the uncertainty principle.

Previously, analogies between classical processes and quantum dynamics have found use in areas as diverse as polymer physics, liquid crystal elasticity, hydrodynamics, and the motion of financial markets [15]. Such analogies are often drawn via a path-integral formalism, but they may be formulated by rotating the time axis into the complex plane. We have shown that this approach can be extended to study active fluids composed of self-propelled particles. In order to account for the self-propulsion, we employ concepts familiar from the study of strongly correlated electron fluids. These analogies have the potential to help discover novel phases of active matter by analogy with their electronic counterparts.

CHAPTER 4

TRANSITIONLESS QUANTUM DRIVING

The evolution in time of a system driven by a time-dependent Hamiltonian can be, in general, quite complicated. In Quantum Mechanics, for example, the absence of energy conservation can yield mixing between the instantaneous eigenstates of the Hamiltonian, i.e., states that satisfy:

$$\hat{H}(t)|\Psi_n\rangle = E_n(t)|\Psi_n\rangle. \tag{4.1}$$

This mixing implies these eigenstates no longer represent stable states of the system. However, there is an approximate regime in which stability can hold. Indeed, if the rate at which the Hamiltonian changes is slow, the mixing between instantaneous states is exponentially small, and the system remains in its instantaneous states, up to a phase, with a high probability. What sets the scale of what can be considered slow is then the time-scale set by the difference between the different eigenstates: $\hbar(E_n(t) - E_m(t))^{-1}$. This is known as the adiabatic theorem [82].

There are many applications in which some adiabatic time-evolution helps to construct exotic initial or entangled states [83, 84, 85, 86]. However, in many setups, such as quantum computing [87], the time-scales needed in order to achieve such time evolution make this application non-viable, and a way to accelerate the adiabatic time evolution is needed. There has been much ongoing research on finding ways to do this effectively and robustly (see Ref. [88]). One way in which this acceleration can be achieved, introduced by Berry in Ref. [8] and known as transitionless quantum driving, involves adding a new piece, $\hat{K}$, to the Hamiltonian in such a way that adiabatic time-evolution becomes exact.

The extra piece that the Hamiltonian needs, called the counterdiabatic term, can always be found exactly as a formal matrix in Hilbert space. This solution though, in its raw form, says little about how the observables of the problem need to combine in order to generate this extra piece, or even if it is a local operator. Here, we understand locality in an analytical sense; we say that an operator is local if, when going to configuration space, its application on a given wavefunction only requires knowledge of the behavior of the wavefunction in a neighborhood of the point being considered. When designing experimental applications this is a desirable property since most experimental situations can deal only with local operators.

In this work, [7], we address these two issues, explicitness and locality, for one dimensional single-particle hamiltonian systems. We do so by explicitly linking the counterdiabatic term with the observables of the system through a commutator equation (see Refs.[7, 89, 90]), which we treat semi-classically; we first study the classical solutions (obtained by exchanging commutators with Poisson brackets), to which we later add quantum corrections through the use of Moyal brackets and the formalism of quantum mechanics in phase space. An analysis of the classical solution for one-dimensional single particle systems reveals that, in general, the counterdiabatic term is not local, as it entails an infinite power series in the momentum operator. However, a well-known notable exception to the previous statement is reached when considering systems subjected to re-scalable potentials (see Ref. [91]). For this particular class of potentials, the counterdiabatic term, which can be computed exactly, is a local operator. Finally, since the lack of locality severely thwarts the range of applicability of the method, and since, in general, locality cannot be achieved, we look for a local approximation to the counterdiabatic term. Taking advantage of the fact that rescalable potentials are exactly solvable, we employ a perturbation scheme, similar to Rayleigh-Shcrödinger, in order to attack more general potentials. We focus in poten-

tials with two natural length-scales (e.g., $\lambda x^2 + \tau x^4$) and we consider the regime in which one of the length-scales (say, the one associated to τx^4) is much bigger than the other one (τx^2), in which case it can be considered as a perturbation. The conclusion is that, at least for some potentials, obtaining a local approximate $\hat{K}$ is achievable. The approximated counterdiabatic term drives the instantaneous perturbed eigenstates of the system. Thus, as long as these perturbed eigenstates are a good approximation to the exact ones, this would grant a good approximation to the exact non local expression. Therefore, through this scheme we obtain an operator that, although it can only approximately stifle non-adiabatic transitions, has the advantage of being local and thus it can possibly be realizable experimentally or mapped to a realizable experimental setup thorugh canonical transformations (see Ref.[91]).

This chapter is structured as follows. In the first two sections we review the adiabatic approximation, Berry's transitionless quantum driving and the counterdiabatic term. Then, in section 4.3, we show a derivation of the commutator equation connecting the counterdiabatic term with the observable of the system. In section 4.4, we study the classical limit of the previous equations, effectively transforming it into a partial differential equation (PDE). We then use this equation to show how rescalable potentials imply local counterdiabatic terms. In section 4.5, we discuss the inclusion of quantum corrections through the use of the Moyal bracket and the formalism of quantum mechanics in phase space. In section 4.6 we study the issue of locality by employing the classical solution and briefly discuss the case of the only rescalable potential that does not lead to a local counterdiabatic term: x^{-2}. Finally, in section 4.7 we cover potentials with multiple length-scales and derive the perturbation scheme. We also explicitly show how this scheme leads to local approximated counterdiabatic terms for the potential $\lambda x^2 + \tau x^4$ and discuss the physical meaning of the perturbed term.

4.1 The adiabatic theorem in quantum mechanics

In this section we provide a brief review of the adiabatic theorem, which was first proved by Born and Fock in 1928 [82]. For all derivations we follow Ref. [11].

Let $\hat{H}(t/\tau)$ be a time-dependent Hamiltonian and τ be the characteristic time-scale of its variation. As we shall see, the adiabatic limit corresponds to $\tau \to \infty$. We call the instantaneous eigenstate basis of this Hamiltonian $\{|\Psi_k(t)\rangle\}_k$, and the corresponding eigenvalues $\{E_k(t)\}_k$; then:

$$\hat{H}(t/\tau)|\Psi_k(t)\rangle = E_k(t)|\Psi_k(t)\rangle. \tag{4.2}$$

We further assume that the spectrum is non-degenerate, i.e., $E_k(t) \neq E_{k'}(t)$ for $k \neq k'$.

One starts by writing the time dependent Schrödinger equation (with $\hbar = 1$) for a general state $|\Psi(t)\rangle$:

$$i\frac{\partial}{\partial t}|\Psi(t)\rangle = \hat{H}(t/\tau)|\Psi(t)\rangle. \tag{4.3}$$

By using that the instantaneous eigenstates form a basis for all t, we can rewrite Eq. (4.3) as

$$|\Psi(t)\rangle = \sum_k c_k(t)e^{-i\theta_k(t)}|\Psi_k(t)\rangle, \tag{4.4}$$

in which we have defined the so-called dynamical phase: $e^{-i\theta_k(t)} \equiv \exp\left(-i\int_0^t d\lambda E_k(\lambda)\right)$. We further assume that the system starts at the n-th instantaneous eigenstate, so that $|\Psi(0)\rangle = |\Psi_n(0)\rangle$, and thus $c_m(0) = \delta_{nm}$. Then, inserting Eq. (4.4) into Eq. (4.3) and taking the inner product with respect to $\exp(i\theta_m(t))|\Psi_m(t)\rangle$ yields

$$\frac{d}{dt}c_m = -\sum_k c_k(t)e^{i(\theta_m(t)-\theta_n(t))}\langle\Psi_m(t)|\left[\frac{\partial}{\partial t}|\Psi_k(t)\rangle\right]. \tag{4.5}$$

In order to simplify the term on the right, notice that, by differentiating Eq. (4.2) on both sides and taking the inner product with respect to $|\Psi_m(t)\rangle$, we find, for $k \neq m$, that

$$\langle\Psi_m(t)|\left[\frac{\partial}{\partial t}|\Psi_k(t)\rangle\right] = \frac{1}{\tau}\frac{\langle\Psi_m(s)|\partial_s H(s)|\Psi_k(s)\rangle}{E_k(s)-E_m(s)}, \tag{4.6}$$

where, in order to make explicit the dependence on τ, we have replaced t by the rescaled variable $s = t/\tau$. Using Eq. (4.6) on Eq. (4.5) leads to the formal solution:

$$\frac{d}{dt}c_m = -c_m(t)\langle\Psi_m(t)|\left[\frac{\partial}{\partial t}|\Psi_m(t)\rangle\right] - \frac{1}{\tau}\sum_k c_k(t)e^{i(\theta_m(t)-\theta_n(t))}\frac{\langle\Psi_m(s)|\partial_s H(s)|\Psi_k(s)\rangle}{E_k(s)-E_m(s)}. \tag{4.7}$$

The adiabatic approximation amounts to neglecting the second term on the right-hand side of Eq. (4.7). This is admissible if:

$$\frac{(E_k-E_m)^{-1}}{\tau} \ll 1, \tag{4.8}$$

i.e., if the time-scale associated with the energy differences between the relevant states are much smaller than the characteristic time-scale for the variation of the Hamiltonian in time, τ. This approximation, together with the initial conditions, gives the result

$$c_k(t) = e^{i\gamma_n(t)}\delta_{kn}, \tag{4.9}$$

where we have defined

$$\gamma_n(t) \equiv i\int_0^t dt'\langle\Psi_n(t')|\left[\frac{\partial}{\partial t'}|\Psi_n(t')\rangle\right]. \tag{4.10}$$

This is a purely real quantity, and thus $e^{i\gamma_n(t)}$ is a complex phase.

In terms of quantum states, we have that

$$|\Psi(t)\rangle = e^{i\gamma_n(t)} e^{-i\theta_n(t)} |\Psi_n(t)\rangle. \tag{4.11}$$

So, up to two phases, the system follows the instantaneous eigenstates of the system. How good is this approximation? In their first proof of the adiabatic theorem, Born and Fock showed that, for $m \neq n$, one has

$$\langle \Psi_m(t)|\Psi(t)\rangle \sim O\left(\frac{1}{\tau}\right). \tag{4.12}$$

More recent proofs (see Refs. [92, 93]) have shown that, under appropriate conditions, one has $\langle \Psi_m(t)|\Psi(t)\rangle \sim O\left(e^{-\frac{1}{\tau}}\right)$.

4.1.1 Berry's phase:

The phase that appears with the adiabatic solution is also of great interest; is origin, as pointed out by Berry in Ref. [94], is purely geometrical, and hence receives the name geometric phase, or Berry's phase. Indeed, if we now let the time-evolution of our Hamiltonian be associated with a vector in parameter space $\boldsymbol{R}(t)$ (i.e., a vector formed from the parameters of the Hamiltonian) then we have that: $\partial_t = \partial_t \boldsymbol{R} \cdot \nabla_{\boldsymbol{R}}$ and hence:

$$\begin{aligned} \gamma_n(t) &= i \int_0^t dt' \frac{d\boldsymbol{R}}{dt'} \langle \Psi_n(t')| \left[\nabla_{\boldsymbol{R}} |\Psi_n(t')\rangle\right] \\ &= i \int_{\boldsymbol{R}(0)}^{\boldsymbol{R}(t)} d\boldsymbol{R'} \cdot \langle \Psi_n(t')| \left[\nabla_{\boldsymbol{R'}} |\Psi_n(t')\rangle\right]. \end{aligned} \tag{4.13}$$

Thus, if time t represents the period over one full cycle in parameter space (i.e., we have cyclic time-evolution), then $\boldsymbol{R(t)}$ describes a closed curve C and we can write:

$$\gamma_n(C) = \oint_C \boldsymbol{A}_n(\boldsymbol{R}) \cdot d\boldsymbol{R}, \tag{4.14}$$

where we have defined the gauge potential $\boldsymbol{A}_n(\boldsymbol{R})$ via

$$\boldsymbol{A}_n(\boldsymbol{R}) = \langle \Psi_n(t')| \left[\nabla_{\boldsymbol{R}} |\Psi_n(t')\rangle\right]. \tag{4.15}$$

Finally, by using the Stokes' theorem we can rewrite this phase as a flux integral over a surface bounded by the path C due to a generalized field

$$\boldsymbol{B}_n(\boldsymbol{R}) = \nabla_{\boldsymbol{R}} \times \boldsymbol{A}_n(\boldsymbol{R}), \tag{4.16}$$

which implies

$$\gamma_n(C) = \oint d\boldsymbol{a} \cdot \boldsymbol{B}_n(\boldsymbol{R}). \tag{4.17}$$

The geometrical character of the Berry phase becomes clearer by noticing that it does not depend on the details of the phase along the path C (although Eq. (4.14) could suggest otherwise). Indeed, in a similar way to a gauge transformation, if we introduce an arbitrary time-dependent phase factor; $\exp(i\delta(\boldsymbol{R}))$, to the definition of $|\Psi\rangle$, viz.: $|\Psi\rangle \rightarrow \exp(i\delta(\boldsymbol{R}))|\Psi\rangle)$, then $\boldsymbol{A}_n(\boldsymbol{R})$ changes as

$$\boldsymbol{A}_n(\boldsymbol{R}) \rightarrow \boldsymbol{A}_n(\boldsymbol{R}) - \nabla_{\boldsymbol{R}}\delta(\boldsymbol{R}), \tag{4.18}$$

which leaves $\boldsymbol{B}$ unchanged. By Eq. (4.17), so does the Berry phase. Thus, $\gamma_n(C)$ depends only on the geometry of the path traced in parametric space.

In the previous derivation we assumed that the spectrum was non-degenerate. What effects could degeneracies have? To begin, even under truly adiabatic time-evolution, mixing between degenerate states can not be avoided. In this case, as pointed out by Wilczek and

Zee [95], the geometric phase $\gamma_n(C)$ can no longer be a c-number, but rather it must be an operator which mixes the the states within each degenerate subspace; in other words; a non-abelian gauge field.

4.2 Transitionless quantum driving: Reverse engineering

As mentioned in the introduction of this chapter, in many applications, such as quantum computing, the natural time-scales of the system are not slow enough for the adiabatic theorem to apply. The fact that adiabatic time-evolution would yield useful or exotic states motivates the question if it is possible to accelerate the adiabatic time-evolution. One approach among many, introduced by Berry in Ref. [8], consists of adding a new operator to the system's Hamiltonian, called the counterdiabatic term. This extra piece is designed to make the adiabatic state an exact solution of the time-dependent Schrödinger equation. Using this condition and a process of reverse engineering, it is always possible to find such an operator.

As in the previous section, consider the quantum hamiltonian $\hat{H}(t)$ with its instantaneous eigenstates and energies been given by $|n(t)\rangle$ and $E_n(t)$, respectively. If the adiabatic time-evolution were exact, $\hat{H}(t)$ would drive the states in the following way:

$$|\Psi_n(t)\rangle = e^{-i\theta_n(t)}e^{i\gamma_n(t)}|n(t)\rangle, \tag{4.19}$$

where, as before, $\exp(-i\theta_n(t))$ and $\exp(i\gamma_n(t))$ stand for the dynamic and geometric phases, respectively. We shall demand this state to be an exact solution for the time-dependent Schrödinger equation driven by the Hamiltonian $\hat{H}(t) + \hat{K}(t)$, where $\hat{K}(t)$ is the counterdiabatic term. This implies that

$$i\frac{d}{dt}|\Psi_n(t)\rangle = (\hat{H}(t) + \hat{K}(t))|\Psi_n(t)\rangle, \tag{4.20}$$

and thus that

$$-\frac{d}{dt}\gamma_n(t)|n(t)\rangle + i\frac{d}{dt}|n(t)\rangle = \hat{K}(t)|n(t)\rangle, \tag{4.21}$$

where we have used the fact that, by definition $\hat{H}(t)|n(t)\rangle = E_n(t)|n(t)\rangle$. Then, by taking the inner product with respect to an arbitrary state $|m(t)\rangle$ we obtain

$$\langle m(t)|\hat{K}(t)|n(t)\rangle = -\frac{d}{dt}\gamma_m(t)\delta_{mn} + i\langle m(t)|\frac{d}{dt}|n(t)\rangle. \tag{4.22}$$

Because for all t's the eigenstates form a basis of the Hilbert space, we then have

$$\hat{K}(t) = \sum_{m,n}\left[-\frac{d}{dt}\gamma_m(t)\delta_{mn} + i\langle m(t)|\frac{d}{dt}|n(t)\rangle\right]|m(t)\rangle\langle n(t)|. \tag{4.23}$$

Using the definition of $\gamma_m(t)$ (see Eq. (4.10)), we are led then to

$$\hat{K}(t) = \sum_{m\neq n}\left[-i\langle m(t)|\frac{d}{dt}|m(t)\rangle\delta_{mn} + i\langle m(t)|\frac{d}{dt}|n(t)\rangle\right]|m(t)\rangle\langle n(t)|. \tag{4.24}$$

We see that the diagonal elements cancel, and thus we obtain

$$\hat{K}(t) = i\sum_{m\neq n}\left[\langle m(t)|\frac{d}{dt}|n(t)\rangle\right]|m(t)\rangle\langle n(t)|. \tag{4.25}$$

Finally, by differentiating the instantaneous eigenvalue equation we, can eliminate of the $\frac{d}{dt}|n(t)\rangle$ term (we are assuming that there are no degeneracies), to obtain

$$\langle m(t)|\frac{d}{dt}|n(t)\rangle = \frac{\langle m(t)|\partial_t\hat{H}(t)|n(t)\rangle}{E_n(t) - E_m(t)}. \tag{4.26}$$

We conclude the derivation by inserting Eq. (4.26) into Eq. (4.25), which gives us

$$\hat{K}(t) = i \sum_{m \neq n} \left[\frac{\langle m(t)|\partial_t \hat{H}(t)|n(t)\rangle}{E_n(t) - E_m(t)} \right] |m(t)\rangle\langle n(t)|. \tag{4.27}$$

If the original Hamiltonian does present degeneracies, it is possible to extend this derivation by taking into consideration the non-abelian Berry's phase [96]. Further developments include extensions to non-hermitian Hamiltonians [97], useful for systems with losses, and many particle systems [98].

Equation (4.27), although correct, express $\hat{K}(t)$ as a formal operator in Hilbert space. As such, *a priori* it offers little insight about how $\hat{K}(t)$ depends on the physical observables of the system, such as the position coordinates, momenta or spin. This lack of explicitness is one of the first things we would like to address. Along the same lines, it is, in general, impossible to know *a priori* if this operator can be easily created experimentally, or if it is local. Generally, the term local is used to describe operators that depend only on the position operator. However, in this work we will use a broader analytical definition of locality; By local we mean that the application of $\hat{K}$ in configuration space over an specific point of a wavefunction only requires knowledge of the behavior of the wavefunction in a neighborhood of this point. In mathematical terms, this implies that the operator must have a finite number of derivatives, and thus it can only have finite powers of $\hat{p}$. See Figure 4.1. Thus, we also focus in finding criteria to help determine when locality can be achieved. In the next section, we introduce a new formalism that offers a better support to get insight into both these issues (explicitness and locality).

Before continuing, though, we would like to mention that the previous expression for $\hat{K}(t)$ assumes a time-evolution that included the geometric phase. If, on the contrary, one is interested into achieving a time-evolution with only the dynamic phase, then the piece one needs to add, $\hat{K}_{\text{dyn}}(t)$, is given by:

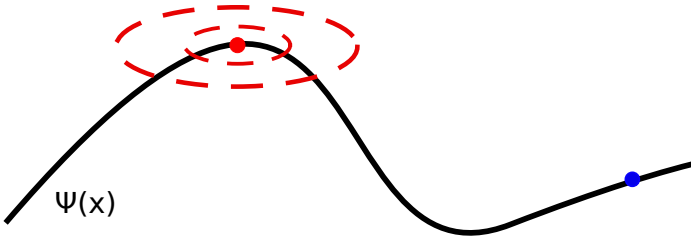

Figure 4.1: Graphical depiction of locality. The application of the operator in configuration space only requires knowledge of the behavior of the wavefunction in a neighborhood of the application point (red point) and hence it is independent of what happens very far away (blue point) from this point.

$$\hat{K}_{\text{dyn}}(t) = i\partial_t\hat{\Lambda}\Lambda^\dagger, \tag{4.28}$$

in where $\hat{\Lambda}$ is the (unitary) time-evolution operator given by

$$\Lambda = \sum_n |n(t)\rangle\langle n(0)|. \tag{4.29}$$

The difference between $\hat{K}(t)$ and $\hat{K}_{\text{dyn}}(t)$ is then given by:

$$\sum_n \left[-i\langle n(t)|\frac{d}{dt}|n(t)\rangle\right]|n(t)\rangle\langle n(t)|, \tag{4.30}$$

which, as we see, is diagonal in the basis of instantaneous eigenstates, and therefore, commutes with $\hat{H}(t)$.

4.3 A commutator equation for $\hat{K}$

As mentioned in the previous section, one of the issues with Eq. (4.27) is explicitness; it does not show how this operator depends on the observables of the problem. One way in which one can solve this issue is to find an equation that directly links $\hat{K}$ with these observables. This is precisely our objective in this section.

We proceed by using a dynamical property of transitionless Hamiltonians. Let $\hat{H}$ be a

time-dependent Hamiltonian and let $\{|\Psi_n(t)\rangle\}_n$ be their instantaneous eigenstates associated to eigenvalues $\{E_n(t)\}_n$. Thus, we have that

$$\hat{H}|\Psi_n(t)\rangle = E_n(t)|\Psi_n(t)\rangle. \tag{4.31}$$

Notice that Eq. (4.31) is valid independent of any time-dependent phase that we could have introduced in the definition of $|\Psi_n(t)\rangle$. Now, let $\hat{\Gamma}(t)$ be a transitionless Hamiltonian associated to these eigenstates, viz. the Hamiltonian that satisfies

$$i\frac{d}{dt}|\Psi_n(t)\rangle = \hat{\Gamma}(t)|\Psi_n(t)\rangle. \tag{4.32}$$

The time-evolution driven by $\hat{\Gamma(t)}$ is then carried out by a unitary operator $\hat{U}_\Gamma(t)$. This operator is obtained by solving

$$i\frac{d}{dt}\hat{U}_\Gamma(t) = \hat{\Gamma}(t)\hat{U}_\Gamma(t), \tag{4.33}$$

and it satisfies

$$|\Psi_n(t)\rangle = \hat{U}_\Gamma(t)|\Psi_n(0)\rangle, \tag{4.34}$$

for all n. Using Eq. (4.34) in Eq. (4.31) leads then to

$$\hat{U}_\Gamma^\dagger(t)\hat{H}(t)\hat{U}_\Gamma(t)|\Psi_n(0)\rangle = E_n(t)|\Psi_n(0)\rangle. \tag{4.35}$$

Thus, $\hat{U}_\Gamma(t)$ can also be seen as a transformation into a co-moving frame in which the eigenstates do not evolve in time. Notice that this is exactly the opposite to what happens in the Heisenberg picture of time-evolution. Indeed, by defining the transformed Hamiltonian

$$\tilde{H}(t) \equiv \hat{U}_\Gamma^\dagger(t)\hat{H}(t)\hat{U}_\Gamma(t), \tag{4.36}$$

we see that

$$\tilde{H}(t)|\Psi_n(0)\rangle = E_n(t)|\Psi_n(0)\rangle. \tag{4.37}$$

The time-evolution under $\tilde{H}$ is trivial, as this operator commute with itself at all different times. Therefore, is no surprise to see that differentiating Eq. (4.37) with respect to time yields

$$\left(\frac{d}{dt}\tilde{H}\right)|\Psi_n(0)\rangle = \left(\frac{d}{dt}E_n(t)\right)|\Psi_n(0)\rangle. \tag{4.38}$$

This implies that $\tilde{H}$ and $\left(\frac{d}{dt}\tilde{H}\right)$ share the same eigenbasis, and thus, they commute

$$\left[\tilde{H}, \frac{d}{dt}\tilde{H}\right] = 0. \tag{4.39}$$

We then go back to the original lab-frame. By directly differentiating Eq. (4.36) and using Eq. (4.33) we find that

$$\frac{d}{dt}\tilde{H} = \hat{U}_\Gamma^\dagger \left[\frac{d}{dt}\hat{H} + i\left[\hat{\Gamma}, \hat{H}\right]\right]\hat{U}_\Gamma, \tag{4.40}$$

which, used in Eq. (4.39), yields the following commutator condition on $\hat{\Gamma}$

$$\left[\hat{H}, \frac{d}{dt}\hat{H} + i\left[\hat{\Gamma}, \hat{H}\right]\right] = 0. \tag{4.41}$$

Notice that $\hat{K}$, as defined in the previous section, Eq. (4.20), drives the transitionless evolution of instantaneous eigenstates that carry Berry's phase, but not the dynamic phase. As such, they must satisfy Eq. (4.41), and we conclude that

$$\left[\hat{H}, \frac{d}{dt}\hat{H} + i\left[\hat{K}, \hat{H}\right]\right] = 0. \tag{4.42}$$

In the course of this work we have discovered that Polkovnikov et. al. [89, 90] have reached

the same equation independently.

As a side note, notice that if the right side of the most-outward commutator of Eq. (4.42) equals zero, this would imply that $\hat{H}$ is an invariant under the time-evolution driven by $\hat{\Gamma}$. Specifically, this is the case in which the spectrum of the Hamiltonian is preserved under time-evolution and only the eigenstates change. Therefore, this is very reminiscent to the theory of exact invariants of Hamiltonians, also known as Lewis-Riesenfeld invariants [99]. As explained in Ref. [88], these invariants can also be used as an alternative shortcut to adiabaticity, different from transitionless quantum driving. In this method the roles of $\hat{H}$ and $\hat{K}$ are reversed. Special interest have received the look for invariants that are quadratic in momentum, since these can be created experimentally. The original work of Lewis-Riesenfeld focused in to the search of invariants for the Harmonic oscillator [99]. As of now, the identification of Hamiltonians that admit an invariant quadratic in momentum has been realized both in classical mechanics [100] and quantum mechanics [101].

Now, it is clear that the solutions to Eq. (4.42) cannot be unique. There are two possible sources of degeneracy, as we now explain.

(i) Note that the modification $\hat{K} \rightarrow \hat{L} + \hat{K}$, where $\hat{L}$ is any operator that commutes with $\hat{H}$, also yields a solution of Eq. (4.42). The reason behind this lies in the arbitrary way in which we can define an instantaneous basis of eigenstates. The different choices of time-dependent phases can be considered as different dynamical phases, and to each of this phases there is an associated $\hat{L}$ operators.

Therefore, in order to consistently find $\hat{K}$ using Eq. (4.42), we need a criterion that can allow us to eliminate these degeneracies. This criterion comes through the following observation: $\hat{K}$ is *orthogonal* to all operators that commute with $\hat{H}$.

In order to make this assertion, one first needs to establish a way to measure angles between operators, viz. we need an inner product. We define the inner product between two operators $\hat{A}$ and $\hat{B}$ via

$$\left\langle \hat{B}, \hat{A} \right\rangle \equiv \mathrm{Tr}\left(\hat{B}^{\dagger}\hat{A}\right). \tag{4.43}$$

However, as the traces of operators defined in infinite dimensional Hilbert spaces do not generally converge, this definitions applies only for spaces of finite dimension. However, if we are only interested into seeing if two operators are orthogonal, we only need to see if this quantity vanishes. By using the bra-ket notation we can always do this test. Now, in addition to the definition (4.43), notice that if the spectrum of $\hat{H}$ is non-degenerate then the set of operators that commute with $\hat{H}$ belongs to the span of $\{|k\rangle\langle k|\}_k$, where we have used the shorthand notation $|\Psi_n\rangle = |n\rangle$. In other words, the operators $\{|k\rangle\langle k|\}_k$ form a basis for all possible operators $\hat{L}$ (i.e., operators that commute with $\hat{H}$). Given this, we see that in order to prove that $\hat{K}$ is perpendicular to all operators $\hat{L}$, it is enough to show that: $\left\langle |k\rangle\langle k|, \hat{K} \right\rangle = 0$ for all k. By using the explicit form of $\hat{K}$, Eq. (4.27) we obtain that

$$\begin{aligned}
\left\langle |k\rangle\langle k|, \hat{K} \right\rangle &= i \sum_{m \neq n} \left[\frac{\langle m|\partial_t \hat{H}|n\rangle}{E_n - E_m} \right] \mathrm{Tr}\left(|k\rangle\langle k|m\rangle\langle n|\right) \\
&= i \sum_{n \neq k} \left[\frac{\langle m|\partial_t \hat{H}|n\rangle}{E_n - E_m} \right] \mathrm{Tr}\left(|k\rangle\langle n|\right) \\
&= 0,
\end{aligned} \tag{4.44}$$

as we evidently have that $\mathrm{Tr}\left(|k\rangle\langle n|\right) = 0$.

Therefore, in order to find $\hat{K}$ we need to solve Eq. (4.42) with the restriction $\hat{K} \in (\mathrm{span}(\{|k\rangle\langle k|\})^C$, where C denotes orthogonal complement.

(ii) A second source of degeneracy comes through the modification $\hat{K} \to \hat{T} + \hat{K}$, in

where $\hat{T}$ has the property that $\left[\hat{T}, \hat{H}\right] = \hat{L}$, for some non-zero operator $\hat{L}$ that commutes with $\hat{H}$. In other words: $\left[\hat{H}, \left[\hat{T}, \hat{H}\right]\right] = 0$. It is clear that $\hat{K}$ does not belong to this class of operators, and that, more importantly, these operators cannot exist in finite-dimensional Hilbert spaces or hamiltonian systems in which the basis of eigenstates is complete (and thus, dense in their corresponding Hilbert spaces). Indeed, notice that by using this orthonormal basis we can write

$$\hat{T} = \sum_{nm} c_{nm} |m\rangle\langle n|, \tag{4.45}$$

with $c_{nm} = \langle m|\hat{T}|n\rangle$, and

$$\hat{H} = \sum_{k} E_k |k\langle\rangle k|. \tag{4.46}$$

Therefore, we have that

$$[\hat{H}, \hat{T}] = \sum_{nm} c_{nm}(E_m - E_n)|m\rangle\langle n|. \tag{4.47}$$

The diagonal elements of this operator, together with the matrix elements associated to degenerate subspaces, are zero. As a consequence, if this operator where to commute with $\hat{H}$, it must be the zero operator.

Thus, for well-defined Hamiltonians we expect this second form of degeneracy to not be an issue. In infinite-dimensional Hilbert spaces, there might exist operators that can formally achieve the condition we just excluded, but they will have a more restricted domain and therefore, they will not be defined for the entirety of the Hilbert space. Finally, Hamiltonians with singular potentials (such as $V(x) \propto 1/x^2$), may also present degeneracies of this sort.

In any case, $\hat{K}$ does not contain any contribution from such kind of operators. Essen-

tially, it is a pure particular solution of Eq. (4.42) and it should have the minimal amount of terms needed. Physically, this is clear, since the source term in Eq. (4.42) is the time dependence of the original Hamiltonian. If this dependence were non-existent, then $\hat{K}$ should vanish identically.

In the following subsection we use an example (used by Berry in Ref. [8]) to illustrate how to solve Eq. (4.42) by employing the orthogonality criterion. In particular, for this example there is no need to worry abut the second kind of degeneracies, since this problem lies in a finite dimensional Hilbert space.

4.3.1 A simple example: A spin under the effects of a time dependent magnetic field

Consider a quantum spin operator $\hat{\boldsymbol{S}}$ under the action of a time dependent magnetic field $\boldsymbol{B}(t)$. The Hamiltonian of such a system is given by:

$$\hat{H} = -\mu \boldsymbol{B}(t) \cdot \hat{\boldsymbol{S}}, \tag{4.48}$$

in where μ is just a proportionality constant. We can then separate the evolution of the magnitude of $\boldsymbol{B}(t)$, $B(t)$, from its direction, $\boldsymbol{n}(t)$, by explicitly writing

$$\hat{H} = -\mu B(t)(\boldsymbol{n}(t) \cdot \hat{\boldsymbol{S}}). \tag{4.49}$$

In this section, we find $\hat{K}$ by solving Eq. (4.42) via the Ansatz

$$\hat{K} = \boldsymbol{\omega} \cdot \hat{\boldsymbol{S}}. \tag{4.50}$$

That is to say, we will find the correct value of the vector $\boldsymbol{\omega}$.

The first step is to find the space of operators with the form (4.50) that commute with

$\hat{H}$. Namely, find all vectors $\boldsymbol{\omega}'$ for which

$$\left[\hat{H}, \boldsymbol{\omega}' \cdot \hat{\boldsymbol{S}}\right] = 0. \tag{4.51}$$

By explicitly expanding the previous expression and using the angular momentum algebra, $[S_i, S_j] = i\varepsilon_{ijk}S_k$, we find that

$$(\boldsymbol{n} \times \boldsymbol{\omega}') \cdot \hat{\boldsymbol{S}} = 0. \tag{4.52}$$

Given the linear independence of the components of $\hat{\boldsymbol{S}}$, this leads to the condition: $\boldsymbol{n} \times \boldsymbol{\omega}' = 0$, or $\boldsymbol{\omega}' \,||\, \boldsymbol{n}$. This tells us then that the vector $\boldsymbol{\omega}$ must lay in the plane perpendicular to $\boldsymbol{n}$. An orthogonal basis for this plane is given by:

$$\boldsymbol{\omega}_1 \equiv \begin{pmatrix} n_2 \\ -n_1 \\ 0 \end{pmatrix}, \boldsymbol{\omega}_2 \equiv \begin{pmatrix} n_1 n_3 \\ n_2 n_3 \\ -(n_2^2 + n_1)^2 \end{pmatrix},$$

in where we have assume that $\boldsymbol{n} = (n_1, n_2, n_3)$. Therefore, we expect to have that

$$\hat{K} = c_1 \boldsymbol{\omega}_1 \cdot \hat{\boldsymbol{S}} + c_2 \boldsymbol{\omega}_2 \cdot \hat{\boldsymbol{S}}. \tag{4.53}$$

Introducing this into Eq. (4.42) and using the definition of $\hat{H}$, Eq. (4.48), we find that

$$[B\boldsymbol{n} \cdot \hat{\boldsymbol{S}}, \dot{B}\boldsymbol{n} \cdot \hat{\boldsymbol{S}} + B\dot{\boldsymbol{n}} \cdot \hat{\boldsymbol{S}} + i[c_1 \boldsymbol{\omega}_1 \cdot \hat{\boldsymbol{S}} + c_2 \boldsymbol{\omega}_1 \cdot \hat{\boldsymbol{S}}, B\boldsymbol{n} \cdot \hat{\boldsymbol{S}}]] = 0, \tag{4.54}$$

in where the dots denote time derivatives. Clearly, the term containing $\dot{B}$ commutes with the left side of the most-outward commutator and therefore does not contribute to $\hat{K}$. Then, we can completely factor out the magnitude of the magnetic field: $\hat{K}$ does not depend on $B(t)$. The reason behind this is that what it drives the mixing between states in the original Hamiltonian $\hat{H}$ is the rotation. Once we move to the rotating frame, the spin always points

in the same direction and the changes in $B(t)$ only contribute to the dynamical phase. Equation (4.54) then simplifies to

$$[\boldsymbol{n}\cdot\hat{\boldsymbol{S}}, \dot{\boldsymbol{n}}\cdot\hat{\boldsymbol{S}} + c_1(\boldsymbol{n}\times\boldsymbol{w_1})\cdot\hat{\boldsymbol{S}} + c_2(\boldsymbol{n}\times\boldsymbol{w_2})\cdot\hat{\boldsymbol{S}}] = 0, \tag{4.55}$$

in where we used the identity $[\boldsymbol{a}\cdot\hat{\boldsymbol{S}}, \boldsymbol{b}\cdot\hat{\boldsymbol{S}}] = i(\boldsymbol{a}\times\boldsymbol{b})\cdot\hat{\boldsymbol{S}}$. Notice though that: $\boldsymbol{n}\times\boldsymbol{w_1} = \boldsymbol{w_2}$ and $\boldsymbol{n}\times\boldsymbol{w_2} = -\boldsymbol{w_1}$. Hence

$$[\boldsymbol{n}\cdot\hat{\boldsymbol{S}}, \dot{\boldsymbol{n}}\cdot\hat{\boldsymbol{S}} + c_1\boldsymbol{w_2}\cdot\hat{\boldsymbol{S}} - c_2\boldsymbol{w_1}\cdot\hat{\boldsymbol{S}}] = 0, \tag{4.56}$$

which finally leads to

$$c_1\boldsymbol{w_1}\cdot\hat{\boldsymbol{S}} + c_2\boldsymbol{w_2}\cdot\hat{\boldsymbol{S}} = (\boldsymbol{n}\times\dot{\boldsymbol{n}})\cdot\hat{\boldsymbol{S}} \tag{4.57}$$

By comparing this with Eqs. (4.50, 4.53) we conclude that $\boldsymbol{\omega} = (\boldsymbol{n}\times\dot{\boldsymbol{n}})$, which is the classical angular velocity of the vector $\boldsymbol{n}$, and consequently

$$\hat{K} = (\boldsymbol{n}\times\dot{\boldsymbol{n}})\cdot\hat{\boldsymbol{S}}, \tag{4.58}$$

which is exactly the same solution reached by Berry in Ref. [8]. Notice that by simply demanding the operator $\hat{K}$ to be perpendicular to operators that with $\hat{H}$, we were able to avoid degeneracies. The method also yields the correct expression for the counterdiabatic term, $\hat{K}$, without requiring any explicit knowledge of the instantaneous eigenstates.

4.4 The bridge to classical mechanics: From commutators to PDE

The use of Eq. (4.42) in the previous example, although successful, was facilitated by the use of a clever Ansatz based in properties of the rotation group. This Ansatz leads to linear expressions and avoids the problem of operator-ordering. In general, solving a commutator equation is much more complicated and in most cases, an impossible task.

Thus, a much more comfortable approach would be one that deals with differential equations instead. Although these might not always be solvable, there are many techniques that allow for perturbative analysis and gain insight into the analytical structure of what we are investigating. As a first approach then, we can try such an approach by studying the classical limit of the problem.

4.4.1 A naive approach: the classical limit

In this section we explore the solutions of Eq. (4.42) in the classical limit, which we reach via the exchange

$$[\hat{A}, \hat{B}] \to i\{A, B\}, \tag{4.59}$$

in where $\{\ ,\ \}$ denotes the Poisson bracket. This change leads then to the following equation

$$\{H, \dot{H} - \{K, H\}\} = 0. \tag{4.60}$$

This results in a linear partial differential equation for K (the classical limit of $\hat{K}$). The advantage of this approach is that this equation provides a much easier way to see the structure of K in terms of observables. On the other hand, we will not know which is the correct order of operators that $\hat{K}$ should have. Nevertheless, the hope is that by obtaining a good Ansatz, we can retrieve the correct order of the operators through the commutator equation. Further below we will see that, in general, this will not be the case, and quantum corrections will be needed.

From now on we restrict ourselves, for simplicity, to one-dimensional systems with Hamiltonians given by $H(x, p)$, in were x denotes the position and p the momenta. Given that the Poisson bracket takes the form

$$\{A, B\} = \frac{\partial A}{\partial x}\frac{\partial B}{\partial p} - \frac{\partial A}{\partial p}\frac{\partial B}{\partial x} \tag{4.61}$$

we obtain that Eq. (4.60) becomes

$$\begin{aligned}(H_x)^2 K_{pp} - 2H_p H_x K_{xp} + H_p^2 K_{xx} \\ + (H_p H_{px} - H_x H_{pp})K_x + (H_x H_{xp} - H_p H_{xx})K_p = H_p H_{tx} - H_x H_{tp}\end{aligned}, \tag{4.62}$$

in where the subscripts denotes partial derivatives with respect to x, p and t.

Among all one-dimensional Hamiltonians, we pay special attention to Hamiltonians of the form

$$H = \frac{p^2}{2m} + V(x, t). \tag{4.63}$$

In the following subsections, we explore under which circumstances one can obtain simple and local expressions for K and in which situations non-locality is inevitable.

4.4.2 The space of operators that commute with H

We start by computing which operators commute with the Hamiltonian (and that therefore we need to avoid). These clearly satisfy the equation

$$\{H, f(x, p)\} = 0, \tag{4.64}$$

or

$$V_x \frac{\partial f}{\partial p} = \frac{p}{m}\frac{\partial f}{\partial x}, \tag{4.65}$$

which can be rewritten as

$$\frac{m}{p}\frac{\partial f}{\partial p} = \frac{1}{V_x}\frac{\partial f}{\partial x}. \tag{4.66}$$

In order to solve this equation, we rescale the position and momentum via

$$\tilde{x} = V(x,t)\,\tilde{p} = \frac{p^2}{2m} \tag{4.67}$$

which leads to

$$\frac{\partial f}{\partial \tilde{p}} - \frac{\partial f}{\partial \tilde{x}}. \tag{4.68}$$

By defining new variables $z = \tilde{p} + \tilde{x}$ and $w = \tilde{x} - \tilde{p}$, we obtain then that

$$\frac{\partial f}{\partial w} = 0. \tag{4.69}$$

The solution to this equation is, not surprisingly, $f = g(z)$, or

$$f(x,p) = g\left(\frac{p^2}{2m} + V(x,t)\right) = g(H), \tag{4.70}$$

in where g is an arbitrary function. Notice then that in this space we will always have even powers of p. These need to be avoided when looking for K. This can also be seen from Eq. (4.23):

$$\hat{K}(t) = \sum_{m,n}\left[-\frac{d}{dt}\gamma_m(t)\delta_{mn} + i\langle m(t)|\frac{d}{dt}|n(t)\rangle\right]|m(t)\rangle\langle n(t)| \tag{4.71}$$

Given that in one-dimensional systems one can always choose the eigenfunctions to be real, the matrix elements of K must be purely imaginary. This would not be the case if we have even powers of the momentum operator taking place in $\hat{K}$, which, in addition, we demand to be hermitian. Given the above arguments, we expect K to be of the form:

$$K(x,p) = f(x)p + g(x)p^3 + h(x)p^5 + \dots . \tag{4.72}$$

Using this Ansatz in Eq. (4.62) we then explore under which situations this series can be truncated, yielding along the way a local operator.

4.4.3 Local potentials

As mentioned in the previous sections,we would like to use Eq. (4.62) to gain insight into the issue of the locality of K. Solving this equation for a general potential is very hard to achieve. An alternative could be to consider a variety of different potentials, compute their associated K and then try to identify which properties of the potential lead to locality. Such an approach would be far from optimal. Instead, in this subsection we undertake the reverse approach; Instead of considering a particular potential, we introduce a local K and see which potentials can yield such a K. That is to say, we use the Ansatz (4.72) and consider Eq. (4.62) as an equation for the potential $V(x,t)$.

Since in principle we are not only worried about locality, but we would also like to have a K that could be easily created in the lab, we first focus in finding the class of potentials compatible with a K of the form:

$$K = f(x,t)p. \tag{4.73}$$

Indeed such a modification of the Hamiltonian is easy to create through the use of electromagnetic fields. Indeed, by introducing electromagnetic potentials $qA/m = -f(x,t)$ and $q\Phi = -mf(x,t)^2/2$, we would have that the Hamiltonian, trough minimal coupling, becomes

$$H = \frac{1}{2m}(p + mf(x,t))^2 - f(x,t)^2 + V(x,t) = \frac{p^2}{2m} + V(x,t) + f(x,t)p. \tag{4.74}$$

We proceed by inserting Eqs . (4.73,4.63) into (4.62), obtaining that

$$\frac{1}{m^2}\left[\frac{\partial^2}{\partial x^2}f\right]p^3 - \frac{1}{m}\left[3\left(\frac{\partial}{\partial x}f\right)\frac{\partial}{\partial x}V + f\frac{\partial^2}{\partial x^2}V + \frac{\partial^2}{\partial x \partial t}V\right]p = 0, \tag{4.75}$$

which, by using the linear independence of the different powers of p, yields

$$\begin{array}{l} \dfrac{\partial^2}{\partial x^2}f = 0 \\ ,3\left(\dfrac{\partial}{\partial x}f\right)\dfrac{\partial}{\partial x}V + f\dfrac{\partial^2}{\partial x^2}V + \dfrac{\partial^2}{\partial x \partial t}V = 0. \end{array}. \tag{4.76}$$

This immediately implies that the only functions $f(x,t)$ that are compatible with a K of the form given in Eq. (4.73) must satisfy

$$f(x,t) = b(t) + a(t)x. \tag{4.77}$$

Using this in Eq. (4.76) gives us that $V(x,t)$ must satisfy:

$$3a\frac{\partial}{\partial x}V + (ax+b)\frac{\partial^2}{\partial x^2}V + \frac{\partial^2}{\partial x \partial t}V = 0. \tag{4.78}$$

We then rewrite this equation as an equation for $U(x,t) = \partial_x V(x,t)$

$$3aU + (ax+b)\frac{\partial}{\partial x}U + \frac{\partial}{\partial t}U = 0. \tag{4.79}$$

In order to simplify this equation we look for a time-dependent shift of the x-coordinate $x' = x - F(t)$. This leads to:

$$3aU + \left(ax' + aF - \frac{d}{dt}F + b \right) \frac{\partial}{\partial x'}U + \frac{\partial}{\partial t}U = 0. \tag{4.80}$$

Now, we can impose that $aF(t) - \frac{d}{dt}F + b = 0$. The solution to this equation is given by:

$$F = \exp\left(\int_0^t d\tau a(\tau) \right) \int_0^t dt' \exp\left(- \int_0^{t'} d\tau' a(\tau') \right) b(t'). \tag{4.81}$$

With this shift, Eq. (4.80) becomes

$$x' \frac{\partial}{\partial x'}U + \frac{1}{a}\frac{\partial}{\partial t}U = -3U. \tag{4.82}$$

We can then rescale position and time via

$$\begin{aligned} \tilde{x} &= \ln(x') \\ \tilde{t} &= \int_0^t d\tau a(\tau) = \ln(\gamma(t)) \end{aligned}, \tag{4.83}$$

in where we defined: $a \equiv \partial_t \ln(\gamma(t))$. In this way, we get:

$$\frac{\partial}{\partial \tilde{x}}U + \frac{\partial}{\partial \tilde{t}}U = -3U. \tag{4.84}$$

By changing coordinates to $z = \tilde{x} + \tilde{y}$ and $w = \tilde{x} - \tilde{y}$, which satisfy: $\partial_{\tilde{x}} + \partial_{\tilde{t}} = 2\partial_z$, we reduce Eq. (4.78) to

$$\frac{\partial}{\partial z}U = -\frac{3}{2}U. \tag{4.85}$$

The solution to this equation is clearly given by $U = \exp(-3z)C(w)$, in where $C(w)$ is an arbitrary function. By going back to x and t, we see then that:

$$U = \frac{1}{(x\gamma)^{3/2}} \tilde{C}\left(\frac{x - F}{\gamma} \right), \tag{4.86}$$

in where $\tilde{C}(x) = C(\ln(x))$. To recover $V(x,t)$, we just need to integrate U with respect to

x:

$$V(x,t) = \int dx \frac{1}{(x\gamma)^{3/2}} \tilde{C}\left(\frac{x-F}{\gamma}\right). \tag{4.87}$$

We then isolate the time-dependance from this last expression by changing variables to $s = x\gamma$. This leads to

$$V(x,t) = \frac{1}{\gamma^2} \int^{\frac{x-F}{\gamma}} ds \frac{1}{s^{3/2}} \tilde{C}(s). \tag{4.88}$$

Finally, by defining $G(s) \equiv \int ds \frac{1}{s^{3/2}} \tilde{C}(s)$ we obtain that the most general solution for $V(x,t)$ has the form of a rescalable potential

$$V(x,t) = \frac{1}{\gamma^2} G\left(\frac{x-F}{\gamma}\right). \tag{4.89}$$

Notice that since G is obtained from integrating C, which is an arbitrary function, G itself is also arbitrary. Potentials with the form (4.89) have been extensively discussed in the literature, and the fact that they yield $K \sim xp$ is well known. For example, in Ref. [91] the authors guess this behavior by inspecting the spectrum of these kind of potentials. Moreover, in an approach more similar to ours, Ref. [90] shows that these potentials solve Eq. (4.62). However, our computations in this subsection have shown that this potentials are not only one possible solution for this equation, but in fact, the most general one.

Until now, we have obtained the rescaling and shift of the potential, γ and F, in terms of a and b, the coefficient of K. However, physically, it makes more sense to have this relationship in the opposite direction. In terms of γ and F, this K is given by:

$$K = \left(\frac{\partial_t \gamma}{\gamma}(x-F)\partial_t F\right) p. \tag{4.90}$$

This explains the simplicity of Eq. (4.89); The time-evolution operators associated to these

Hamiltonians are unitary transformation that produce global rescaling and translations of the position. Indeed, if we ignore translations, the quantum operator associated to K would be given by

$$\hat{K} = \frac{\partial_t \gamma}{2\gamma}(\hat{x}\hat{p} + \hat{p}\hat{x}) \tag{4.91}$$

There are no other possible symmetric orderings for the term xp. Then the time-evolution operator associated to $\hat{K}$ is given by

$$\hat{U}_{\hat{K}} = \exp\left(\frac{1}{2}\ln\left(\frac{\gamma(t)}{\gamma(0)}\right)(\hat{x}\hat{p} + \hat{p}\hat{x})\right), \tag{4.92}$$

which is a squeezing operator. In particular, it satisfy:

$$\begin{aligned} \hat{U}^{\dagger}_{\hat{K}}\hat{x}\hat{U}_{\hat{K}} &= \exp\left(\ln\left(\frac{\gamma(t)}{\gamma(0)}\right)\right)\hat{x} = \frac{\gamma(t)}{\gamma(0)}\hat{x} \\ \hat{U}^{\dagger}_{\hat{K}}\hat{p}\hat{U}_{\hat{K}} &= \exp\left(-\ln\left(\frac{\gamma(t)}{\gamma(0)}\right)\right)\hat{p} = \frac{\gamma(0)}{\gamma(t)}\hat{p} \end{aligned} \tag{4.93}$$

Hence, when going to the co-moving frame, the Hamiltonian becomes

$$\hat{U}^{\dagger}_{\hat{K}}\left(\frac{\hat{p}^2}{2m} + \frac{1}{\gamma^2(t)}V\left(\frac{x}{\gamma(t)}\right)\right)\hat{U}_{\hat{K}} = \left(\frac{\gamma(0)}{\gamma(t)}\right)^2\left(\frac{\hat{p}^2}{2m} + \frac{1}{\gamma^2(0)}V\left(\frac{x}{\gamma(0)}\right)\right), \tag{4.94}$$

which clearly commutes with itself at different times, and thus cannot produce mixing between states.

Thus, if one only has access to electromagnetic fields, one can only aspire to achieve transition-less quantum driving of Hamiltonians with simple global rescalings. This observation manifest explicitly through Eq. (4.89).

In general, having rescalable potentials seems to simplify the process of finding appro-

priate counterdiabatic terms, i.e., $\hat{K}$. First noticed by Jarzynski in Ref. [102] for power law traps and expandable boxes, later extended in Ref. [91] to general scalable potentials and finally generalized by del Campo in Ref. [103] to systems of many interacting particles, this feature usually leads to local operators.

It is curious though that with only one power of p only global transformations are allowed. One fair question that once could ask then is if by including higher powers of p, say p^3, one could obtain more general transformations, such as local re-scaling. This seems to be the case. The question of which potentials match these transformations though is much more harder to answer. A procedure similar to the one followed in this subsection would end up in a non-linear integro-partial-differential equation for $V(x,t)$, at which point we can not even guarantee the existence of a solution. However, by truncating the series in powers of p, and thus imposing locality, we can still learn something about the conditions that V must satisfy.

4.5 Quantum corrections and the Moyal bracket

Until now we have assumed that by replacing the commutator with the Poisson bracket we would obtain all the terms of $\hat{K}$, and thus, just needed to find the correct ordering of these terms. As we saw in the previous section, this strategy works perfectly when dealing with rescalable potentials or K's linear in p. However, there is no fundamental reason why this should be the case and in principle $\hat{K}$ could have terms proportional to $\hbar$ that would disappear in the classical limit. In fact, this is indeed the case.

As noticed in in Refs. [104, 105], the classical and quantum solution are, in general, different. These references study the situations in which the spectrum of the system is constant. In this case the commutator equation simplifies to $\partial_t \hat{H} + i[\hat{K}, \hat{H}] = 0$. In this

simplified situation, one can then try to replicate what we did in the previous section, i.e., look for the most general potential compatible with a certain form of $\hat{K}$, but now for $K = p^3 + f(x)p + g(x)$. By inserting this into the classical Eq. (4.62) and collecting powers of p, one gets that

$$\begin{aligned} &\frac{\partial V}{\partial t} + f(x)\frac{\partial V}{\partial x} = 0, \\ &\frac{1}{m}\frac{\partial f}{\partial x} - 3\frac{\partial V}{\partial x} = 0, \ . \\ &\frac{1}{m}\frac{\partial g}{\partial x} = 0. \end{aligned} \tag{4.95}$$

This system of equations is clearly solved by taking $f = 3mV(x,t)$ and $g = C = \text{const.}$ This leads then to:

$$K = p^3 + 3mV(x,t)p + C, \tag{4.96}$$

and the following condition for $V(x,t)$ (see Ref. [105])

$$\frac{\partial V}{\partial t} = -3mV(x,t)\frac{\partial V(x,t)}{\partial x}. \tag{4.97}$$

Notice that expression (4.96) only has one possible symmetric form. Thus, we must have that the operator $\hat{K}$ must be given by

$$\hat{K} = \hat{p}^3 + \frac{3}{2m}(\hat{p}V(x,t) + V(x,t)\hat{p}) + C. \tag{4.98}$$

We can then put this expression into the original commutator equation for $\hat{K}$. By doing so, one quickly notices that the terms containing the same power of $\hat{p}$ do not cancel unless they are normal ordered. This process though, introduces new terms that do not appear in the classical equation and that lead to a different condition for V. Indeed, in the quantum case one gets that, for a $\hat{K}$ such as (4.98), the potential must satisfy (see Ref. [104])

$$\frac{\partial V}{\partial t} = -3m\frac{\partial V}{\partial x}V + \frac{1}{4}\frac{\partial^3 V}{\partial x^3}. \tag{4.99}$$

As we see then, the classical and quantum conditions for the potential differ by the presence of the term $\frac{1}{4}\frac{\partial^3 V}{\partial x^3}$. The quantum equation is the KDV equation of integrable systems [106], which reveals a deep connection between integrability and transitionless driving. On the other hand, the classical condition is the dispersion-less version of the KDV equation. Thus, the inherent non-locality of quantum mechanics results in dispersion, which must be taken into account if one wants to counter transitions.

More importantly, from the results above we can conclude that, in general, the classical limit is not enough to obtain $\hat{K}$, and that we must incorporate quantum corrections in our formalism. The challenge consist in finding a way to incorporate this corrections and still be able to establish the problem in terms of PDE's. The key to this problem lies in finding a proper exact representation of the commutator. Luckily, there is a formalism that achieve exactly this objective; quantum mechanics in phase space and the use of Moyal brackets.

Quantum mechanics in phase space is an alternative way to do quantum mechanics. It is build over the seminal works of Weyl, Wigner, Groenewold and Moyal (see Refs. [107, 108, 13, 14]). The idea is that well-defined operators $\hat{O}(\hat{x},\hat{p})$ are in biyection with functions of phase space variables $O_W(x,p)$. We call this function the Weyl symbol of $\hat{O}$. The mapping between the two is the Wigner transformation:

$$O_W(x,p) = \int d\xi \left\langle x - \frac{\xi}{2}\right| \hat{O} \left| x + \frac{\xi}{2}\right\rangle e^{ip\xi/\hbar}, \tag{4.100}$$

and the inverse mapping is the Weyl transformation:

$$\hat{O} = \frac{1}{(2\pi\hbar)^2}\int dx\, dp\, da\, db\, O(x,p) e^{\frac{1}{\hbar}(a(x-\hat{x})+b(p-\hat{p})}, \tag{4.101}$$

which is also known as Weyl quantization. In general, the result of this transformation is a Weyl-ordered operator, i.e., a completely symmetrization of the products of $\hat{p}$ and $\hat{x}$. Notice that these mappings are linear and thus the Weyl symbol of the sum of two operators is the sum of the Weyl symbols of each operator. However, things are not so simple when having to deal with the Weyl symbol of the product of two operators. Essentially, given that in general two operators do not commute, the normal product between scalar cannot yield the proper mapping. Indeed, one needs to use the Moyal product:

$$(\hat{A}\hat{B})_W(x,p) = \sum_{n=0}^{\infty} \frac{1}{n!} A_W \left[\left(\frac{i\hbar}{2} \right)^n \left(\overleftarrow{\partial_x}\overrightarrow{\partial_p} - \overleftarrow{\partial_p}\overrightarrow{\partial_x} \right)^n \right] B_W. \tag{4.102}$$

The anti-symmetrization of this product is the Moyal bracket:

$$[\hat{A}, \hat{B}]_W = i\hbar\{A_W, B_W\}_M \equiv A_W 2i \sin\left(\frac{\hbar}{2} (\overleftarrow{\partial_q}\overrightarrow{\partial_p} - \overleftarrow{\partial_p}\overrightarrow{\partial_q}) \right) B_W \tag{4.103}$$

which is an exact representation of the commutator.

Now, let us go back to our original problem. We saw that if one wants to find a solution of the commutator equation the Poisson bracket is not enough. We must incorporate quantum corrections. In order to this, we do quantum mechanics in phase space by replacing the commutators in the commutator equation with Moyal brackets

$$\{H_W, (\partial_t H)_W - \{K_W, H_W\}_M\}_M = 0 \tag{4.104}$$

Equation. (4.104) is a partial differential equation for the Weyl symbol of $\hat{K}$, K_W. The idea is then to solve for K_W and then use the Weyl transformation, Eq. (4.101), to obtain $\hat{K}$.

The price to pay for this exchange is that, in general, we will not obtain exact expressions but rather semi-classical expansions, i.e., series in powers of $\hbar^2$. By analyzing the structure of the Moyal bracket it is easy to see why is this the case: we have an infinite

number of derivatives in Eq. (4.104). However, for polynomial potentials it is clear that these series are truncated and thus we have a finite number of corrections. In a similar fashion, notice that by following this procedure we also have solved the operator-ordering problem. Indeed, the Weyl transformation will provide us with the correct ordering. Also, note that, although the structure of the Moyal bracket is quite complicated, it simplifies greatly when we use it in Eq. (4.104); since the Hamiltonian does not have terms that depend on both position and momentum, only derivatives that are purely spatial or purely of momentum will contribute. Therefore, when expanding the Moyal bracket, we only need to focus on the most external terms. When computing quantum corrections, the situation is even simpler. Indeed, the third derivative of the Hamiltonian with respect to the momentum always vanishes, since $H_W \sim p^2$. Thus, when expanding the Moyal bracket we only need to keep the terms of the form $\overleftarrow{\partial}_p^n \vec{\partial}_q^n$.

4.6 Asymptotic behavior and locality

Although the classical solution is not the exact solution to our problem, it is the leading order contribution. As such, we can use it to gain insight about the locality of $\hat{K}$. Essentially, if the classical solution is non-local, the quantum solution must also be non-local. In this section, we will use the classical solution to obtain criteria under which locality cannot be achieved.

Consider potentials of the form

$$V(x,t) = \lambda(t)V(x). \tag{4.105}$$

In order for these potentials to rescale as Eq. (4.89), and hence have a K linear in p, we must have that $V(x)$ belongs to one of the following three cases

- The power law: $V(x) = x^N \quad (N \neq -2)$

- The logarithm: $V(x) = \ln(|rx|)$
- The exponential under translations: $V(x) = e^{rx-b}$

The first case is obvious. In the second one, notice that $\ln(rx/\gamma) = \ln(rx) - \ln(\gamma)$ and that this last term can only contribute through the dynamical phase. Finally, the exponential is only covered under translations, i.e., $\partial_t \gamma = 0$. Notice also that, among the power laws, there is a notable exemption: x^{-2}. Since this potential rescales in the same way as the momentum, there is no way to avoid mixings using only a global rescaling. In this specific case one can still compute the (classical) correct form of K, although it is highly non local.

One question that one can ask then is if there are other potential $V(x)$ such that one can still have a local form for K (i.e., a K with a truncated expansion in powers of p). In general, this will not be possible. In fact one can show that for any potential that has as an asymptotic behavior a power law, logarithmic grow or exponential grow (or decay), but it is not exactly a rescalable potential, the associated K cannot be local. The argument goes as follows; Suppose that there exists a local K that satisfy Eq. (4.62) for a potential of the form (4.105). Then, K can be written as

$$K = \sum_{n=1}^{N} f_n(x) p^{2n-1} \tag{4.106}$$

with N finite. By collecting powers of p, this would yield $N+1$ differential equations. The last one always has the form:

$$\frac{d^2}{dx^2} f_N(x) = 0, \tag{4.107}$$

and thus we must have $f_N(x) = a_N x + b_N$. However, if asymptotically $V(x)$ has a power law, exponential or logarithmic behavior, we know that in this regime we should have $K \to c\,xp$, in where c is just a constant. This implies that, asymptotically: $f_N(x) \to 0$. Given that $f_N(x)$ is linear in x, this can only happen if $f_N(x) = 0$ everywhere. As a conse-

quence, we have that f_{N-1} must satisfy $\frac{d^2}{dx^2} f_{N-1}(x) = 0$, yielding the same conclusion as before. Operating by induction, we conclude then that K must be linear in p. This can only happen if $V(x)$ has one of the forms described before. If this is not the case, then we have reached a contradiction. Since the only assumption we took was that we could truncate the expansion of K in powers of p, this leads to the conclusion that such a truncation cannot be achieved, and hence K must be non-local.

4.6.1 The inverse square potential exception: Explicit solution

As discussed in the previous section, the potentials $\lambda(t)x^N$ have a local $\hat{K}$ for all $N \neq 2$. In the case $N = 2$, this potential scales in the same way than the kinetic energy, and thus one cannot fix the mixing between states by a simple rescaling. In this section we obtain an explicit expression for the classical form of $\hat{K}$ associated to this potential. As we will see, it is highly non-linear and it posses a complicated analytical structure which leads to completely different behaviors when going from the attractive ($\lambda(t) < 0$) to the repulsive case ($\lambda(t) > 0$). This behavior is due in part to the high singular behavior of the potential. By doing this and trying to find the first quantum corrections we also see that classical mechanics and quantum mechanics differ greatly for this potential. Indeed, as mentioned in Ref. [109], the quantum version of this problem is full of mathematical problems: *A priori* it is not clear that this potential leads to a hermitian hamiltonian and self adjoint extensions become necessary. In addition, when the system is capable of holding boundstates, it holds one for every negative energy, leading then to a continuum spectrum without a groundstate. This is a strong red flag. Complementing this is the fact that there is no way to form an expression with units of energy using the fundamental constants that appear in the Hamiltonian (see Ref. [109]). The pathological behavior of this operator can also be appreciated by noticing that:

$$[\hat{H}, [\hat{H}, \hat{p}\hat{x} + \hat{x}\hat{p}]] = 0, \tag{4.108}$$

which, as we saw in previous sections, should not happen for well defined operators. Notice that this also implies that terms of the form xp are homogeneous solution to Eq. (4.62). However, to analyze this issues lies out of the scope of this work. We restrict ourselves to simply obtaining an explicit expression for the leading order term in K_W. The latter issue will only imply that this expression cannot have as a contribution terms with the form xp.

First, let us compute the classical solution: K. We start by suggesting the following Ansatz:

$$K = f(x)p + g(x)p^3 + h(x)p^5 + z(x)p^7 + \dots \tag{4.109}$$

in Eq. (4.62) for $V(x,t) = \lambda(t)/x^2$. By collecting powers of p this yields the following set of equations

$$\begin{aligned}
&\frac{24\lambda^2 g(x)}{x^6} - \frac{6\lambda f(x)}{mx^4} + \frac{6\lambda f'(x)}{x^3 m} + \frac{2\hat{\lambda}}{mx^3} = 0, \\
&\frac{14\lambda g'(x)}{mx^3} - \frac{18\lambda g(x)}{mx^4} + \frac{f''(x)}{m^2} + \frac{80\lambda^2 h(x)}{x^6} = 0, \\
&\frac{22\lambda h'(x)}{mx^3} - \frac{30\lambda h(x)}{mx^4} + \frac{168\lambda^2 z(x)}{x^6} + \frac{g''(x)}{m^2} = 0, \\
&\vdots
\end{aligned} \tag{4.110}$$

in where the subscripted dots denote time derivatives and the primes denote spatial derivatives. Counting powers in x leads to the the conclusion that $f(x) \propto x$, $g(x) \propto x^3$, $h(x) \propto x^5$ and $z(x) \propto x^7$. This power counting is done by demanding that we only add the minimum necessary terms in order to successfully cancel the source term, i.e., the term proportional to $\dot{\lambda}$. Seeing this, we can hypothesize that:

$$K = \sum_{n=1}^{\infty} c_n (xp)^{2n-1}. \tag{4.111}$$

As discussed before, we must have $c_1 = 0$. Introducing this Ansatz into Eq. (4.62) we obtain a system of equations for the coefficients c_n. Solving this system for the first coefficients yields

$$c_2 = -\frac{\dot{\lambda}}{\lambda}\frac{1}{12\lambda m}, \quad c_3 = \frac{\dot{\lambda}}{\lambda}\frac{1}{40\lambda^2 m^2}, \quad c_3 = -\frac{\dot{\lambda}}{\lambda}\frac{1}{112\lambda^4 m4}, \ldots, \tag{4.112}$$

which turn out to be consistent with the sequence

$$c_n = \frac{\dot{\lambda}}{\lambda}\frac{(-1)^n}{2^{n+1}(2n+1)(\lambda m)^n}. \tag{4.113}$$

This suggest that K is given by

$$K = \frac{\dot{\lambda}}{\lambda}\sum_{n=0}^{\infty}\frac{(-1)^n}{2^{n+1}(2n+1)(\lambda m)^n}(xp)^{2n+1} - \frac{\dot{\lambda}}{2\lambda}(xp), \tag{4.114}$$

in where we have added and subtracted a term proportional to xp. We do this in order to find a closed expression for the infinite sum. Although this series has a finite radius of convergence, $r = \sqrt{2m|\lambda|}$, it can be computed exactly. For positive λ we obtain

$$K = \frac{\dot{\lambda}}{\lambda}\left[\sqrt{\frac{m\lambda}{2}}\arctan\left(\frac{xp}{\sqrt{2m\lambda}}\right) - \frac{1}{2}xp\right], \tag{4.115}$$

while in the negative λ case, we find that

$$K = \frac{\dot{\lambda}}{\lambda}\left[\sqrt{\frac{m\lambda}{2}}\operatorname{arctanh}\left(\frac{xp}{\sqrt{2m\lambda}}\right) - \frac{1}{2}xp\right] \tag{4.116}$$

as one may expect from analytical continuation. Notice however that, written in this way, this function is real only for $|xp| < \sqrt{2m\lambda}$, and we know that K must lead to an hermitian operator. Thus, it cannot have an complex classical limit. However, recall that Eq. (4.62)

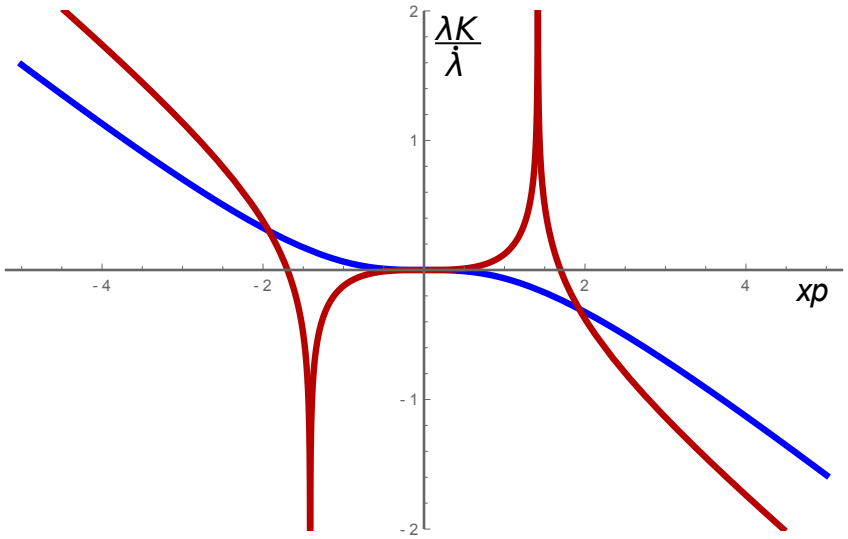

Figure 4.2: Plot of $\lambda K/\dot{\lambda}$ for the inverse square potential (in both its attractive and repulsive cases) as a function of xp. In order to make this plot we also fixed $\sqrt{m|\lambda|} = 1$. The red line represents the attractive ($\lambda < 0$) case while the blue line represents the repulsive ($\lambda > 0$) case. These functions were obtained by extending the limit of the power series (4.113) to the entire domain.

is a linear equation with real coefficients, and thus real and imaginary parts of a given complex solution do not mix. Hence, they must also be solutions. Since the real part agrees completely with our expression for K inside the radius of convergence, we can just write

$$K = \frac{\dot{\lambda}}{\lambda}\Re\left(\sqrt{\frac{m\lambda}{2}}\arctan\left(\frac{xp}{\sqrt{2m\lambda}}\right) - \frac{1}{2}xp\right), \tag{4.117}$$

which is valid for any λ. A plot of this function, for both $\lambda > 0$ and $\lambda < 0$ can be found in Figure 4.2.

One interesting feature of the classical atractive solution is the presence of divergent vertical asymptotes at $xp = \pm\sqrt{2m|\lambda|}$. Classically, xp reaches this value when the particle crosses the origin in a bound state. Also, that value of xp marks the boundary between bound and free states. Indeed, for $|xp| > \sqrt{m\lambda}$ we have free states and for $|xp| < \sqrt{m\lambda}$ we have boundstates. Finally, we observe that in the asymptotic regime $|x| \to \infty$, K acquires a linear behavior with a slope given by $-\frac{\dot{\lambda}}{2\lambda}$ for both the repulsive and attractive cases. This is the same slope that one gets for K for a logarithmic potential.

Once we have obtained the classical solution, we look for the first quantum correction. In order to obtain this correction, we assume that:

$$K_W = K + \hbar^2 K_1 + \dots, \tag{4.118}$$

where K_1 is the first quantum correction. Using this Ansatz into Eq. (4.104) and collecting powers of $\hbar$ we obtain an equation for K_1. By assuming that this correction can also be expanded in series of p, we obtain that the first correction is given by

$$K_1 = \frac{1}{2}\frac{px}{\lambda} - \frac{7}{6}\frac{p^3x^3}{\lambda^2} + \frac{11}{5}\frac{p^5x^5}{\lambda^3} - \frac{25}{7}\frac{p^7x^7}{\lambda^4} + \frac{95}{18}\frac{p^9x^9}{\lambda^5} + \dots \tag{4.119}$$

Notice that the absolute values of the coefficients of this expansion seem to form an increasing sequence. As such, the right-hand side of Eq. (4.119) should not converge and the first quantum correction blows up. This can be understood by noticing that in classical mechanics there is nothing special about the x^{-2} potential as we can find orbital solutions. However, the quantum problem is quite a different story, being unsolvable in principle. This discrepancy between both theories gets manifested by the divergence of the quantum corrections.

4.7 Multiple-scale potentials and the perturbation scheme

Until now, the literature seems to have been centered around re-scalable potentials. However, most potentials will have multiple scales. For example consider a simple harmonic oscillator with a small anharmonicity correction, i.e., $V(x,t) = \lambda x^2 + \tau x^4$. Here, the x^2 and the x^4 terms scale in a different way and thus a global rescaling will not be enough to fix the time-evolution of the system; indeed, we will need some sort of local rescaling. In general, as we deducted in section 4.6, this will not be a local operator, and therefore, probably not realizable experimentally. However, if one assumes that one of the length-scales of this

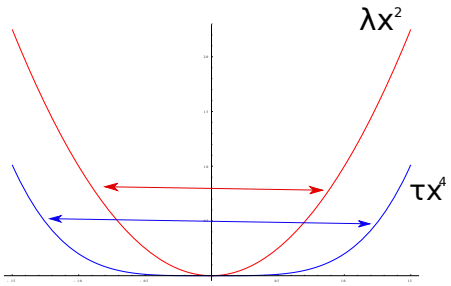

Figure 4.3: Potential with multiple scales. The total potential is $\lambda x^2 + \tau x^4$. In this diagram we show the contributions from each term and how each term has its own natural length-scale. We are interested into studying the limit case in which one length-scale, in this case, the one associated to τx^4, is much bigger that the other one, i.e., λx^2.

potential is much larger than the other one (see Figure 4.3), one could have a situation in which a local operator could be a good approximation. Indeed, in this situation one should focus first in globally fixing the shorter length-scale, which yields a local operator. Over this length-scale the other potential will remain approximately constant. Over longer scales however, we will need to add corrections. If one only requires an approximate driving of the states, then this corrections may be achieved by local operators, as they will only have to fix a neighborhood of each point. This opens the door to a potential perturbative scheme.

The formalism is achieved by assuming that $\hat{H} = \hat{H}_0 + \tau V(x,t)$, in where $\tau V(x,t)$ is the long-scale potential that we will consider as a perturbation and τ is a small parameter. We write the potential in this way, explicitly separating V from τ, in order to book keep the order of each correction. In a similar way, we can expand $\hat{K}$ in series of τ

$$\hat{K} = \hat{K}_0 + \tau \hat{K}_1 + \tau^2 \hat{K}_2 + \dots, \tag{4.120}$$

in where K_0 is the counterdiabatic term associated to H_0, i.e.,

$$\left[\hat{H}_0, \partial_t \hat{K}_0 + \frac{i}{\hbar}\left[\hat{K}_0, \hat{H}_0\right]\right] = 0. \tag{4.121}$$

Then, we replace this expansion in the commutator equation and proceed in a way similar

to the Rayleigh-Schrödinger perturbation scheme. By collecting powers of τ we obtain a set of coupled commutator equations. In these equations though, the equation for the N-th correction only depends on the first N previous terms. Since $\hat{K}_0$ is known, we can then, in principle, systematically solve for each correction.

For example, the general equation for the first correction is

$$\frac{i}{\hbar}[\hat{H}_0,[\hat{K}_1,\hat{H}_0]]+[V,\partial_t\hat{H}_0]+[\hat{H}_0,\partial_t V]+\frac{i}{\hbar}[\hat{H}_0,[\hat{K}_0,V]]+\frac{i}{\hbar}[V,[\hat{K}_0,\hat{H}_0]]=0. \quad (4.122)$$

In principle, one could write equations like this for each correction. However, since commutators are not easy to handle, we solve these equations by exchanging the commutator with Moyal brackets. Then, Eq. (4.121) becomes

$$\{H_{0W}+\tau V_W,\partial_t H_{0W}+\tau\partial_t V_W-\{K_{0W}+\tau K_{1W}+\ldots,H_{0W}+\tau V_w\}_M\}_M=0 \quad (4.123)$$

Therefore, in the most general case, this would mix two schemes of approximation: the perturbative approximation and the semi-classical approximation. Thus, for each perturbative correction we write

$$K_{1W}=K_{1W}^0+\hbar^2K_{1W}^2+\hbar^4K_{1W}^4+\ldots. \quad (4.124)$$

Namely, each perturbative correction can be thought as a classical correction plus quantum corrections. This quantum corrections are then computed in exactly the same way as the classical perturbative corrections: by solving equations recursively. However, as we mentioned before, there are potentials for which the semi-classical expansion is finite and, in this cases, we are left only with an infinite perturbative approximation.

In order to solve Eq. (4.123) we then propose the following scheme. First solve the classical unperturbed problem

$$\{H_{0W}, \partial_t H_{0W} - \{K^0_{0W}, H_{0W}\}\} = 0, \tag{4.125}$$

where $\{\ ,\ \}$ denotes the Poisson bracket. Afterwards, compute the quantum corrections using

$$\left\{ H_{0W} + \tau V_W, \partial_t H_{0W} + - \left\{ \sum_{n=0}^{N} \hbar^{2n} K^{2n}_{0W}, H_{0W} \right\}_M \right\}_M = 0. \tag{4.126}$$

Again, this is achieved by expanding the equation and collecting powers of $\hbar^2$. In the next step, solve for the first classical perturbation

$$\{H_0 + \tau V, \partial_t V - \{K^0_{0W} + \tau K^0_{1W} + \ldots, H_{0W} + \tau V_w\}\} = 0, \tag{4.127}$$

and later compute the quantum corrections via

$$\{H_{0W} + \tau V_W, \partial_t V_W - \{\sum_{n=0}^{N} \hbar^{2n} K^{2n}_{0W} + \tau \sum_{n=0}^{N} \hbar^{2n} K^{2n}_{1W}, H_{0W} + \tau V_w\}_M\}_M = 0. \tag{4.128}$$

We repeat this process until we obtain an expression for K_W corrected perturbatively and semi-classically up to the desired orders.

Now, recall that, in order to solve for this terms, we need to solve PDE's. Again these PDE's are solved by assuming that each correction can be expanded in odd powers of p

$$K^{2n}_{mW} = \sum_{k \text{ odd}} f^{2n}_{k,m}(x) p^k. \tag{4.129}$$

If the corrections are local, then these series can be truncated.

4.7.1 Physical meaning of the perturbative solutions

Until now we have assumed that K_W can be expanded in a power series of τ and developed an scheme to obtain these corrections systematically. We have not stopped to think what is the physical meaning of having such a corrected operator. The main objective of this subsection is to clarify this point.

Recall that for any well-behaved potential there is a unique exact solution of Eq. (4.104), K_W, whose associated operator satisfies the equation

$$i\partial_t|\Psi_n(t)\rangle = \hat{K}|\Psi_n(t)\rangle, \tag{4.130}$$

where $|\Psi_n(t)\rangle$ is the adiabatic time-evolution of the exact instantaneous eigenstate of $\hat{H}$ without the dynamical phase, i.e., including just the geometrical phase. On a side note, notice that since in one dimension we can always choose to have real eigenstates there will be no geometrical phase.

Now, formally, we can also expand K_W in a power series of τ

$$K_W = \sum_{k=0} \tau^k K_{kW}. \tag{4.131}$$

Since the actual value of τ is arbitrary and this expansion must be true for any of such values, this expansion must match the one we obtain by collecting powers of τ by means of the Moyal bracket. This expansion will have then, through the Weyl transformation, a similar expansion for the associated operator $\hat{K}$

$$\hat{K} = \sum_{k} \tau^k \hat{K}_k. \tag{4.132}$$

This operator must continue to satisfy Eq. (4.130). However, since $|\Psi_n(t)\rangle$ are instanta-

neous eigenstates, they also have a perturbative expansion, which can be obtained through the usual time-independent perturbation theory scheme. Then, we can write

$$|\Psi_n(t)\rangle = \sum_{k=0} \tau^k |\Psi_{n,k}(t)\rangle. \tag{4.133}$$

Using this in Eq. (4.130), and keeping terms up to order τ^N, we see that

$$i\partial_t \sum_{k=0}^{N} \tau^k |\Psi_{n,k}(t)\rangle = \left(\sum_{k=0}^{N} \tau^k \hat{K}_k\right)\left(\sum_{k=0}^{N} \tau^k |\Psi_n(t)\rangle\right) + O(\tau^{N+1}). \tag{4.134}$$

This last equation clearly reveals the physical role of an operator $\hat{K}$ corrected up to order N: it is the operator that drives the corrected instantaneous eigenstates up to order N in τ. This also tells us when this perturbative solution is a good approximation. $\hat{K}$ will keep non-adiabatic mixings small as long as the the corrected instantaneous eigenstates are, by themselves, a good approximation of the exact instantaneous eigenstates. This means that, depending on the perturbative potential, the degree of precision that we achieve can be different for each eigenstate.

4.7.2 Example: $V(x,t) = \lambda(t)x^2 + \tau(t)x^4$

In this section we will illustrate our approximation scheme by solving Eq. (4.104) for the potential $V(x,t) = \lambda(t)x^2 + \tau(t)x^4$, with the role of the perturbation being taken by $\tau(t)x^4$. We choose this specific potential for two reasons; first, we know that the number of quantum corrections at each order will be finite. Second, we can use our knowledge of the quantum harmonic oscillator and the physical interpretation of the corrected $\hat{K}$ in order to guess an appropriate Ansatz for each correction.

We start then by compute K_{0W}. Since this is a re-scalable potential, we know that we must have $K_{0W} \propto xp$. Indeed, it is not hard to obtain that

$$K_{0W} = -\frac{\dot{\lambda}}{4\lambda} xp. \tag{4.135}$$

The next step consists in finding the classical first perturbative correction. In order to do so, we recall that this correction should make $\hat{K}$ drive the eigenstates corrected up to first order. This first order correction mixes the eigenstates of the harmonic oscillator, $|n\rangle$, for which the matrix element $\langle n|x^4|m\rangle$ does not vanish. Since these are harmonic oscillator states, these matrix elements only connect states that differ in up to four quantum numbers, which can be easily be seen by replacing $\hat{x}$ and $\hat{p}$ in terms of creation and annihilation operators. In addition, by remembering that even powers of $\hat{p}$ are linked to operators that commute with $\hat{H}$ we must have that the correction can only have odd powers of $\hat{p}$. The only combinations of $\hat{x}$ and $\hat{p}$ that achieve both these objectives (up to operator ordering) are: $\hat{x}\hat{p}^3$ and $\hat{x}^3\hat{p}$. Inspired by this, we propose the Ansatz

$$K_{1W} = c_1 x^3 p + c_2 x p^3. \tag{4.136}$$

Inserting this into the classical equation we get that:

$$K_{1W} = -\frac{\dot{\lambda}}{\lambda} \frac{2\lambda\dot{\tau} - 3\tau\dot{\lambda}}{\lambda\dot{\lambda}} \left(\frac{5}{32} x^3 p + \frac{3}{64} \frac{xp^3}{m\lambda} \right). \tag{4.137}$$

Notice that this is indeed a local operator, which confirms our impression that we could have an approximate local operator.

The next step in our scheme would be to compute the quantum corrections to the previous expression. However, when using Eq (4.104), we see that, up to first order in τ, the equation is satisfied exactly, and thus, there are no quantum corrections to the first order.

In order to obtain the next correction, we can use the same logic than before: think in which states can be connected by the perturbation at each order and suggest an Ansatz.

Then, using this Ansatz, compute the classical solution and then use Eq. (4.104) to get the quantum corrections.

Proceeding in this way, we get that, up to second order in τ

$$\begin{aligned} K = -\frac{\dot{\lambda}}{\lambda}\Bigg\{ & \frac{1}{4}xp + \frac{2\lambda\dot{\tau} - 3\tau\dot{\lambda}}{\lambda\dot{\lambda}\tau}\Bigg[\tau\left(\frac{5}{32}x^3p + \frac{3}{64}\frac{xp^3}{m\lambda}\right) \\ & -\tau^2\left(\frac{19}{64}\frac{x^5p}{\lambda} + \frac{13}{48}\frac{x^3p^3}{m\lambda^2} + \frac{13}{256}\frac{xp^5}{m^2\lambda^3}\right) + \hbar^2\tau^2\frac{9}{128}\frac{xp}{m\lambda^2}\Bigg]\Bigg\} \end{aligned} \tag{4.138}$$

As we see, the first quantum correction appears at the second perturbative order. Moreover, all the corrections are local. This continues to be true when going to third order. Finally, notice the overall factor $2\lambda\dot{\tau} - 3\tau\dot{\lambda}$ multiplying all the corrective terms. This factor must be present because, for a fine tuning of the time dependence of the parameters λ and τ, the potential $\lambda x^2 + \tau x^4$ can become a rescalable potential, in which case the counterdiabatic term must be proportional to xp.

Finally, recall that for this particular potential, the perturbative expansion is only a good approximation for low energy states. Indeed, low energy states are well localized around the origin and therefore, they don't see too much of the perturbation. However, as the energy of these states increases, they become less and less localized, until they reach a point in which their natural length-scales are comparable to the one of the perturbation. At this point, the perturbed states are no longer a good approximation, and hence, the corrected $\hat{K}$ does not keep us close to the exact instantaneous eigenstates.

We would like to finish this section by mentioning that these features are not exclusive of the τx^4 perturbation. Indeed, we could have used any even power of x as our perturbation and we would still have obtained local corrections. However, when increasing the

degree of the perturbation we would have also add higher order quantum corrections.

4.8 Final remarks

The capability of finding counterdiabatic terms cannot be taken into real applications unless we know the explicit relationship between this operator and the observables of the system. Moreover, even if we were to know this relationship, if this operator is non-local we might not be able to create it in the lab. Therefore, there is a need to find explicit expressions for $\hat{K}$ and find regimes in which local operators can be found.

In this work, we have found a way to explicitly link $\hat{K}$ with the observables of the system through a commutator equation. Since these equations are not easy to solve, we exchange commutators with partial derivatives by exchanging the commutator with Moyal brackets. The necessity of using the Moyal bracket, and not simply the Poisson bracket, comes from the fact that $\hat{K}$ receives quantum corrections, which yield a semi-classical expansion for $\hat{K}$. As the leading order term in this expansion, the classical limit can be used to gain insight into the possible locality of $\hat{K}$. By proceeding in this way, we learned that, in most cases, K is not local. In general, potentials with multiple length-scales do not have local counterdiabatic terms unless they are fine tuned so they can be rescaled. However, if in such potentials one length-scale is much bigger than the other ones, there is a chance that one could get an approximate local operator. In order to test this idea, we developed a perturbation scheme for $\hat{K}$. The result of such approximation is an operator that drives the perturbed eigenstates of the system. We tested this idea with the potential $\lambda x^2 + \tau x^4$, and, as expected, we obtained local corrections. This seems to confirm the view of the counterdiabatic term as a generator of local scaling and translations.

REFERENCES

[1] M. Doi, "Second quantization representation for classical many-particle system," *J. Phys. A: Math. Gen.*, vol. 9, no. 9, p. 1465, 1976.

[2] ——, "Stochastic theory of diffusion-controlled reaction," *J. Phys. A: Math. Gen.*, vol. 9, no. 9, p. 1479, 1976.

[3] C. Domb and J. L. Lebowitz, Eds., ser. Phase Transitions and Critical Phenomena. Academic Press, 2001, vol. 19.

[4] de Gennes and G. P., "Soluble model for fibrous structures with steric constraints," *The Journal of Chemical Physics*, vol. 48, no. 5, pp. 2257–2259, 1968.

[5] Benjamin Loewe and Paul M. Goldbart, "Systems of directed polymers in non-trivial geometries," *In preparation*,

[6] Benjamin Loewe, Anton Souslov, and Paul M. Goldbart, "Flocking from a quantum analogy: Spin-orbit coupling in an active fluid," *In preparation*,

[7] Benjamin Loewe, Rafael Hipolito, and Paul M. Goldbart, "A semi-classical approach to transitionless quantum driving," *In preparation*,

[8] M. V. Berry, "Transitionless quantum driving," *J. Phys. A: Math. Theor.*, vol. 42, p. 365 303, 36 Aug. 2009.

[9] E. Noether, "Invariante variationsprobleme," *Nachrichten von der Gesellschaft der Wissenschaften zu Gttingen, Mathematisch-Physikalische Klasse*, vol. 1918, pp. 235–257, 1918.

[10] Herbert Goldstein, Charles P. Poole, and John L. Safko, *Classical Mechanics*, 3rd ed. Addison-Wesley, Jun. 2001.

[11] J. J. Sakurai and Jim Napolitano, *Modern quantum mechanics*, 2nd edition. Pearson, 2010.

[12] P. A. M. Dirac, "The fundamental equations of quantum mechanics," *Proceedings of the Royal Society of London A: Mathematical, Physical and Engineering Sciences*, vol. 109, no. 752, pp. 642–653, 1925.

[13] H. J. Groenewold, "On the principles of elementary quantum mechanics," *Physica*, vol. 12, no. 7, pp. 405–460, 1946.

[14] J. E. Moyal, "Quantum mechanics as a statistical theory," *Math. Proc. Cambridge Philos. Soc.*, vol. 45, no. 1, pp. 99–124, Jan. 1949.

[15] Hagen. Kleinert, *Path Integrals in Quantum Mechanics, Statistics, Polymer Physics, and Financial Markets)*, 5th ed. World Scientific, Jun. 2009.

[16] A. Zee, *Quantum field theory in a nutshell*. Princeton University Press, 2010.

[17] M. E. Peskin and D. V. Schroeder, *An Introduction to Quantum Field Theory*. Westview Press, 1995.

[18] Kenneth G. Wilson, "The renormalization group: Critical phenomena and the Kondo problem," *Rev. Mod. Phys.*, vol. 47, pp. 773–840, 4 Oct. 1975.

[19] R. Bausch, H. K. Janssen, and H. Wagner, "Renormalized field theory of critical dynamics," *Zeitschrift für Physik B Condensed Matter*, vol. 24, no. 1, pp. 113–127, 1976.

[20] Vadim Linetsky, "The path-integral approach to financial modeling and options pricing," *Computational Economics*, vol. 11, no. 1, pp. 129–163, 1997.

[21] Norbert Wiener, "The average of an analytic functional," *Proc. Natl Acad. Sci.*, vol. 7, pp. 253–260, 9 Sep. 1921.

[22] Paul A. M. Dirac, "The Lagrangian in Quantum Mechanics," *Physikalische Zeitschrift der Sowjetunion*, vol. 3, pp. 64–72, 1933.

[23] R. P. Feynman, "Space-time approach to non-relativistic quantum mechanics," *Rev. Mod. Phys.*, vol. 20, pp. 367–387, 2 Apr. 1948.

[24] D. Zeb Rocklin, Shina Tan, and Paul M. Goldbart, "Directed-polymer systems explored via their quantum analogs: Topological constraints and their consequences," *Phys. Rev. B*, vol. 86, p. 165 421, 16 Oct. 2012.

[25] Anton Souslov, D. Zeb Rocklin, and Paul M. Goldbart, "Organization of strongly interacting directed polymer liquids in the presence of stringent constraints," *Phys. Rev. Lett.*, vol. 111, p. 096 401, 9 Aug. 2013.

[26] D. Zeb Rocklin and Paul M. Goldbart, "Directed-polymer systems explored via their quantum analogs: General polymer interactions and their consequences," *Phys. Rev. B*, vol. 88, p. 165 417, 16 Oct. 2013.

[27] Anton Souslov, Benjamin Loewe, and Paul M. Goldbart, "Emergent tilt order in Dirac polymer liquids," *Phys. Rev. E*, vol. 92, p. 030 601, 3 Sep. 2015.

[28] M. Girardeau, "Relationship between systems of impenetrable bosons and fermions in one dimension," *J. Math. Phys.*, vol. 1, no. 6, pp. 516–523, 1960.

[29] N. C. Bartelt, T. L. Einstein, and Ellen D. Williams, "The influence of step-step interactions on step wandering," *Surf. Sci.*, vol. 240, no. 1, pp. L591 –L598, 1990.

[30] Anatoli Polkovnikov, Yariv Kafri, and David R. Nelson, "Vortex pinning by a columnar defect in planar superconductors with point disorder," *Phys. Rev. B*, vol. 71, p. 014 511, 1 Jan. 2005.

[31] Manas Kulkarni and Austen Lamacraft, "Finite-temperature dynamical structure factor of the one-dimensional bose gas: From the gross-pitaevskii equation to the kardar-parisi-zhang universality class of dynamical critical phenomena," *Phys. Rev. A*, vol. 88, p. 021 603, 2 Aug. 2013.

[32] L. Chetouani, L. Dekar, and T. F. Hammann, "Green's functions via path integrals for systems with position-dependent masses," *Phys. Rev. A*, vol. 52, pp. 82–91, 1 Jul. 1995.

[33] B. Gaveau, E. Mihóková, M. Roncadelli, and L. S. Schulman, "Path integral in a magnetic field using the trotter product formula," *Am. J. Phys*, vol. 72, no. 3, pp. 385–388, 2004.

[34] R. Feynman and A. Hibbs, *Quantum mechanics and path integrals*. McGraw-Hill, 1965.

[35] V. V. Dodonov, A. B. Klimov, and D. E. Nikonov, "Quantum particle in a box with moving walls," *J. Math. Phys.*, vol. 34, no. 8, pp. 3391–3404, 1993.

[36] Sara Di Martino, Fabio Anzà, Paolo Facchi, Andrzej Kossakowski, Giuseppe Marmo, Antonino Messina, Benedetto Militello, and Saverio Pascazio, "A quantum particle in a box with moving walls," *J. Phys. A: Math. Theor.*, vol. 46, no. 36, p. 365 301, 2013.

[37] Thomas Kramer, Stephanie Scholz, Michael Maskos, and Klaus Huber, "Colloid–polymer mixtures in solution with refractive index matched acrylate colloids," *J. Colloid Interface Sci.*, vol. 279, no. 2, pp. 447–457, 2004.

[38] Radu P. Mondescu and M. Muthukumar, "Brownian motion and polymer statistics on certain curved manifolds," *Phys. Rev. E*, vol. 57, pp. 4411–4419, 4 Apr. 1998.

[39] H. Kleinert and A. Chervyakov, "Perturbation theory for path integrals of stiff polymers," *J. Phys. A: Math. Gen.*, vol. 39, no. 26, p. 8231, 2006.

[40] Frank Schweitzer, *Brownian agents and active particles: Collective dynamics in the natural and social sciences*, 3rd edition. Springer-Verlag Berlin Heidelberg, 2003.

[41] Tim Sanchez, Daniel T. N. Chen, Stephen J. DeCamp, Michael Heymann, and Zvonimir Dogic, "Spontaneous motion in hierarchically assembled active matter," *Nature*, vol. 491, no. 7424, pp. 431–434, 2013.

[42] H. P. Zhang, Avraham Be'er, E.-L. Florin, and Harry L. Swinney, "Collective motion and density fluctuations in bacterial colonies," *Proceedings of the National Academy of Sciences*, vol. 107, no. 31, pp. 13 626–13 630, 2010.

[43] J. Buhl, D. J. T. Sumpter, I. D. Couzin, J. J. Hale, E. Despland, E. R. Miller, and S. J. Simpson, "From disorder to order in marching locusts," *Science*, vol. 312, no. 5778, pp. 1402–1406, 2006.

[44] M. Ballerini, N. Cabibbo, R. Candelier, A. Cavagna, E. Cisbani, I. Giardina, V. Lecomte, A. Orlandi, G. Parisi, A. Procaccini, M. Viale, and V. Zdravkovic, "Interaction ruling animal collective behavior depends on topological rather than metric distance: Evidence from a field study," *Proceedings of the National Academy of Sciences*, vol. 105, no. 4, pp. 1232–1237, 2008.

[45] Andrea Cavagna and Irene Giardina, "Bird Flocks as Condensed Matter," *Annual Review of Condensed Matter Physics.*, vol. 5, no. 1, pp. 183–207, Mar. 2014.

[46] Antoine Bricard, Jean-Baptiste Caussin, Nicolas Desreumaux, Olivier Dauchot, and Denis Bartolo, "Emergence of macroscopic directed motion in populations of motile colloids.," *Nature*, vol. 503, no. 7474, pp. 95–8, 2013.

[47] L. Giomi, N. Hawley-Weld, and L. Mahadevan, "Swarming, swirling and stasis in sequestered bristle-bots," in *Proceedings of the Royal Society of London A: Mathematical, Physical and Engineering Sciences*, The Royal Society, vol. 469, 2013, p. 20 120 637.

[48] M. C. Marchetti, J. F. Joanny, S. Ramaswamy, T. B. Liverpool, J. Prost, Madan Rao, and R. Aditi Simha, "Hydrodynamics of soft active matter," *Rev. Mod. Phys.*, vol. 85, pp. 1143–1189, 3 Jul. 2013.

[49] Tamás Vicsek, András Czirók, Eshel Ben-Jacob, Inon Cohen, and Ofer Shochet, "Novel type of phase transition in a system of self-driven particles," *Phys. Rev. Lett.*, vol. 75, pp. 1226–1229, 6 Aug. 1995.

[50] Guillaume Grégoire and Hugues Chaté, "Onset of collective and cohesive motion," *Phys. Rev. Lett.*, vol. 92, p. 025 702, 2 Jan. 2004.

[51] Hugues Chaté, Francesco Ginelli, and Raúl Montagne, "Simple model for active nematics: Quasi-long-range order and giant fluctuations," *Phys. Rev. Lett.*, vol. 96, p. 180 602, 18 May 2006.

[52] H. Chaté, F. Ginelli, G. Grégoire, F. Peruani, and F. Raynaud, "Modeling collective motion: Variations on the vicsek model," *The European Physical Journal B*, vol. 64, no. 3, pp. 451–456, 2008.

[53] N. D. Mermin and H. Wagner, "Absence of ferromagnetism or antiferromagnetism in one- or two-dimensional isotropic heisenberg models," *Phys. Rev. Lett.*, vol. 17, pp. 1133–1136, 22 Nov. 1966.

[54] John Toner and Yuhai Tu, "Long-range order in a two-dimensional dynamical XY model: How birds fly together," *Phys. Rev. Lett.*, vol. 75, pp. 4326–4329, 23 Dec. 1995.

[55] John Toner, Yuhai Tu, and Sriram Ramaswamy, "Hydrodynamics and phases of flocks," *Ann. Phys.*, vol. 318, no. 1, pp. 170–244, 2005, Special Issue.

[56] Eric Bertin, Michel Droz, and Guillaume Grégoire, "Boltzmann and hydrodynamic description for self-propelled particles," *Physical Review E*, vol. 74, no. 2, p. 22 101, 2006.

[57] ——, "Hydrodynamic equations for self-propelled particles: Microscopic derivation and stability analysis," *J. Phys. A: Math. Theor.*, vol. 42, no. 44, p. 445 001, 2009.

[58] Baskaran Aparna and M. Cristina Marchetti, "Nonequilibrium statistical mechanics of self-propelled hard rods," *J. Stat. Mech: Theory Exp.*, vol. 2010, no. 04, P04019, 2010.

[59] Alexandre Morin, Nicolas Desreumaux, Jean-Baptiste Caussin, and Denis Bartolo, "Distortion and destruction of colloidal flocks in disordered environments," *Nat. Phys.*, vol. 13, no. 1, pp. 63–67, Oct. 2016.

[60] Hugo Wioland, Francis G. Woodhouse, Jörn Dunkel, John O. Kessler, and Raymond E. Goldstein, "Confinement Stabilizes a Bacterial Suspension into a Spiral Vortex," *Phys. Rev. Lett.*, vol. 110, no. 26, p. 268 102, Jun. 2013.

[61] Tommaso Brotto, Jean-Baptiste Caussin, Eric Lauga, and Denis Bartolo, "Hydrodynamics of confined active fluids.," *Phys. Rev. Lett.*, vol. 110, no. 3, p. 038 101, Jan. 2013.

[62] D. J. G. Pearce and M. S. Turner, "Emergent behavioural phenotypes of swarming models revealed by mimicking a frustrated anti-ferromagnet.," *Journal of the Royal Society, Interface / the Royal Society*, vol. 12, no. 111, p. 20 150 520, Oct. 2015.

[63] Antoine Bricard, Jean-Baptiste Caussin, Debasish Das, Charles Savoie, Vijayakumar Chikkadi, Kyohei Shitara, Oleksandr Chepizhko, Fernando Peruani, David Saintillan, and Denis Bartolo, "Emergent vortices in populations of colloidal rollers," *Nat. Commun.*, vol. 6, pp. 1–8, Jun. 2015.

[64] Hugo Wioland, Francis G. Woodhouse, Jörn Dunkel, and Raymond E. Goldstein, "Ferromagnetic and antiferromagnetic order in bacterial vortex lattices," *Nat. Phys.*, Jan. 2016.

[65] A. Souslov, B. C. van Zuiden, D. Bartolo, and V. Vitelli, "Topological sound in active-liquid metamaterials," Oct. 21, 2016. arXiv: 1610.06873v2 [cond-mat.soft].

[66] F. G. Woodhouse and J. Dunkel, "Active matter logic for autonomous microfluidics," Oct. 18, 2016. arXiv: 1610.05515v2 [physics.bio-ph].

[67] B. Gaveau, T. Jacobson, M. Kac, and L. S. Schulman, "Relativistic extension of the analogy between quantum mechanics and brownian motion," *Phys. Rev. Lett.*, vol. 53, pp. 419–422, 5 Jul. 1984.

[68] B. Gaveau and L. S. Schulman, "Dirac equation path integral: Interpreting the Grassmann variables," *Il Nuovo Cimento D*, vol. 11, no. 1-2, pp. 31–51, 1989.

[69] T. Jacobson and L. S. Schulman, "Quantum stochastics: The passage from a relativistic to a non-relativistic path integral," *J. Phys. A: Math. Gen.*, vol. 17, no. 2, p. 375, 1984.

[70] C. W. Gardiner, *Handbook of stochastic methods for physics, chemistry and the natural sciences*, 3nd edition. Springer, 1985.

[71] N. G. Kampen, *Stochastic processes in physics and chemistry*, 3rd edition. North Holland, 2007.

[72] F. D. C. Farrell, M. C. Marchetti, D. Marenduzzo, and J. Tailleur, "Pattern formation in self-propelled particles with density-dependent motility," *Phys. Rev. Lett.*, vol. 108, p. 248 101, 24 Jun. 2012.

[73] Fernan Jaramillo and Kurt Wiesenfeld, "Mechanoelectrical transduction assisted by brownian motion: A role for noise in the auditory system," *Nat. Neurosci.*, vol. 1, no. 5, pp. 384–388, Sep. 1998.

[74] Aparna Baskaran and M. Cristina Marchetti, "Hydrodynamics of self-propelled hard rods," *Phys. Rev. E*, vol. 77, p. 011 920, 1 Jan. 2008.

[75] ——, "Enhanced diffusion and ordering of self-propelled rods," *Phys. Rev. Lett.*, vol. 101, p. 268 101, 26 Dec. 2008.

[76] Shradha Mishra, Aparna Baskaran, and M. Cristina Marchetti, "Fluctuations and pattern formation in self-propelled particles," *Phys. Rev. E*, vol. 81, p. 061 916, 6 Jun. 2010.

[77] P. Romanczuk, M. Bär, W. Ebeling, B. Lindner, and L. Schimansky-Geier, "Active brownian particles," *The European Physical Journal Special Topics*, vol. 202, no. 1, pp. 1–162, 2012.

[78] F. Peruani, A. Deutsch, and M. Bär, "A mean-field theory for self-propelled particles interacting by velocity alignment mechanisms," *The European Physical Journal Special Topics*, vol. 157, no. 1, pp. 111–122, 2008.

[79] Yoshiki Kuramoto, "Self-entrainment of a population of coupled non-linear oscillators," in *International Symposium on Mathematical Problems in Theoretical Physics: January 23–29, 1975, Kyoto University, Kyoto/Japan*, Huzihiro Araki, Ed. Berlin, Heidelberg: Springer Berlin Heidelberg, 1975, pp. 420–422.

[80] ——, *Chemical oscillations, waves, and turbulence*. Springer Science & Business Media, 1984, vol. 19.

[81] Sigbjørn Løland Bore, Michael Schindler, Khanh-Dang Nguyen Thu Lam, Eric Bertin, and Olivier Dauchot, "Coupling spin to velocity: Collective motion of hamiltonian polar particles," *J. Stat. Mech: Theory Exp.*, vol. 2016, no. 3, p. 033 305, 2016.

[82] M. Born and V. Fock, "Beweis des adiabatensatzes," *Zeitschrift für Physik*, vol. 51, no. 3, pp. 165–180, 1928.

[83] Gong-Wei Lin, Ming-Yong Ye, Li-Bo Chen, Qian-Hua Du, and Xiu-Min Lin, "Generation of the singlet state for three atoms in cavity qed," *Phys. Rev. A*, vol. 76, p. 014 308, 1 Jul. 2007.

[84] Mei Lu, Yan Xia, Jie Song, and He-Shan Song, "Driving three atoms into a singlet state in an optical cavity via adiabatic passage of a dark state," *J. Phys. B: At., Mol. Opt. Phys.*, vol. 46, no. 1, p. 015 502, 2013.

[85] Shi-Biao Zheng, "Nongeometric conditional phase shift via adiabatic evolution of dark eigenstates: A new approach to quantum computation," *Phys. Rev. Lett.*, vol. 95, p. 080 502, 8 Aug. 2005.

[86] N. Sangouard, X. Lacour, S. Guérin, and H. R. Jauslin, "Cnot gate by adiabatic passage with an optical cavity," *The European Physical Journal D - Atomic, Molecular, Optical and Plasma Physics*, vol. 37, no. 3, p. 451, 2005.

[87] Yan Liang, Chong Song, Xin Ji, and Shou Zhang, "Fast cnot gate between two spatially separated atoms via shortcuts to adiabatic passage," *Opt. Express*, vol. 23, no. 18, pp. 23 798–23 810, Sep. 2015.

[88] E. Torrontegui, S. Ibáñez, S. Martínez-Garaot, M. Modugno, A. del Campo, D. Guéry-Odelin, A. Ruschhaupt, X. Chen, and J. Muga, "Chapter 2 - shortcuts to adiabaticity," in *Advances in Atomic, Molecular, and Optical Physics*, ser. Advances In Atomic, Molecular, and Optical Physics, P. Berman E. Arimondo and C. Lin, Eds., vol. 62, Academic Press, 2013, pp. 117–169.

[89] D. Sels and A. Polkovnikov, "Minimizing irreversible losses in quantum systems by local counter-diabatic driving," Jul. 19, 2016. arXiv: 1607.05687v2 [quant-ph].

[90] M. Kolodrubetz, P. Mehta, and A. Polkovnikov, "Geometry and non-adiabatic response in quantum and classical systems," Feb. 2, 2016. arXiv: 1602.01062v3 [cond-mat.quant-gas].

[91] Sebastian Deffner, Christopher Jarzynski, and Adolfo del Campo, "Classical and quantum shortcuts to adiabaticity for scale-invariant driving," *Phys. Rev. X*, vol. 4, p. 021 013, 2 Apr. 2014.

[92] M. V. Berry, "Histories of adiabatic quantum transitions," *Proceedings of the Royal Society of London A: Mathematical, Physical and Engineering Sciences*, vol. 429, no. 1876, pp. 61–72, 1990.

[93] G. Nenciu, "Linear adiabatic theory. exponential estimates," *Comm. Math. Phys.*, vol. 152, no. 3, pp. 479–496, 1993.

[94] M. V. Berry, "Quantal phase factors accompanying adiabatic changes," *Proc. R. Soc. Lond. A*, vol. 392, no. 1802, pp. 45–57, 1984.

[95] Frank Wilczek and A. Zee, "Appearance of gauge structure in simple dynamical systems," *Phys. Rev. Lett.*, vol. 52, pp. 2111–2114, 24.

[96] J. Zhang, Thi Ha Kyaw, D. M. Tong, Erik Sjöqvist, and Leong-Chuan Kwek, "Fast non-abelian geometric gates via transitionless quantum driving," *Sci. Rep.*, vol. 5, 18414 EP, Dec. 2015.

[97] S. Ibáñez, S. Martínez-Garaot, Xi Chen, E. Torrontegui, and J. G. Muga, "Shortcuts to adiabaticity for non-hermitian systems," *Phys. Rev. A*, vol. 84, p. 023 415, 2 Aug. 2011.

[98] Adolfo del Campo, Marek M. Rams, and Wojciech H. Zurek, "Assisted finite-rate adiabatic passage across a quantum critical point: Exact solution for the quantum ising model," *Phys. Rev. Lett.*, vol. 109, p. 115 703, 11 Sep. 2012.

[99] H. R. Lewis Jr. and W. B. Riesenfeld, "An exact quantum theory of the time-dependent harmonic oscillator and of a charged particle in a time-dependent electromagnetic field," *J. Math. Phys.*, vol. 10, no. 8, pp. 1458–1473, 1969.

[100] H. Ralph Lewis and P. G. L. Leach, "A direct approach to finding exact invariants for one-dimensional time-dependent classical Hamiltonians," *J. Math. Phys.*, vol. 23, no. 12, pp. 2371–2374, 1982.

[101] A. K. Dhara and S. V. Lawande, "Feynman propagator for time-dependent lagrangians possessing an invariant quadratic in momentum," *J. Phys. A: Math. Gen.*, vol. 17, no. 12, p. 2423, 1984.

[102] Christopher Jarzynski, "Generating shortcuts to adiabaticity in quantum and classical dynamics," *Phys. Rev. A*, vol. 88, p. 040 101, 4 Oct. 2013.

[103] Adolfo del Campo, "Shortcuts to adiabaticity by counterdiabatic driving," *Phys. Rev. Lett.*, vol. 111, p. 100 502, 10 Sep. 2013.

[104] Manaka Okuyama and Kazutaka Takahashi, "From classical nonlinear integrable systems to quantum shortcuts to adiabaticity," *Phys. Rev. Lett.*, vol. 117, p. 070 401, 7 Aug. 2016.

[105] ——, "Quantum-classical correspondence of shortcuts to adiabaticity," *J. Phys. Soc. Jpn.*, vol. 86, no. 4, p. 043 002, 2017.

[106] Dr. D. J. Korteweg and Dr. G. de Vries, "Xli. on the change of form of long waves advancing in a rectangular canal, and on a new type of long stationary waves," *Philosophical Magazine Series 5*, vol. 39, no. 240, pp. 422–443, 1895.

[107] H. Weyl, "Quantenmechanik und gruppentheorie," *Zeitschrift für Physik*, vol. 46, no. 1, pp. 1–46, 1927.

[108] E. Wigner, "On the quantum correction for thermodynamic equilibrium," *Phys. Rev.*, vol. 40, pp. 749–759, 5 Jun. 1932.

[109] Andrew M. Essin and David J. Griffiths, "Quantum mechanics of the 1x2 potential," *Am. J. Phys*, vol. 74, no. 2, pp. 109–117, 2006.